Silicone-based Implants for the treatment of the inner ear

Adam Qnouch

UNIVERSITE DE LILLE – DROIT ET SANTE
FACULTE DES SCIENCES PHARMACEUTIQUES ET BIOLOGIQUES
Ecole Doctorale Biologie-Santé

Silicone-based Implants for the Treatment of the Inner Ear

Implants en silicone pour le traitement de l'oreille interne

THESE DE DOCTORAT

Soutenue le 15/11/2021

ADAM QNOUCH

Dirigée par:

Dr. Florence Siepmann – Directrice

Dr. Juergen Siepmann – Co-directeur

Composition du Jury :

Monsieur SIEPMANN Juergen *Professeur à l'Université de Lille 2*	Co-directeur de Thèse
Madame Evelyne Ferrary *Professeur à l'Université Pierre et Marie Curie*	Rapporteur
Madame BOCHOT Amélie *Professeur à l'Université Paris-Sud*	Rapporteur
Madame SIEPMANN Florence *Professeur à l'Université de Lille 2*	Directrice de Thèse

Remerciements

Je tiens à remercier chaleureusement toutes les personnes qui m'ont soutenu durant ma thèse.

Je voudrais remercier les Professeurs Juergen et Florence Siepmann pour m'avoir accueilli dans leur laboratoire, merci de m'avoir donné l'opportunité de travailler sur un sujet aussi intéressant, pour toutes vos discussions enrichissantes, ainsi que votre bonne humeur à toute épreuve.

Je remercie aussi le Professeur Jean-François Willart, qui a eu la gentillesse de m'aider pour les études de caractérisation, sa disponibilité ainsi que ses idées qui ont grandement contribué à l'avancement de mon projet de thèse. Encore merci !

Je voudrais également remercier le Professeurs Amélie Bochot, qui m'a non seulement soutenu lorsque j'étais encore étudiant à l'Université Paris-Saclay, mais aussi durant ma thèse en faisant partie de mon comité de suivi de thèse.

Je remercie aussi le Professeur Evelyne Ferrary pour ses commentaires toujours très pertinents au cours de nos réunions de projet biannuelles, ainsi que d'avoir accepté de faire partie de mon jury de thèse.

Je souhaite remercier tout particulièrement les étudiants que j'ai pu encadrer durant mes trois années de thèse, qui m'ont assisté au cours de mes expériences et m'ont permis de porter un nouveau regard sur mes travaux. Merci à Victoria, Jean, Candice et Chaimaa.

Un grand merci aussi à toute l'équipe U1008 pour leur accueil ainsi que l'ambiance d'entraide au sein du laboratoire, en particulier à Susanne Muschert, Youness Karrout, Mounira Hamoudi, Hugues Florin, Jérémy Vérin, Martin Foissart et Muriel Deudon.

Je remercie également mes camarades doctorants pour avoir instauré une ambiance amicale et leur soutien indéfectible. Ting pour m'avoir transmis autant de connaissances sur mon sujet en si peu de temps, Martin pour m'avoir initié aux afters, Doha pour son incroyable abnégation, Fahima pour son immense ouverture d'esprit, Corinna pour sa grande gentillesse, Céline pour

avoir proposé autant de sorties entre doctorants, Yanis pour son aide inestimable sur la dernière partie de ma thèse.

Je tiens enfin à remercier mes amis ainsi que ma famille, sans qui rien de tout cela n'aura été possible, et qui malgré la distance m'ont permis d'avancer dans les moments les plus compliqués. Merci énormément à vous tous.

Table of contents

List of abbreviations

WHO	World Health Organization
SNHL	Sensorineural hearing loss
NIHL	Noise-induced hearing loss
SSNHL	Sudden sensorineural hearing loss
PTA	Pure-tone average
HIR	Hearing improvement rate
HA	Hyaluronic acid
CGP	Chitosan glycerol-phosphate
PLGA	Poly(lactic-co-glycolic acid)
PHEA	Poly(2-hydroxyethyl aspartamide)
DPOAE	Distortion product otoacoustic emissions
PRN	Post-rotary nystagmus
DNQX	6,7-dinitroquinoxaline-2,3-dione
EC	Encapsulated Cell
BDNF	Brain-derived neurotrophic factor
BTE	Behind the ear
ITE	In the ear
CI	Cochlear implant
PEG	Polyethyleneglycol

1. Introduction

1.1 Sound Perception

There are three main components to the human auditory system: the outer ear, the middle ear, and the inner ear[1] (figure 1.1).

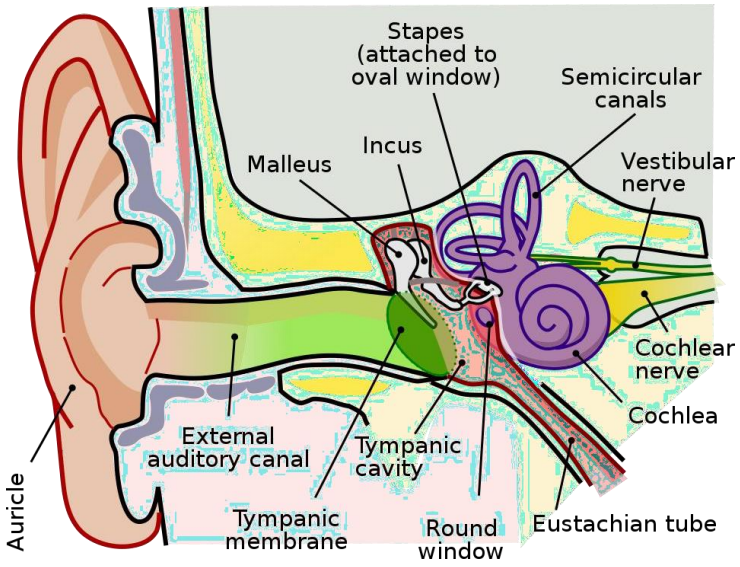

Figure 1.1. Anatomy of the ear: division into the outer (auricle, external auditory canal, tympanic membrane), the middle (tympanic cavity, malleus, incus, stapes, round window, Eustachian tube), and the inner ear (cochlea, semicircular canals, cochlear and vestibular nerves), adapted from [2]

The **outer ear** includes the pinna, the visible part of the ear, as well as the ear canal which terminates at the eardrum, also called the tympanic membrane. The pinna serves to focus sound waves through the ear canal toward the eardrum. The eardrum being an airtight membrane, arriving sound waves cause it to vibrate following the waveform of the sound.[1]

The **middle ear** consists of a small air-filled chamber that is located medial to the eardrum. Within this chamber are three small bones, known collectively as the ossicles. They include the malleus, incus, and stapes (also known as the hammer, anvil and stirrup

respectively). They aid in the transmission of the vibrations from the eardrum into the inner ear, where the cochlea resides. The stapes transmits sound waves to the inner ear through the oval window, a flexible membrane separating the air-filled middle ear from the fluid-filled inner ear. The round window, another flexible membrane, allows for the smooth displacement of the inner ear fluid caused by the entering sound waves.[3]

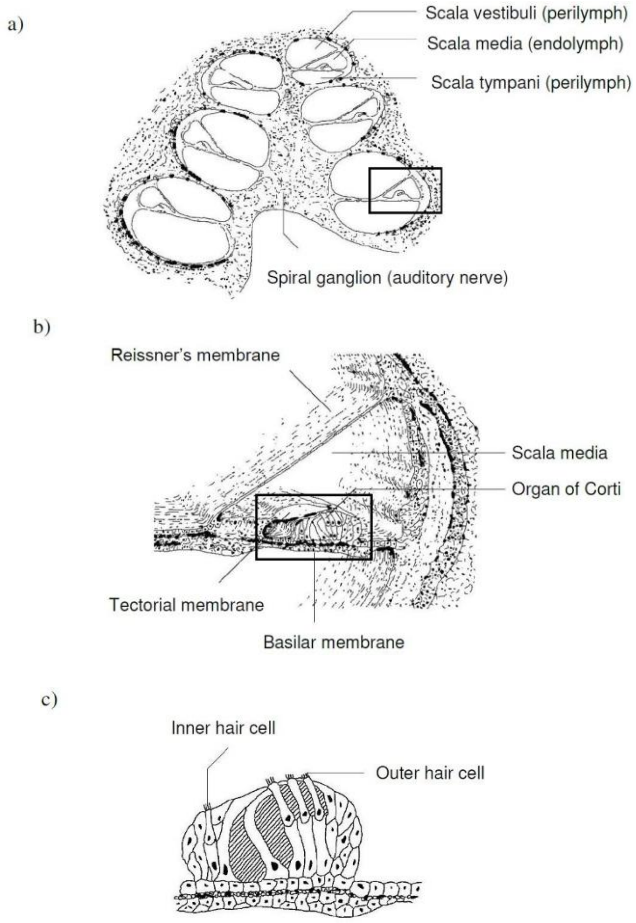

Figure 1.2. Anatomy of the cochlea: Section through the cochlea: a) cochlea with three coiled up fluid filled spaces: scala vestibuli, media and tympani; b) zoom into the scala media with the Organ of Corti – the organ containing the sensory cells; c) zoom into the Organ of Corti with three rows of outer hair cells and one row of inner hair cells, adapted from[4]

The **inner ear** is home to the cochlea, a snail-like structure that consists of three fluid-filled canals: scala tympani, scala media and scala vestibuli (figure 1.2.a)[4]. The scala tympani and vestibuli are filled with perilymph, which shares a similar composition to other extracellular fluids. Both scalae share a volume of 70 µL in humans and 2.78 µl in gerbils.

Table 1.1. Characteristics of fluids inside the cochlea: Perilymph and Endolymph in humans, adapted from[5,6]

	Perilymph	**Endolymph**
Volume, µL	70	8
Volume (gerbil), µL	2.78	0.38
Na+, mM	160	1
K+, mM	4-5	150
Cl-, mM	120	130
H2CO3, mM	20	30
Ca2+, mM	1.2	0.02
Glucose, mM	4	0.5
Proteins, g L-1	1	0.15
pH	7.4	7.4
Osmolality, mOsm kg-1	290	315
Potential, mV	0	+80

On the other hand, scala media – situated between the two other scalae – is filled with endolymph. Endolymph has an unusual composition, notably with its increased concentration of potassium ions (150 mM) leading to a higher potential (+80 mV) in its fluids. The endolymphatic space is generally nearly ten times lower than the perilymph volume (Table 1.1).

The three scalae are separated from one another by two membranes: Reissner's membrane is found between the scala vestibuli and media, while the basilar membrane is between the scala media and tympani (Figure 1.2.b). The basilar membrane is tonotopic, meaning that each frequency has a characteristic place of resonance along it. Characteristic frequencies being high at the basal entrance to the cochlea (20000 Hz), and low at the apex (20 Hz).[7] The basilar membrane is situated inside the organ of Corti (figure 1.2.c), which is the main organ of mechanical to neural transduction. Basically, the basilar membrane will start to vibrate when waves from the middle ear propagate through the endolymph. The subsequent motions will trigger the depolarization of hair cells, which are specialized auditory receptors located within the organ of Corti. Hair cells are responsible for the translation of mechanical waves into electrical signals, leading to the perception of sound in the brain.[4]

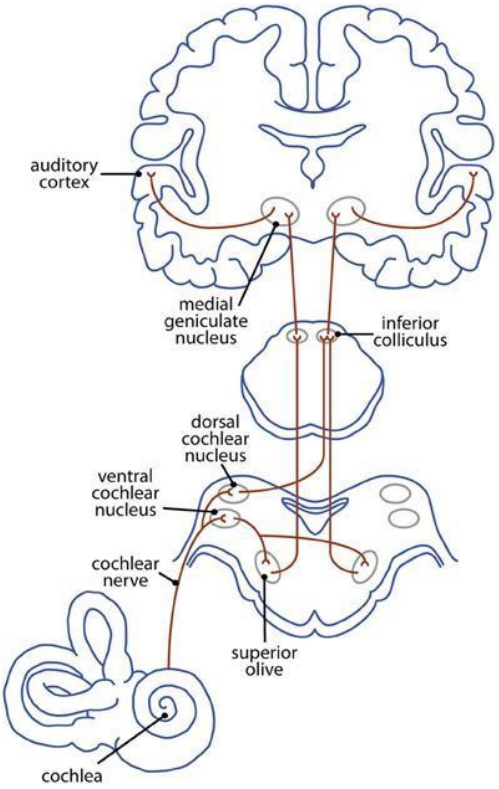

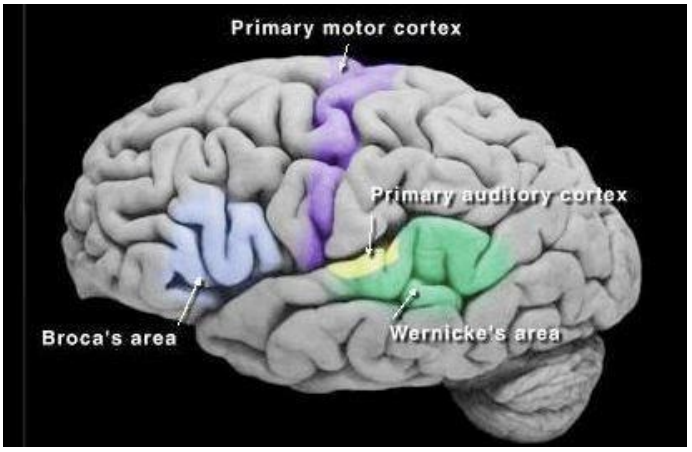

Figure 1.3. Relay stations in the auditory pathway: Afferent nerves arising from the cochlea send their information to the cochlear nuclei in the medulla, the inferior colliculi in the midbrain, and the primary auditory cortex in the middle third of the superior temporal gyrus, close to the Wernicke's area, adapted from[8]

The sound information from the cochlea travels to the primary **auditory cortex** in the temporal lobe (figure 1.3.a)[8]. Around the primary auditory cortex lies the Wernicke's area, a cortical area involved in interpreting sounds that is necessary to understand spoken words (figure 1.3b).[9]

Disturbances at any of these levels can cause hearing problems[10,11], difficulties in maintaining the balance of the body (Menière's disease)[12], or auditory hallucinations[13]. Although, given the highly sensitive nature of the human auditory system, many barriers are present to ensure its protection, in which we will expand for the upcoming chapter.

1.2 Barriers of the human auditory system

Figure 1.4. Image of a human tympanic membrane, adapted from[14]

The tympanic membrane – also called eardrum – is the first barrier protecting the human auditory system (Figure 1.4). It is found between the outer and middle ear, at the very end of the external auditory canal. The tympanic membrane has an area of 85 to 90 mm^2 and consists of three layers: the outer layer, continuous with the skin on the external canal; the inner layer, continuous with the mucous membrane lining the middle ear; and, between the two, a layer of radial and circular fibres that gives the membrane its tension and stiffness[15]. This combination of layers protects the middle ear from toxic substances entering through the ear canal. The tympanic membrane has low permeability to most substances and is considered an essentially impenetrable barrier in drug delivery to the ear[16]. It may be perforated due to diseases or trauma, causing partial hearing loss and potential middle ear infection. However, in order to deliver drugs to the middle ear for inner ear drug delivery, the integrity of the tympanic membrane must be compromised during intratympanic administration. It is important to note that even when intratympanic delivery is done, drugs administered into the middle ear can be cleared from the Eustachian tube, causing drug loss and short residence. As such, reducing drug

clearance to prolong drug residence in the middle ear is of the upmost importance for an efficient drug delivery [16].

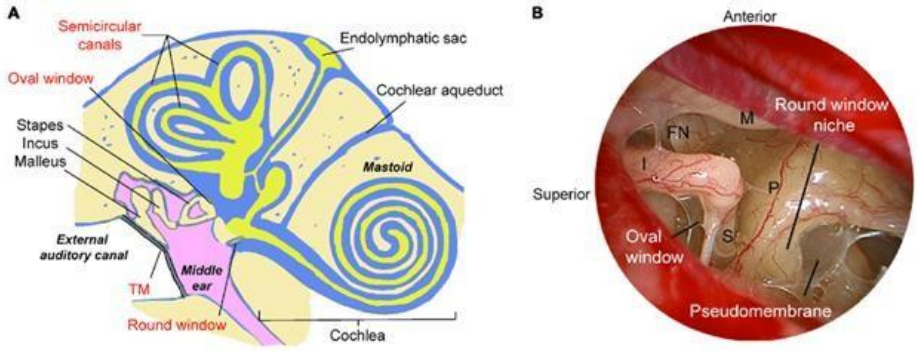

Figure 1.5. Anatomy of the oval and round window: A) schematic view of the localization of oval and round window within the middle and inner ear, B) endoscopic view of the human middle ear, adapted from[17]

The oval and round window (Figure 1.5) are the second set of barriers, they connect the middle ear with the cochlea and are surrounded by the petrous bone, one of the densest bones in the human body. The round window is connected to the scala tympani at the basal turn of the cochlea. It consists of three layers: an external, or mucous, derived from the mucous lining of the tympanic cavity; an internal, from the lining membrane of the cochlea; and an intermediate, or fibrous layer. The round window niche has an opening width of about 0.5 to 3 mm, the membrane has a thickness of about 50 to 100 μm in humans compared to 10 to 14 μm in rodents[18,19]. The ovoid surface of the round window is around 2.2 mm^2 in humans compared to 1 mm^2 in rodents and can have various shapes. The oval window is in contact with the perilymph of the scala vestibuli at the base of the stapes. The stapes' footplate is attached to the oval window by the annular ligament and has a normal thickness of 0.3 to 0.5 mm in humans[18]. The length of the footplate has been measured to be 2.5 to 3.36 mm compared to a width of 0.7 to 1.66 mm. It has been calculated[20] that the surface area of the stapes footplate is about 3.97 mm^2. Although there is limited literature studying the permeability of oval window,

experimental results[21,22] have suggested that the oval window is more permeable to compounds than the round window membrane and may be a promising alternative route of drug delivery to treat vestibular disorders. The round window membrane is still considered as the primary passage of intratympanic drugs, even though it is also one of the most important physical barriers for inner drug delivery. To add to its limitations, the varied shapes of the ear canal in humans often introduce difficulty in visualizing the round window membrane during intratympanic administration. When the round window membrane is obstructed, this can lead to interpatient variability in intratympanic administration[16].

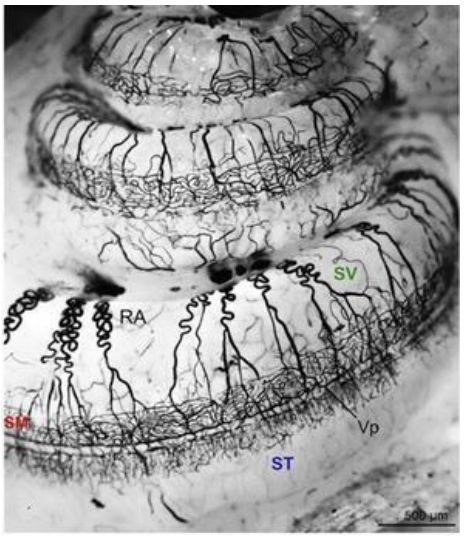

Figure 1.6. Image of blood vessels in a cat cochlea highlighted by ink perfusion, adapted from[23]

Finally, we have the **blood-cochlea barrier** (Figure 1.6). Also called the blood-perilymph barrier, its function is similar to the blood-brain barrier, as it limits the diffusion of drugs from the systemic blood circulation into the inner ear. The drugs entry is blocked by tight junctions without fenestration, a result of the capillary endothelium special composition[24]. Nevertheless, it seems that drugs can still enter the inner ear depending on their chemical characteristics. Small lipophilic ones can enter the perilymph more easily than big hydrophilic,

charged or protein binding drugs[25]. Positively charged drugs are also less likely to enter the endolymphatic space from the perilymph because of the electrical gradient (Table 1.1). It is important to keep in mind that noise exposure, inflammation, and the administration of diuretics or osmotic agents can easily disturb the blood-cochlea barrier[6].

Despite the presence of many barriers protecting the human auditory system, this region remains extremely fragile, and disturbances in any of its levels can cause hearing problems in a wide range of patients. As such, the next chapter will be focusing on hearing loss.

1.3 Hearing loss

Hearing loss is a partial or total inability to hear (deafness)[26]. It is diagnosed when hearing testing finds that a person is unable to hear 25 decibels in at least one ear. There are five **grades of hearing impairment**, which can range from mild to profound[27] (table 1.2):

Table 1.2. Hearing impairment according to the definition of the WHO.

Grade	Threshold shift of the better ear, dB	Effect
0	25 or less	No trouble
1	26 to 40	Slight/mild impairment, trouble hearing and understanding soft speech, also speech from a distance or with background noise
2	41 to 60	Moderate impairment, trouble hearing regular speech, even at a close distance
3	61 to 80	Severe impairment, only very loud speech or loud sounds in the environment can be heard
4	81 or greater	Profound impairment, even loud sounds are not heard

There are also several **types of hearing loss** depending on the concerned region[28] (table 1.3):

Table 1.3. Types of hearing loss with the concerned region.

Type of hearing loss	Concerned region
Conductive	Disease of external and/or middle ear
Sensorineural	Disease of the cochlea and/or nerve
Mixed	Combination of conductive and sensorineural

According to the WHO[29], 466 million people (6.1% of the world's population) are estimated to be living with hearing loss, and this number is expected to rise to 900 million by 2050. On this day, 34 million children have deafness or hearing loss problems, of which 60% of cases are due to preventable causes. On the other end of the lifespan, approximately one third of people over age 65 are affected by disabling hearing loss, with the majority of these cases in South Asia, Asia Pacific and sub-Saharan Africa. The impacts of hearing loss are broad and can be profound, they include a loss of the ability to communicate with others, which can lead to social isolation, loneliness and frustration. Many areas lack sufficient accommodations for hearing loss, which effect academic performance and options for employment. Low- and middle-income countries bear a disproportionate burden from hearing loss.

WHO estimates that global hearing aid production covers only 3% of the need in these countries. Children with hearing loss have a delayed language development, and deaf children in developing countries rarely receive any schooling at all. Unaddressed hearing loss costs the global economy US$ 750 billion annually due to health sector costs, costs of educational support, loss of productivity and societal costs. Even more worrying, 1 billion young people (12-35 years) are at risk for hearing loss due to recreational exposure to loud sounds.[29]

The **causes of hearing loss** can be either congenital or acquired (table 1.4):

Table 1.4. Causes of hearing loss with their occurrence and etiology.

Cause of hearing loss	Occurrence	Etiology
Congenital	During or shortly after birth	57% is idiopathic, genetic factors account for 25% of the cases, 18% are infections transmitted by the mother (rubella, toxoplasmosis) or inappropriate use of drugs during pregnancy[30]
Acquired	At any age, suddenly or over a long period of time	Mainly idiopathic, can develop with age of after acute or long term noise exposure[11], usage of ototoxic drugs (chemotherapeutic agents, aminoglycoside antibiotics, anti-malaria drugs)[31–33], some infections (measles, mumps or meningitis)[34] autoimmune diseases (systemic lupus erythematosus, multiple sclerosis, vascular events)[35–37]

The **therapeutic treatment** of patients suffering from hearing loss is extremely challenging, not only are there multiple concerned regions, but also the causes of hearing loss – be it congenital or acquired – are mostly non-identified. For the upcoming chapter we will solely focus on sensorineural hearing loss and its treatments.

1.4 Sensorineural hearing loss and its treatments

Sensorineural hearing loss is the collective term for hearing damage to the cochlea and auditory nerve, which is by far the most prevalent type of hearing loss in adults, accounting for over 90% of all cases[38]. Presbycusis (age-related hearing loss) is the most common cause of SNHL, the second one being exposure to environmental noise, also known as noise-induced hearing loss (NIHL). Using headphones at high volumes over time, being regularly in loud

environments such as a loud workplaces, sporting events, concerts, or using noisy machines can constitute a risk for noise-induced hearing loss.[11]

In the case of sudden sensorineural hearing loss (SSNHL), which is most commonly defined as a sensorineural hearing loss of 30 dB or greater occurring within a 72-hour period, identifiable causes are only found for 7 % up to 45 % of patients[34], which raises the question of how to treat them, or even the necessity to do so, as idiopathic SSNHL spontaneously resolves itself in 32 % to 65 % of patients[39]. Still, numerous agents have been investigated for the **treatment of idiopathic SSNHL.**[40]

Wilson et al. treated 33 patients with varied doses of dexamethasone (ranging from 0.75 mg twice daily to 4.5 mg twice daily) or methylprednisolone (ranging from 4 mg daily to 16 mg 3 times daily) and reported that the anti-inflammatory effect of each dose seemed roughly equivalent. Pure-tone average (PTA) was measured at 1 and 3 months after onset of hearing loss. Results were categorized into "recovery" and "no recovery" groups. No recovery was defined as less than 50% recovery of hearing. They found a statistically significant greater rate of recovery for patients treated with steroids (61%) compared with placebo (32%)[41].

Alternatively, Cinamon et al. administered prednisone 1 mg/kg daily to 11 treatment subjects and measured PTA, speech frequency, high tone hearing levels, and discrimination scores at 6 days (soon after treatment) and 14 to 90 days (follow-up after treatment). Patients were categorized into "improvement" and "no improvement" groups with respect to average hearing level (increase of hearing level at least 15 dB), average speech frequency, and average high tone hearing level. They reported no significant differences between steroids and placebo on all outcome measures[42].

Even though its effect could not always be demonstrated in the literature, steroid usage was still considered as the gold standard in the treatment of SSHL. Various non-steroidal agents were also investigated in many other studies, their effectiveness generally assessed in

comparison to a more conventional steroid therapy. Cinamon et al. treated 10 patients with carbogen inhalation (5% carbon dioxide and 95% oxygen) for 30 minutes, 6 times per day for 5 days and another 11 patients with prednisone, 1 mg/kg daily for 5 days. They reported an improvement in average hearing level (15 dB), speech frequency, and high tone hearing levels soon after treatment (6 days) and at follow-up (33 days in average). However, they found no significant differences between treatment with carbogen or treatment with steroids[42].

Kubo et al. devised 2 treatment groups: 82 patients received a total of 80 U of intravenous batroxobin over 13 days plus oral placebo, while 80 patients in a second treatment arm received a combination of intravenous and oral betamethasone plus placebo intravenous saline solution over 13 days. While there was a fair number of patients with improved PTA after 2 weeks of treatment. There was once again no difference between batroxobin and steroids[43].

Seeing as there is generally no reported improvement when comparing non-steroidal agents to steroidal ones, some teams choose to study instead the combination of both. Nageris et al. conducted a prospective, randomized, double-blind, placebo-controlled trial. 28 patients with idiopathic sudden sensorineural hearing loss were treated with either steroids and oral magnesium (study group) or with steroids and a placebo (control group). PTA was measured after 4 weeks of treatment, and they reported a significantly greater rate of recovery among patients treated with steroids plus magnesium, compared to steroids plus placebo[44].

In the same logic, Joachims et al. compared patients who were treated with vitamin E in addition to standard treatment (steroids, carbogen, and magnesium) versus standard treatment alone (control group). The recovery rate, calculated as hearing gain divided by the difference in hearing level between the affected and unaffected ear, was better than 75% in 41 of 66 (62.12%) patients. This rate was achieved in 26 (78.78%) patients in the study group treated with vitamin E, compared with 15 (45.45%) patients in the control group. These results showed

that the addition of vitamin E achieved better recovery, and more importantly that antioxidants may play a significant role in the treatment of idiopathic sudden hearing loss in addition to steroids[45].

Topuz et al. compared 34 patients receiving hyperbaric oxygen plus standard treatment (prednisone, diazepam, and pentoxifylline) vs 21 patients receiving standard treatment alone. They found a greater rate of improvement, defined as gain of hearing of at least 10 dB on PTA, in the hyperbaric oxygen group[46].

Table 1.4. Summary of agents investigated for the treatment of idiopathic SSNHL.

Study	Treatment	Result
Wilson et al, 1980	Steroid therapy vs placebo	Statistically significant greater rate of recovery for patients treated with steroids (61%) than with placebo (32%), measured at an undefined time after treatment
Cinamon et al, 2001	Steroid therapy vs placebo	No significant differences between any of the treatment groups
Cinamon et al, 2001	Steroid therapy vs carbogen inhalation	Improvement in average hearing level, speech frequency, and high tone hearing levels soon after treatment and at follow-up, but no significant differences between treatment with carbogen or treatment with steroids
Kubo et al, 1988	Steroid therapy vs intravenous batroxobin	Overall improvement in the PTA after 2 weeks of treatment, but no difference between batroxobin and steroids
Nageris et al, 2004	Magnesium plus steroid therapy vs steroid therapy	Statistically greater rate of hearing improvement (at least 10 dB) in the magnesium group than in the control group
Joachims et al, 2003	Vitamin E plus steroid therapy vs steroid therapy	The improvement rate was significantly greater in the vitamin E group (78.8%) than in the standard group (45.5%)
Topuz et al, 2004	Hyperbaric oxygen plus steroid vs steroid therapy	Statistically significant greater hearing gains in the hyperbaric oxygen group than in the control group in 4 of 5 frequencies

When surveyed in 2009, 98 % of U.S. otolaryngologists reported treating idiopathic SSNHL with **oral administration of steroids**[47]. Corticosteroids are thought to improve idiopathic SSNHL by reducing inflammation and edema in the inner ear[48,49]. An initial study combined the data from two separately administered double-blinded randomized controlled trials of a total of 67 patients using different corticosteroid regimens, finding an improved hearing recovery in patients receiving steroids (78 %) compared to placebo (38 %)[41]. However, subsequent attempts to replicate this study reveal inconsistent findings with regard to the benefit of corticosteroids in idiopathic SSNHL, and there are issues in terms of methodology with many of these trials[40,42,49]

Systemic administration of corticosteroids is also feasible, generally in addition to an antiviral agent, but the results are no better. Two studies included in a Cochrane review showed no improvement when aciclovir was administered additionally to prednisolone[50,51]. Patients treated with valaciclovir in addition to prednisone or aciclovir administered additionally to hydrocortisone showed no hearing improvement either[52,53]. This lack of efficacy can be explained by the following: administration by conventional means (especially oral and systemic routes) allows only small quantities of the drug to reach the cochlea, since the passage from the systemic circulation to the inner ear is severely impeded by the presence of the blood-cochlear barrier, whose role is to protect the highly sensitive inner ear. Therefore, high dosage of drugs are required to bypass this barrier, potentially accompanied by serious side effects due to considerable concentrations in other parts the body, while not providing enough therapeutic effects locally[54].

Given the aforementioned limitations of conventional routes, **local drug delivery** imposes itself as the most promising approach, given that it goes beyond the blood-cochlea barrier to offer precise release kinetics and specific targeting[16] (figure 1.7). Salt et al. reviewed the **pharmacokinetics** underlying local therapy of the ear with the drugs commonly used in

clinical practice as examples. Interestingly, they found that it is critically important to know the exact chemical form of the drugs being used, as small differences in molecular configuration can influence polarity and lipophilicity, therefore altering the pharmacokinetic properties of the molecule. For example, dexamethasone had a more polar form than dexamethasone-phosphate, suggesting it would be more permeable through membranous barriers. In contrast, gentamicin is highly polar and hydrophilic, suggesting it would less readily go through cellular boundaries. The same physical parameters also play a major role in the aqueous solubility of different drugs. Small, nonpolar lipophilic drugs such as the base forms of dexamethasone and methylprednisolone are relatively insoluble in water. Adding polar groups to the molecule such as the phosphate or succinate groups for dexamethasone and methylprednisolone respectively will greatly increase aqueous solubility. They found that the use of these polar, more soluble forms of steroids successfully increased the total drug amount delivered in intravenous formulations. When given intravenously the soluble formulation is rapidly dispersed by blood flow before the polar groups are cleaved in tissues, forming the less-soluble active molecule. It is important to note that there is little consideration of how such molecular transformations influence the pharmacokinetics of the drug when used with local applications to the ear. Their analysis confirmed that while dexamethasone enters the ear far more readily than dexamethasone-phosphate, it can only be applied at low concentration due to its limited solubility. On the other hand, due to the declining middle ear concentration combined with ongoing elimination, perilymph concentration falls rapidly with time for dexamethasone-phosphate applications. Dexamethasone-phosphate thus provides only a brief exposure and dexamethasone is limited by its solubility[55].

By understanding the pharmacokinetics underlying local delivery to the inner ear, it is possible to develop appropriate systems for their administration.

El Kechai et al. have recently written an extensive review on the recent advances in local drug delivery to the inner ear, citing two major strategies to deliver drugs locally: intratympanic and intracochlear administration[6].

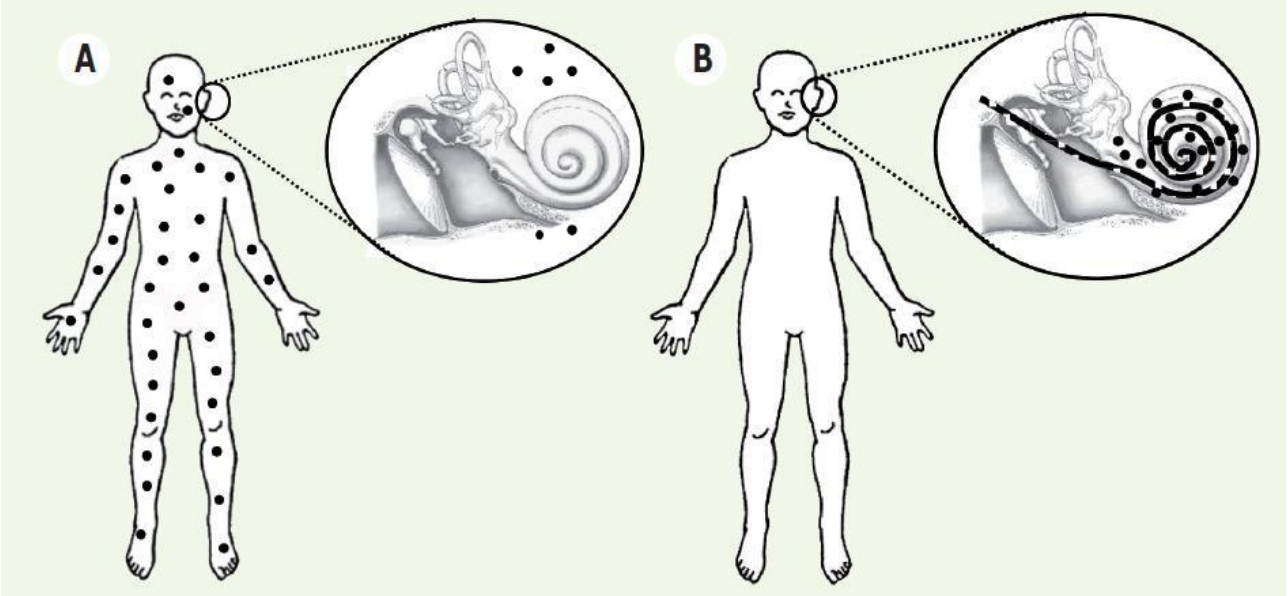

Figure 1.7. Schematic representation of the distribution of the active ingredients in the human body after: (A) administration by a conventional route (oral, systemic), or (B) administration using local drug delivery. The black dots represent molecules of active ingredients, adapted from[54]

Intratympanic administration consists of using the middle ear as a reservoir for drugs, so they can diffuse through the round window and access the inner ear. The key parameter influencing drug concentration in the perilymph is the residence time of drugs close to the round window[56]. The most basic method of intratympanic administration consists of piercing the tympanic membrane using a thin needle and filling the tympanic cavity with a drug solution, generally steroids[57] (figure 1.8). The outcome is looking quite promising for patients suffering from SSNHL, as those whose first line treatment with systemic steroids failed showed a reduction in hearing thresholds when treated with an intratympanic injection[58]. Ng et al.

performed a meta-analysis of studies where intratympanic steroids were used as a salvage treatment. There was a statistically significant reduction in hearing threshold on pure-tone audiometry in patients who received salvage intratympanic steroids than in those who did not. Moreover, subgroup analysis showed that administration by intratympanic injection rather than a round window catheter yielded significant improvement in outcome, and that the usage of dexamethasone yielded better outcomes than the use of methylprednisolone. Interestingly, another meta-analysis by Garavello et al. showed that while intratympanic steroid administration seemed to confer a certain degree of benefit as a salvage therapy, those effects were not as significant when intratympanic administration was used as the primary therapy[59].

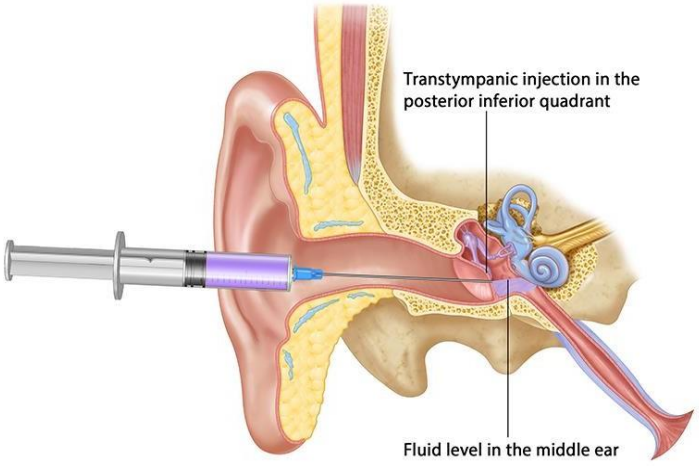

Figure 1.8. Schematic representation of an intratympanic injection. The purple liquid in the middle ear represents a drug solution, adapted from[60]

As seen earlier, drug residence near the round window is a key parameter for its diffusion to the inner ear, however, intratympanic injection is a technique that requires repeated injections – 2 to 5 times a week – given that the drug solution is rapidly eliminated from the middle ear via the Eustachian tube[61]. In order to increase the amount of drugs that stays in the

middle ear, several implantable medical devices were developed for intratympanic administration, including the Silverstein MicroWick, which involves the use of a small wick that is inserted through a tympanic membrane vent tube into the round window. Once the wick has been inserted, the patient can self-administer eardrops into the ear canal, where they are absorbed by the wick and transported to the round window membrane and to the inner ear fluids[62]. Barriat et al. showed that the delivery of methylprednisolone using those devices could improve hearing and speech intelligibility in patients after failure of conventional therapy[63]. Methylprednisolone was administered for 10 days after the onset of the hearing loss, of the 26 patients enrolled, 14 patients (54%) showed an improvement in the pure tone average (PTA) with an overall improvement in PTA of 13.5 ± 7.3 dB for the 26 patients enrolled. The auditory capacity index, defined as the mean speech discrimination score obtained at 40, 55 and 70 dB, improved by 24.2 ± 8.7% in 26 patients. Among the 12 patients with a stable PTA, 9 also showed an increase in speech intelligibility.

The use of microcatheters is also feasible, they are temporarily implanted (few days to weeks) in the posterior wall of the bony ear canal middle ear and connected to an external pump. Briefly, the surgical implantation and fixation technique are characterized by six elements: 1) a medial and a lateral tunnel connected by a groove in the posterior wall of the bony ear canal, 2) stabilization of the catheter with bone wax and soft tissue plugs in the tunnels, 3) an ear canal packing, 4) a series of fixating sutures along the catheter, 5) an adhesive dressing, and 6) additional tapes at the connecting line between pump and catheter. At the end of the implantation period, the catheter is removed by a second surgical procedure allowing for the evaluation of its position and the condition of the middle ear space[64]. Plontke et al. conducted a randomized, double blind, placebo-controlled trial for microcatheters delivering dexamethasone sodium phosphate to patients suffering from SSNHL. Intention-to-treat analysis for the primary outcome criterion during the placebo controlled study period (14 days) showed

an average hearing improvement in the treatment group of 13.9 dB and in the placebo group of 5.4dB. This difference in hearing improvement between the two groups was statistically not significant (P =.26). Of the secondary outcome parameters, the largest benefit of local salvage therapy was found for maximum speech discrimination with an improvement of 24.4% in the treatment and 4.5% in the placebo group (P =.07). After a 3 month follow-up period (i.e. after all patients received intratympanic dexamethasone-phosphate) hearing improvement in the two groups was very similar[65]. Another non-randomized, prospective, controlled study by Li et al. was aimed at evaluating the efficacy of intratympanic dexamethasone perfusion versus injection for the treatment of sudden sensorineural hearing loss. The perfusion was made via round window microcatheter by an electronic pump at a rate of 10 μl/min twice daily for 7 days. Hearing improvement rate (HIR) of SSNHL in the perfusion group was 40.6%, which was significantly higher than in the injection and control groups (20.6 and 7.7%, respectively)[66].

Hydrogels are another type of medical devices that were tested for intratympanic administration. They have a high viscosity and viscoelastic properties that avoid rapid flow through the Eustachian tube, thus allowing longer residence times in the middle ear, while also limiting the number of injections[6]. Wang et al. evaluated thermo-reversible triblock copolymer poloxamer 407 hydrogels containing dexamethasone. They found significant drug levels within the perilymph for at least 10 days, even though an assessment of auditory functions revealed a small transient shift in hearing threshold, most probably of conductive nature, which resolved itself within a week[67]. Borden et al. demonstrated that a hyaluronic-acid (HA)-based hydrogel could provide sustained dexamethasone phosphate release in a guinea pig model, with measurable drug levels in the perilymph up to 72 h after treatment, even though a high variability in dexamethasone phosphate concentration was observed between the samples[68]. Paulson et al. studied a chitosan-glycerophosphate (CGP)-hydrogel based system for the delivery of dexamethasone. The system was designed to release 92% of the dexamethasone

load over 4 consecutive days. Drug levels were detected in the perilymph for 5 days in a mice model, even though auditory function testing revealed a temporary hearing loss in the immediate postoperative period, which resolved by the 10th postoperative day[69].

Nanoparticulate systems, also called nanocarriers, have sizes below 1 μm and possess the ability to directly carry drugs to a target site, avoiding any potential toxic effect on healthy tissues. Some nanocarriers (typically 200 nm or smaller)[70] are even able to cross the round window, granting the possibility to introduce drugs into the cochlea while also avoiding surgical trauma. Nanoparticles can be used to counteract low drug solubility and problems with degradation or short half-life of the drug[6]. Du et al. evaluated the targeting and release kinetics of PLGA-magnetite-dexamethasone-acetate nanoparticles in anesthetized guinea pigs. A permanent magnet was placed opposite the round window membrane for 1 hour to improve targeting. The nanoparticles had an average size of 482.8 ± 158 nm and an average zeta potential of −19.9 ± 3.3 mV. In 1 hour, there was significantly increased cochlear targeted delivery of dexamethasone-acetate compared with diffusion alone[71]. Kim et al. studied the permeability and safety of a drug delivery system for the inner ear using a poly(2-hydroxyethyl aspartamide) (PHEA) polymersome. One month old male C57/BL6 mice were used. They administered the same amount of a fluorescent dye – Nile red – into the middle ear in two forms: loaded in PHEA polymersomes or diluted in ethanol. 24 hours after administration, the cochlea was harvested and the visible red particles counted. Hearing and histological tests were also conducted for safety evaluation. The number of red particles in the organ of Corti was increased significantly in the nanoparticles group, with some subjects even showing uptake in inner hair cells. However, safety tests showed a decrease in the responses of distortion product otoacoustic emissions (DPOAE), as well as a mildly swollen middle ear mucosa compared to the control group[72].

Table 1.5. Summary of intratympanic methods for the treatment of idiopathic SSNHL.

Study	Treatment method	Result
Ng et al, 2015	Intratympanic injection	Meta-analysis: statistically significant reduction in hearing thresholds of patients who received salvage intratympanic steroids when first line treatment with systemic steroids failed
Garavello et al, 2012	Intratympanic injection	Meta-analysis: intratympanic steroid administration has a certain benefit as a salvage therapy, but the effects are not as significant when as the primary therapy
Barriat et al, 2011	Silverstein Microwick	Administration of steroids to the inner ear through the round window route using a Silverstein Microwick showed improved pure tone average (PTA) and speech intelligibility
Plontke et al, 2009	Microcatheters vs placebo	There was a tendency toward better hearing improvement in the treatment group, which was not statistically significant compared to the placebo group
Li et al, 2013	Microcatheters vs injection	Microcatheters delivering dexamethasone in the case of refractory SNHL showed significant hearing improvement (40.6%) compared to injected and control groups (20.6 and 7.7% respectively)
Wang et al, 2009	Poloxamer 407 hydrogel	Significant dexamethasone levels within the perilymph for at least 10 days, but a small transient shift in hearing thresholds that resolved itself after a week
Borden et al, 2011	Hyaluronic acid hydrogel	Dexamethasone phosphate drug levels were measurable up to 72 h after treatment, but high variability in concentrations was observed between samples
Paulson et al, 2008	Chitosan-glycerophosphate hydrogel	Drug levels were detected in the perilymph for 5 days in a mice model, but there was a temporary hearing loss which resolved by the 10th postoperative day
Du et al, 2013	PLGA-magnetite nanoparticles	1 hour after a permanent magnet was placed opposite the round window membrane, PLGA-magnetite-Dexamethasone-Acetate nanoparticles showed significantly increased drug levels in the cochlea compared to diffusion
Kim et al, 2015	PHEA-nanoparticles	Significantly increased permeability with the nanoparticles

In contrast to intratympanic administration, **intracochlear administration** consists of introducing the drug directly into the cochlea, thus avoiding middle ear barriers that limits diffusion-based therapies. The most basic approach is intracochlear injection: following a cochleostomy (surgery to open a path into the cochlea, figure 1.9), very few microliters of a drug solution are injected using fine gauge needles. Kawamoto et al. used this method for gene-based therapy. Briefly, a cochleostomy was performed on young guinea pigs, then approximately 5 µl of adenoviral suspension was slowly injected into the scala tympani perilymph through the cochleostomy. Four days after the inoculation, animals were exposed to 4 kHz octave band noise, presented at 115 dB SPL for 5 hours. Seven days after the noise exposure, animals were euthanized and their inner ear removed for hair cell counting. The results showed that intracochlear injection with adenovirus did not compromise either hair cell counts nor ABR thresholds[56].

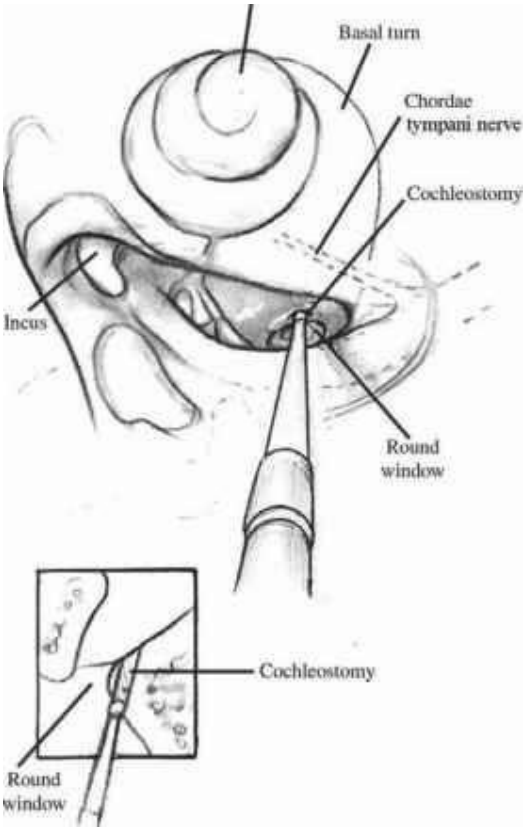

Figure 1.9. Schematic representation of a cochleostomy: a hole is drilled into the scala tympani or the round window, opening a path to the cochlea, adapted from[75]

While simple injections are a good way to study pharmacokinetics or assess the effect of a drug on inner ear cells, there is still a possibility of cochlear fluid leakage that can wash the drug solution, meaning that the drug concentrations are difficult to keep constant[76].

Similar to microcatheters that were already described above for intratympanic administration, osmotic pumps are another mean to ensure a better control over the drug concentration compared to a simple injection. They are implanted subcutaneously with a medial and a lateral tunnel connected by a groove in the posterior wall of the bony ear canal, then stabilized with bone wax and soft tissue plugs. Those systems grant constant drug delivery for days up to weeks, and thanks to their use of osmotic pressure, the delivery rates are low but permanent[77]. Horiike et al. showed that the administration of edaravone using an osmotic pump had a better suppression of streptomycin-induced vestibulotoxicity in guinea pigs compared to systemic administration[78]. Shimogori et al. evaluated the effect of betamethasone on the vestibular function in a guinea pig model of peripheral vestibular disorder. The right lateral semicircular canal was surgically damaged, and after surgery, animals were treated with various concentrations of betamethasone or saline solutions, which were administrated directly into the scala tympani by an osmotic pump. Rotation tests were performed, and the post-rotatory nystagmus (PRN) ratio (PRN number after counterclockwise rotation/PRN number after clockwise rotation) was calculated. The PRN ratio was recovered to normal at 5 days after treatment in the betamethasone administrated groups, but it did not recover to normal until 14 days after treatment in the saline administrated group. Those results also show that steroid hormones may play an important role in the recovery of vestibular functions[79].

Reciprocating perfusion systems combine microsystems and microfluidics technologies to create new drug delivery devices that are able to provide drugs to the inner ear more precisely[70]. For that matter Sewell et al. developed a microfluidics-based intracochlear drug delivery device. Briefly, drugs are stored in a concentrated stabilized form, and introduced into

the perilymph under microprocessor control by a miniaturized low-power high-precision micropump. The micropump is infusing and withdrawing inner ear fluids in a cyclic manner nearly simultaneously so that the volume inside the cochlea stays constant[80]. The system uses a reciprocating fluid delivery regimen to deliver drugs through a single cannula acting as both inlet and outlet. A glutamate receptor blocker, 6,7-dinitroquinoxaline-2,3-dione (DNQX), was administered to guinea pigs using this system. Drug delivery in the scala tympani was proven to be safe and effective. Moreover, equilibration of the drug in the basal turn occurred rapidly (within tens of minutes) and was dependent on reciprocating flow parameters[81].

Encapsulated cells (EC) are devices that have been clinically tested for the treatment of neurodegenerative diseases[82]. The EC device consists of a semipermeable membrane enclosing genetically modified human cells that release neurotrophic factors. Recently, Fransson et al. explored the feasibility of using this device for the treatment of hearing loss. The effects of BDNF releasing device implanted in deafened guinea pigs were investigated for four weeks, and results showed that the treatment significantly preserved the spiral ganglion neurons and maintained their electrical responsiveness[83].

Nanotechnology can also be used for intracochlear delivery. Wang et al. developed a new drug carrier system that uses mesoporous silica nanoparticles as a building block to form larger (~ 500 μm) supraparticles. Mesoporous particle-based therapeutic carriers have attracted considerable interest given their ability to provide a number of advantages in drug delivery such as high surface area, facile surface chemistry modification, adjustable pore sizes, tunable particle sizes, excellent biocompatibility, as well as the ability to protect the drug from endogenous proteases that cause degradation of the drug molecule. The studied supraparticles were found to have high payloads of brain-derived neurotrophic factor (BDNF) and could be surgically implanted into the cochlea of the guinea pig for neuronal rescue[84]. Wise et al. recently investigated the safety and efficacy of these nano-engineered silica

supraparticles. The supraparticles were bilaterally implanted into the basal turn of the cochlea in profoundly deafened guinea pigs. BDNF was delivered over a period of 4 weeks and spiral ganglion neurons survival was observed over a wide extent of the cochlea. Only a mild localized tissue response was observed at the site of implantation[85].

Cochlear prosthesis-mediated drug delivery is another interesting technique to achieve intracochlear administration, in which we will expand later on (chapter 1.6 Drug-eluting cochlear implants).

Table 1.6. Summary of intracochlear methods for the treatment of idiopathic SSNHL.

Study	Treatment method	Result
Kawamoto et al, 2001	Intracochlear injection	Intracochlear injection with adenovirus into did not compromise either hair cell counts or ABR thresholds
Horiike et al, 2004	Osmotic pump vs systemic administration	Administration of edaravone using an osmotic pump had a better suppression of streptomycin-induced vestibulotoxicity in guinea pigs compared to systemic administration
Shigomori et al, 2000	Osmotic pump vs saline solution	The PRN ratio was recovered to normal at 5 days after treatment in the betamethasone administrated groups, compared to 14 days in the saline groups
Sewell et al, 2009	Microfluidics	DNQX delivery in the scala tympani was proven to be safe and effective
Fransson et al, 2018	Encapsulated cells	BDNF treatment significantly preserved the spiral ganglion neurons and maintained their electrical responsiveness.
Wise et al, 2016	Mesoporous silica supraparticles	BDNF was delivered over a period of 4 weeks and spiral ganglion neurons survival was observed over a wide extent of the cochlea. Only a mild localized tissue response was observed at the site of implantation.

Depending on the intended treatment, both intratympanic and intracochlear administrations have various benefits and drawbacks that can be summarized below (table 1.7):

Table 1.7. Comparison between intratympanic and intracochlear administration: benefits and limitations, adapted from [6]

	Intratympanic administration	Intracochlear administration
Benefits	- Treatment of middle and inner ear diseases - Minimized systemic exposure - Short and middle term local drug delivery (several days to weeks) - Minimally invasive - Usually outpatient procedure - Adapted for nanocarriers, hydrogels and medical devices	- Treatment of inner ear diseases - Minimized systemic exposure - Long term local drug delivery (several months to years) - Avoids the diffusion through the round window, direct access to the cochlea - Adapted for nanocarriers, liquid formulations and medical devices - Drugs can be delivered along with a cochlear implant
Limitations	- Require diffusion through the round window for access to the cochlea - High inter-individual variability - Clearance through the Eustachian tube - Risk of introducing pathogens in the middle ear - Risk of tympanic membrane perforation	- Invasive - Requires hospitalization - Potential toxicity of a high drug concentration in the cochlea - Risk of introducing pathogens in the inner ear

Local drug delivery to the inner ear progressed rapidly in the last decade, as many systems were developed[6,80], showing great promise for the treatment of inner ear specific diseases. However, while they offer many benefits in case of emergencies (i.e, sudden sensorineural hearing loss) and for the protection of hair cells in the cochlea, they are not the first line of treatment for patients with **severe to profound hearing loss**. In this particular form, the impairment is best managed with the use of hearing aids, or cochlear implants for the most severe cases[86].

1.5 Hearing aids and cochlear implants

Hearing aids are electronic devices designed to improve hearing by making sounds more audible. A hearing aid has three basic parts: a microphone, amplifier, and speaker. The hearing aid receives sound through a microphone, which converts the sound waves to electrical signals and sends them to an amplifier. The amplifier increases the power of the signals and then sends them to the ear through a speaker.

We can distinguish between two major classes: Behind the ear (BTE) and In the ear (ITE) hearing aids (figure 1.10). BTE hearing aids consist of a hard-plastic case worn behind the ear and connected to a plastic earmold that fits inside the outer ear. The electronic parts are held in the case behind the ear. Sound travels from the hearing aid through the earmold and into the ear. ITE hearing aids fit completely inside the outer ear. Some ITE aids may have certain added features installed, such as a telecoil. A telecoil is a small magnetic coil that allows users to receive sound through the circuitry of the hearing aid, rather than through its microphone. This makes it easier to hear conversations over the telephone.[87]

Figure 1.10. The two major classes of hearing aids: Behind the ear (left) and In the ear (right), adapted from [87]

Cochlear implants (CI) are surgically implanted neuroprosthetic devices (figure 1.11). CI bypasses the normal acoustic hearing process to replace it with electric signals which directly stimulate the auditory nerve[88].

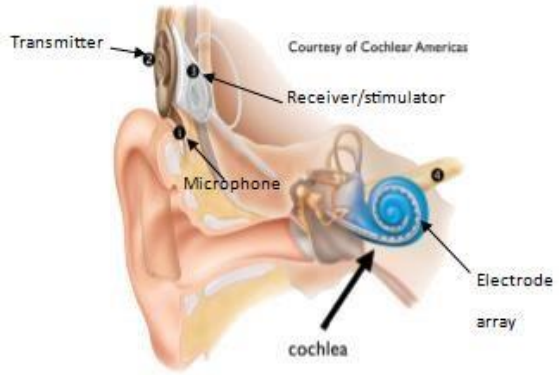

Figure 1.11. Main components of a cochlear implant inserted in a human ear: external parts comprises (1) microphone and (2) transmitter, internal parts comprises (3) receiver/stimulator and (4) electrode array inside the cochlea, adapted from[89]

The implant has two main components: An external part with one or more microphones that pick up sound from the environment, a speech processor which selectively filters sound to prioritize audible speech, and a transmitter that sends the processed sound signals across the skin to the internal device by radio frequency transmission. The internal part starts with a receiver/stimulator, which receives the radio transmission and converts it into electric impulses, those impulses are finally sent to an electrode array embedded in the cochlea[89].

The electrode array is inserted in the cochlea with a surgical procedure that is performed under general anaesthesia. There is considerable interest in the preservation of residual hearing during cochlear implantation, given the recently demonstrated auditory benefits of electric acoustic stimulation. However, due to the **highly invasive nature of the surgery**, the subsequent trauma may cause a significant and immediate loss of hearing, or a delayed one which may occur days to months after implantation[90,91].

Despite its very good results in children and adults in auditory rehabilitation, cochlear implantation is responsible for cell destruction in both internal hair cells, external hair cells, and spiral ganglion cells[92,93]. The **inflammatory response** induces fibrosis and endocochlear neo-

osteogenesis[94,95], with the extent of this fibrosis being correlated to the loss of residual hearing[96,97]. Apoptosis of auditory neurons as a consequence of **oxidative stress** was also observed[98]. It has been shown that the increase in impedance (electrical resistance) is correlated with the importance of the fibrotic reaction around the implant[99]. The increase in impedance create the need to increase the intensity of the electrical stimulus to maintain good performances, which in the end is deleterious to the cochlear structures[100,101].

The current problem of cochlear implantation is therefore to preserve the cochlear structure and residual neurosensory cells as much as possible in order to improve the performance and longevity of these implants. Several measures have already been developed to reduce surgical trauma, including lubricants[102], intraoperative systemic corticosteroid therapy[103], preoperative intra-tympanic corticosteroid therapy[104] and optimization of the insertion axis of the electrode holder[105].

The administration of drugs via the electrode holder, using the implant itself as the vector for pharmacological therapy is currently one of the most attractive ways of reducing the undesirable tissue and cellular effects linked to implant trauma. We will focus on this topic for the next chapter.

1.6 Drug eluting cochlear implants

Figure 1.12. Macroscopic image of an intracochlear electrode implant embedded in a silicone matrix loaded with dexamethasone, adapted from [54]

As seen earlier, intracochlear administration is one of the two main strategies for local drug delivery to the inner ear. While injections or the use of micropumps are one way to achieve this administration, cochlear implants constitutes another vector in which drugs can be introduced to the inner ear[106,107] . There are many benefits in using this technique, first, the inserted electrode is usually coiled up all the way inside the snail-like structure of the cochlea, meaning that the area available for drug release is highly optimised. The second reason comes from the very material constituting the implant: a polymeric network, generally a **silicone matrix** (figure 1.12). Silicone matrices are ideal for trapping drugs, given that they are generally hydrophobic and limit water penetration into their system[108]. This offers the opportunity to accurately control the release rate of drugs, and by adjusting the formulation parameters (silicone type, amount of additives or drug loading), it is even possible to make the release last for months or years[6,25]. This capacity is vital when addressing cochlear implants, as they are destined to stay in the patient's ears for many years following surgery[109,110]. Ensuring long release periods can help control the inflammatory response, thus granting patients long-lasting advantages.

This idea was already put to use for others hard to reach sites in the human body, for example the eye[111], heart[112] or vagina[113]. There are also several commercialized products with drug-eluting matrix systems[114,115]. Interestingly, a double-bind human study even showed that implanted dexamethasone-eluting electrodes in pacemakers could release dexamethasone for over 10 years, resulting in better thresholds values compared to drug-free systems. According to the authors, 20 % of the dexamethasone was still present after 10 years, meaning that the drug could still be released for many more years[112].

Drug-eluting matrix systems for the inner ear were also extensively studied in the last decade. Farahmand Ghavi et al. explored the effect of matrix crosslinking and drug loading on the release profiles of dexamethasone[91]. Farhadi et al. evaluated the effect of dexamethasone-

eluting electrodes on the inflammatory response of implanted guinea pigs, thus showing significant reduction in fibrocyte, macrophage, and giant cell infiltration at day 3 as well as lymphocyte, macrophage infiltration, and capillary formation at day 13, indicating an attenuation of the inflammatory response in the presence of dexamethasone[116]. Meanwhile, Douchement et al. showed that electrode arrays with prolonged release of dexamethasone improved short-term preservation of residual hearing after implantation for the frequencies 500, 1000, 4000, and 16 000 Hz in gerbils. The long-term results at 1 year also confirmed these data for higher frequencies[117].

While very promising, the development of such devices is made difficult by their very own advantage: **long release periods**.

As seen earlier, varying formulation parameters is essential to adjust desired drug release kinetics. However, given the long period of time drugs need to be fully released, said optimization can quickly become cumbersome, since very little information is available in a *quantitative* way[118], unless highly time-consuming and cost-intensive series of trail-and-error experiments are made. Fortunately, some research teams took interest in the use of **mathematical modelling** to predict drug delivery. In silico optimization can help reach good estimates for composition, geometry, dimensions and preparation procedures for various drug delivery systems, thus significantly reducing the number of experiments needed for product development[119,120].

Siepmann and Siepmann made an extensive review on the current state of the art of mathematical modelling of drug delivery, including empirical/semi-empirical and mechanistic realistic models. More or less complex mathematical theories can be used to quantify the involved mass transport processes and describe drug release from polymeric systems (figure 1.13)[121].

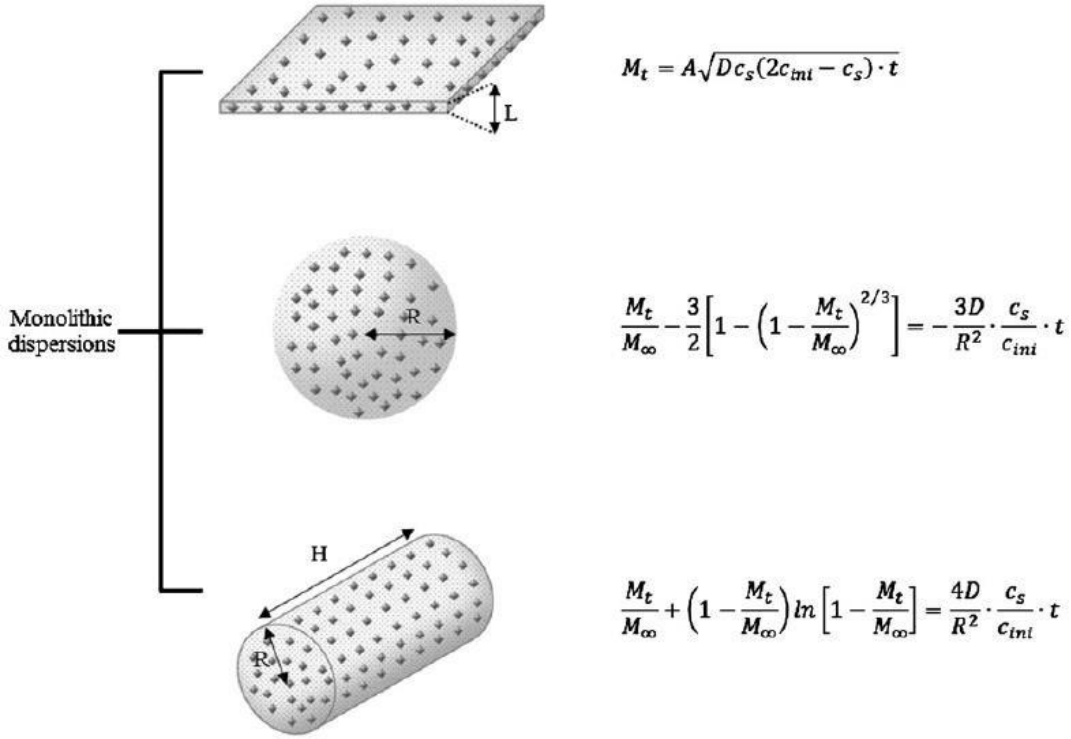

Figure 1.13. Overview on the mathematical equations, which can be used to quantify drug release from monolithic dispersions (initial drug concentration > drug solubility) in slab, sphere and cylinder geometries. M_t and M_∞ denote the cumulative amounts of drug released at time t and at infinite time, respectively; D is the diffusion coefficient of the drug within the system; c_s denotes the drug solubility in the wetted matrix (not in the release medium); c_{ini} represents the initial drug concentration in the system. A is the total surface area of the film exposed to the release medium, R the radius of the sphere or the cylinder, adapted from [121]

More specifically to the inner ear, Krenzlin et al. studied the **predictability** of dexamethasone release from cochlear implants by using a mathematical equation based on Fick's second law of diffusion. After determining the diffusion coefficient of dexamethasone within the matrix via drug release measurements from thin, macroscopic films. The validity of the theoretical model predictions was evaluated by comparison with experimental results obtained with a cochlear implant. The latter consisted of miniaturized electrodes, which were embedded in a silicone matrix loaded with various amounts of dexamethasone[122].

This simplified model helped predict the drug release kinetics from miniaturized electrodes, allowing Gehrke et al. to expand on a quantitative analysis. Dexamethasone was incorporated into thin films based on different types of silicones (e.g. varying in the type of side chains and contents of amorphous silica), optionally containing different types and amounts of poly(ethylene glycol) (PEG) (5 % or 10 %). Furthermore, the initial drug content was altered (from 10 % to 50 %). In most cases, an analytical solution of Fick's second law could be used to describe the resulting drug release kinetics from the films and to determine the respective "apparent" diffusion coefficient of the drug (which varied from 2×10^{-14} to 2×10^{-12} $cm^{2/s}$, depending on the system's composition). The knowledge of the "apparent" drug diffusivity can be used to theoretically predict the resulting release kinetics from dosage forms of arbitrary size and shape. For instance, dexamethasone release was theoretically predicted from cylindrical extrudates based on a selection of different silicone types. These predictions could be confirmed by independent experiments, and thus, the impact of the investigated formulation parameters could be **quantitatively described.**[118]

1.7 Objectives

The main objectives of this thesis were to further expand on the works of Krenzlin et al. and Gehrke et al. for a better understanding of dexamethasone-eluting cochlear implants through new means of characterization, and by optimizing the formulation parameters by adding various drugs to complement the therapeutic effect of dexamethasone.

1) Long-term in vitro release of dexamethasone-loaded cochlear implants:

By the start of this thesis, dexamethasone release could be predicted using Fick's second law of diffusion, but so far, the independent experiments used to confirm our theory would only last for a few months. Now that the most promising silicone and drug loading rates were selected, the decision was made to study the in vitro release of dexamethasone-loaded cochlear implants for as long as possible (i.e, many years).

2) Development and characterization of silicone matrices combining dexamethasone and dexamethasone phosphate:

Silicone matrices loaded with dexamethasone were shown to be able to provide continuous release over several months/years, but it has to be pointed out that the anti-inflammatory action of the drug is particularly vital during the first few days after implant placement. In order to minimize the consequences of the induced trauma at these early time points, it may be a good idea to boost the drug release during this crucial period.

Dexamethasone's low solubility in water (89 mg/L)[123] is one of the main reasons why it can release so slowly, so having an anti-inflammatory drug that exhibits a higher solubility could grant us the possibility of a faster release at early time points. Dexamethasone phosphate proved to be the most likely candidate, since it is a highly hydrophilic form of dexamethasone with tremendous solubility values (1.52 g/L)[124].

It was theorized that with the addition of dexamethasone phosphate, the water uptake would be higher inside the silicone matrices, solubilizing the drug crystals faster, and providing

a burst release that can help us achieve elevated anti-inflammatory concentrations for the first days after surgery, thus complementing the slow and continuous release of dexamethasone.

2. Materials and methods

2.1. Materials

Kits for the preparation of silicone elastomers (MED-4735; NuSil Technology, Carpinteria, USA); dexamethasone and dexamethasone sodium phosphate (dexamethasone phosphate) (Discovery Fine Chemicals, Dorset, UK); calcium chloride dihydrate, magnesium sulfate tetrahydrate, potassium chloride, sodium chloride and 4-(2-hydroxyethyl) piperazine-1-ethanesulfonic acid (HEPES) (HEPES Pufferan; Carl Roth, Lauterbourg, France); acetonitrile (HPLC grade; Fisher Scientific, Illkirch, France); MilliQ water (obtained with a Millipore Integral 5 apparatus; Millipore Corporation, Billerica, USA). The dexamethasone sodium phosphate powder was used as received, or (if indicated) milled as follows: 1 g drug was milled in a stainless-steel jar with a stainless-steel ball for 3 min at 30 Hz (Retsch MM400; Retsch, Haan, Germany).

2.2. Preparation of drug loaded films

Equal amounts of MED-4735 Parts A and B (approximately 5 g each) were passed separately 10 times through a two-roll mill (Chef Premier KMC 560/AT970A; Kenwood, Havant, UK). To initiate polymer crosslinking, both parts were manually blended and the mixture was passed 10 times through the mill. Subsequently, appropriate amounts of dexamethasone powder (as received) and/or dexamethasone sodium phosphate powder (as received or milled) were added and the mixture was passed another 40 times through the mill to obtain a homogenous film. Crosslinking was completed by a thermal treatment in an oven at 60 °C for 24 h. The thickness of the resulting films was determined with a micrometer gauge (Digimatic Micrometer; Mitutoyo, Tokyo, Japan).

2.3. Preparation of drug loaded cochlear implants

Blends of MED-4735 Parts A & B and dexamethasone/dexamethasone sodium phosphate were prepared as described in Section 2.2. Preparation of drug loaded films. The obtained mass was injected into a stainless-steel mold, containing glued iridium platinum electrode contacts with wires (Oticon Medical, Vallauris, France). The implant dimensions were suitable for use in humans (Krenzlin et al.). The mold was placed under a hydraulic press at 4.5 bars and heated to 110 °C for 10 min. Ethanol (96% v/v) was injected into the mold in order to dissolve the glue and allow for implant removal.

2.4. Scanning Electron Microscopy (SEM)

SEM pictures of drug powders were obtained with a JEOL Field Emission Scanning Electron Microscope (JSM-7800F, Tokyo, Japan). Samples were fixed with a ribbon carbon double-sided adhesive and covered with a fine chrome layer.

2.5. X-ray diffraction

A Panalytical X'pert Pro diffractometer (PANalytical, Almelo, Netherlands) in transmission mode with an incident beam parabolic mirror (λ Cu, Kα = 1.54 Å) was used to record X-ray diffraction patterns. The samples were placed inside Lindemann glass capillaries (diameter 1 mm; Hilgenberg, Malsfeld, Germany), which were fixed on a spinning sample holder.

2.6. Drug release measurements

2.6.1. From thin films

Film pieces (1 × 1 cm) were placed into amber glass flasks containing 10 mL (if not otherwise stated) artificial perilymph: an aqueous solution of 1.2 mmol calcium chloride dihydrate, 2 mmol magnesium sulfate tetrahydrate, 2.7 mmol potassium chloride, 145 mmol sodium chloride and 5 mmol HEPES Pufferan. The flasks were horizontally shaken in an incubator (80 rpm; GFL 3033; Gesellschaft fuer Labortechnik, Burgwedel, Germany) at 37 °C. At predetermined time points, 1 mL samples were withdrawn and replaced with fresh artificial perilymph (unless otherwise stated). The drug concentration in the withdrawn samples was determined by HPLC analysis using an Alliance e2695 apparatus (Waters Division, Milford, USA), equipped with an UV detector. Samples (50 μL) were injected into a reverse phase column C18 (Gemini 3 μm, 110 Å, 100 × 4.6 mm, Phenomenex, Le Pecq, France) (mobile phase = acetonitrile:water 33:67 V:V, flow rate = 1.2 mL/min). Dexamethasone and dexamethasone sodium phosphate were detected at λ = 220 nm. If indicated, the release medium was completely renewed every day or every week.

2.6.2. From cochlear implants

Implants were placed into 2 mL HPLC glass vials (Screw-top amber glass; Sigma Aldrich, St. Quentin Fallavier, France) containing 0.2 mL inserts and 70 μL artificial perilymph. The vials were horizontally shaken at 80 rpm (37 °C, GFL 3033). At predetermined time points, the release medium was completely renewed. The drug content in the samples was determined as described for the thin films. Each experiment was performed in triplicate, mean values +/− standard deviations are reported.

2.7. Monitoring of system swelling

Thin films and cochlear implants were treated as for the in vitro drug release measurements described in Section 2.6. Drug release measurements.

2.7.1. Thin films

Dynamic changes in the thickness and wet mass of the films upon exposure to artificial perilymph were measured using a micrometer gauge and a precision balance (Precisa 120A; Precisa, Dietikon, Switzerland). Measurements were performed before and after exposure to the release medium. At predetermined time points, film samples were withdrawn, surface water was carefully removed using Kimtech tissue paper (Kimberly-Clark, Reigate, UK), and the films' thickness and wet mass were determined.

2.7.2. Cochlear implants

Dynamic changes in the dimensions of the cochlear implants upon exposure to artificial perilymph were monitored using a Nikon Eclipse SMZ-U microscope, equipped with an AxioCam ICc 1 Zeiss camera (Zeiss, Oberkochen, Germany). At predetermined time points, samples were withdrawn and analyzed.

2.8. Drug stability in aqueous media

About 5 mg dexamethasone or dexamethasone sodium phosphate (as indicated) were dissolved in 100 mL MilliQ water, artificial perilymph, or aqueous solutions of either 1.2 mmol calcium chloride, 2 mmol magnesium sulfate tetrahydrate, 2.7 mmol potassium chloride, 145

mmol sodium chloride or 5 mmol HEPES. The samples were placed in a horizontal shaker at 37 °C (80 rpm; GFL 3033). At predetermined time points, 100 μL samples were withdrawn and their drug content was determined by HPLC-UV analysis, as described in Section 2.6. Drug release measurements.

2.9. Raman imaging

Implants were analyzed using a Renishaw InVia Raman spectrometer, coupled to a Leica microscope. The 785 nm line emitted from a Renishaw laser diode was focused via an x50 long working distance Leica objective. Under these conditions, ~ 200 μm^3 volumes were analyzed within the samples at each XY position. The spectral resolution was about 2 cm^{-1} in the investigated spectral window (500 – 1000 cm^{-1}). Raman mapping was performed by scanning 100 x 100 μm^2 up to 500 x 500 μm^2 areas, using the classical sequential (point by point) method (from 1 μm up to 5 μm between points). During Raman mapping, 600 up to 10000 spectra were collected with an acquisition time ranging between 1 s up to 3 s. Raman images were calculated using the DCLS (Direct Classical Least Square) method, fitting each spectrum to a linear combination of Raman spectra of the sample components.

2.10. In vivo study

Cochlear implants (initially drug-free or loaded with 1 or 10 % dexamethasone) were inserted into the inner ears of Mongolian gerbils. The systems were explanted after 1 or 24 months (as indicated), cut with a scalpel and analyzed by Raman imaging. All French and European requirements for animal studies were fulfilled and the authorization of a local ethics committee obtained.

2.11. Differential Scanning Calorimetry (DSC)

DSC thermograms were recorded with a DSC Q10 (TA Instruments, Guyancourt, France) using a heating rate of 5°C/min. During all measurements the calorimeter head was flushed with highly pure nitrogen gas. Temperature and enthalpy readings were calibrated at 5°C/min using pure indium. The samples were placed in closed aluminium pans.

3. Results and discussion
3.1 Accelerating drug release at early time points
3.1.1 Introduction

The aim of this study was to increase the initial “burst release” (drug release during the first days/weeks) from silicone-based cochlear implants allowing for controlled dexamethasone release for several years. The strategy was to add freely water-soluble dexamethasone sodium phosphate (“dexamethasone phosphate”), rendering the systems more hydrophilic and, thus, facilitating water penetration into the polymeric matrices. Increased water contents can be expected to accelerate drug dissolution and diffusion out of the implants. The chemical structures of dexamethasone and dexamethasone phosphate are illustrated at the top of Figure 3.1. At the bottom, SEM pictures of the drug powder raw materials (as received) are shown. Since the manufacturing and characterization of miniaturized cochlear implants is not straightforward, experiments were also conducted with macroscopic films of identical composition as the polymeric matrices separating the metal electrodes (and controlling drug release).

Dexamethasone (Dex) **Dexamethasone phosphate (Dex-P)**

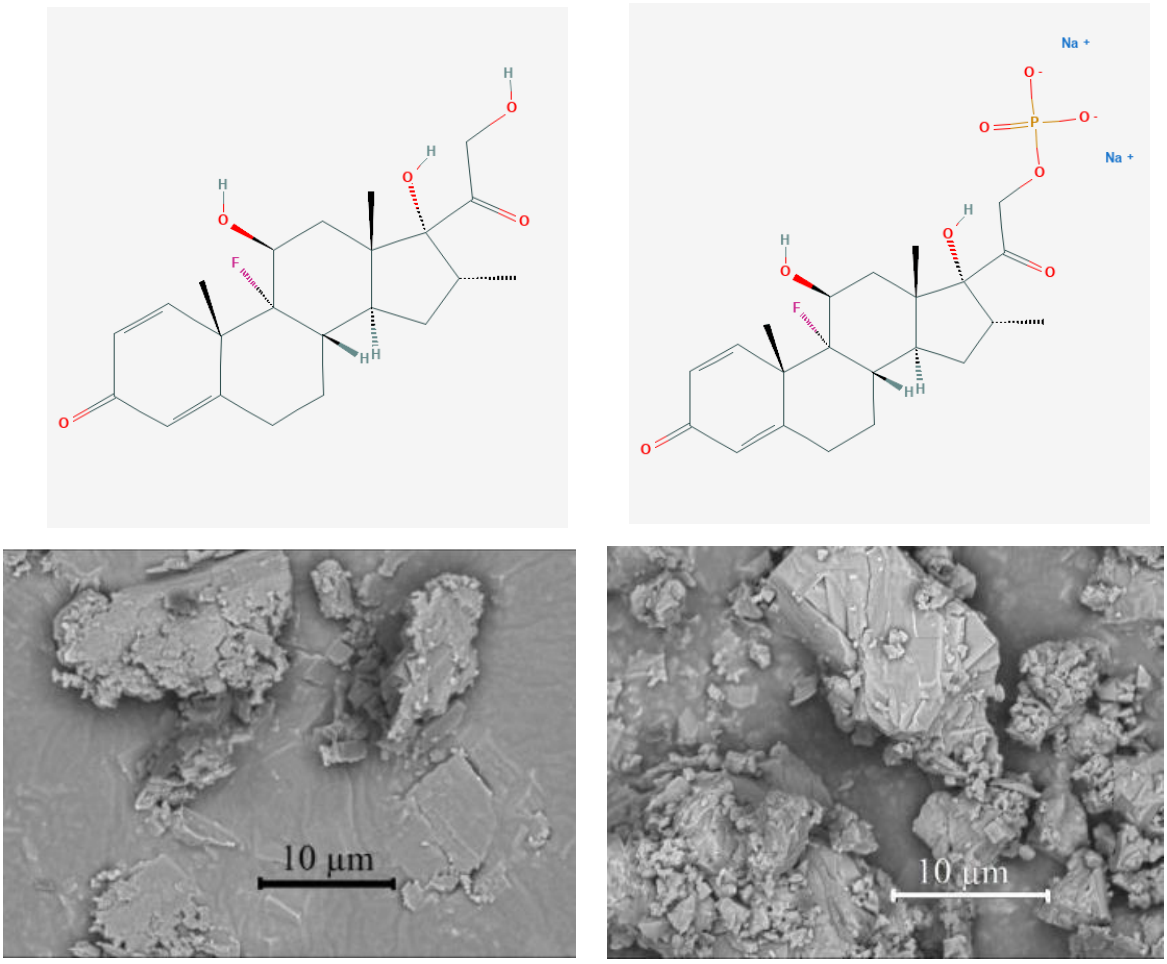

Figure 3.1. Chemical structures and SEM pictures of dexamethasone and dexamethasone phosphate powders (as received). Source of the chemical structures: PubChem [Internet][123,124].

3.1.2 Thin polymeric films

The optical macroscopy picture at the top of Figure 3.2 shows a thin silicone film loaded with 1% w/w dexamethasone phosphate, which was prepared with drug powder as received. As it can be seen, large white transparent). This can be explained by the hydrophilic character of the dexamethasone phosphate and the hydrophobic nature of the polymer: The 2 phases “do not like each other” and drug particle agglomeration reduces the surface of the interface. In the case of the less hydrophilic parent drug dexamethasone, it has previously been reported that the drug was homogeneously distributed within the same silicone matrix, in the form of tiny crystals using a similar preparation procedure[122] (dexamethasone being less hydrophilic). In order to provide a more homogenous drug particle distribution within the polymeric system also for dexamethasone phosphate, the latter was milled for different time periods prior to incorporation into the silicone matrix. The idea was to start with smaller particles, eventually allowing to end up with smaller agglomerates. Optical macroscopy pictures of the obtained films are shown in the middle and at the bottom of Figure 3.2.

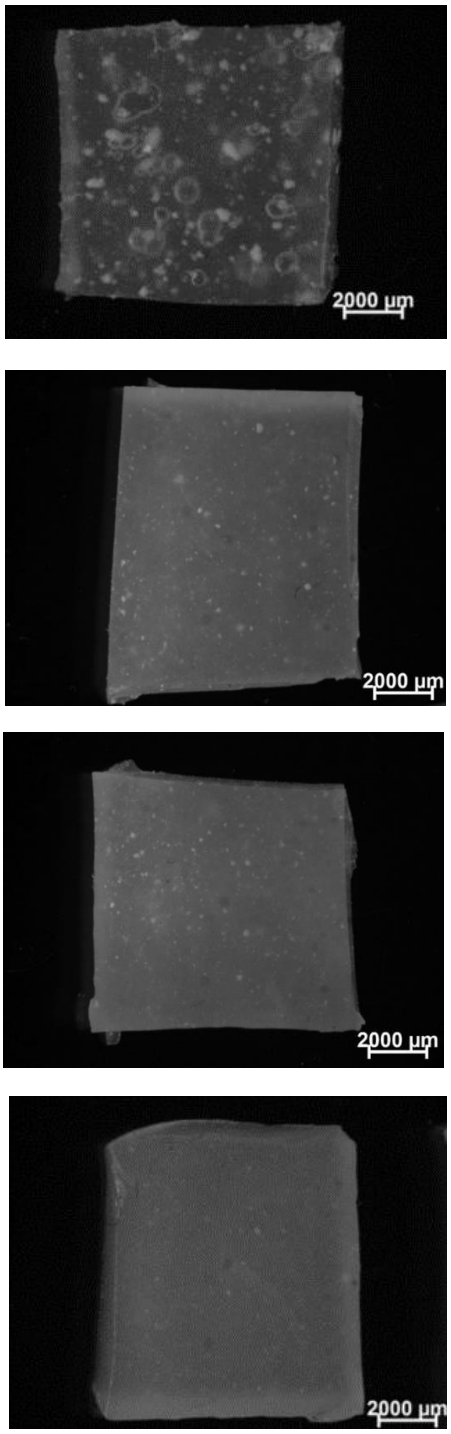

no milling

30 s milling

1 min milling

3 min milling

Figure 3.2. Macroscopic pictures of silicone films loaded with 1 % w/w dexamethasone phosphate. The drug powder was optionally milled for different time periods before incorporation into the silicone (as indicated).

Clearly, the formation of large drug agglomerates could be substantially reduced by the milling step: With increasing milling time, the number and size of visible agglomerates decreased. Since milling can induce changes in the solid state of a drug (e.g., one polymorphic form might be transformed into another, or a crystalline drug might become amorphous), X-ray diffraction patterns of the milled and non-milled powders were recorded. As it can be seen in Figure 3.3, no differences were visible: The drug remained crystalline, and kept its polymorphic form.

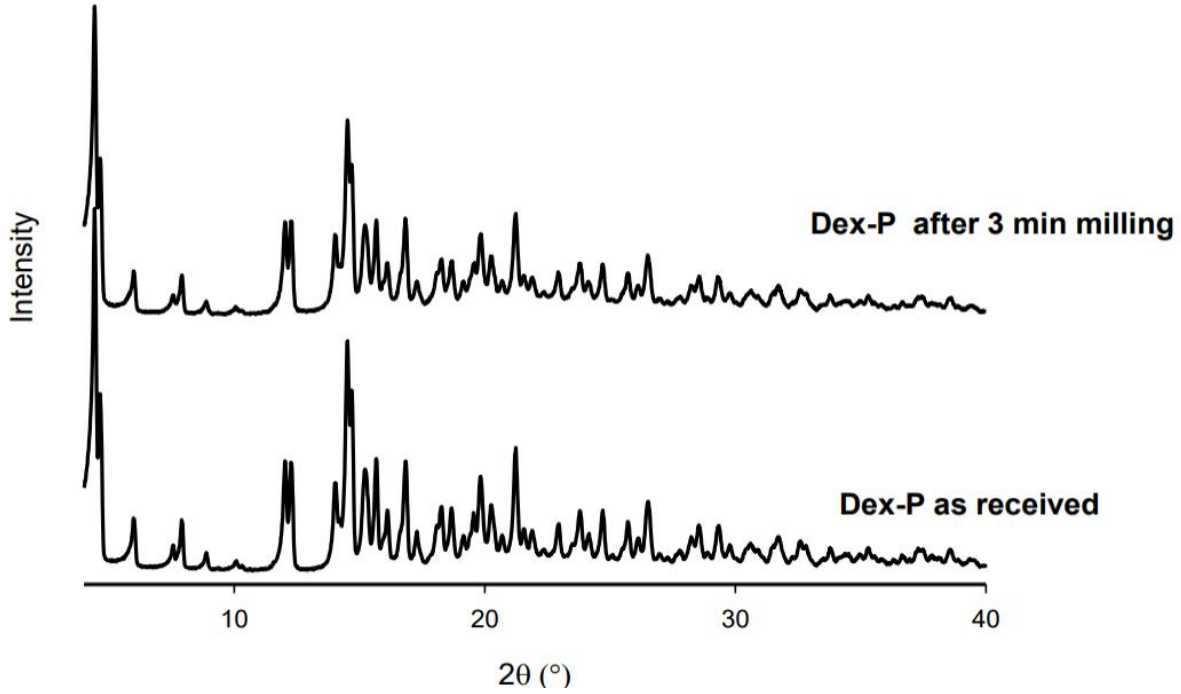

Figure 3.3. X-ray diffraction patterns of dexamethasone phosphate powder: as received and after 3 min milling.

The effects of drug milling for up to 3 min on the resulting drug release kinetics from thin silicone films loaded with 1% dexamethasone phosphate are shown in Figure 3.4. Sink conditions were provided throughout the experiments. As it can be seen, in the case of non-

milled drug powder: (i) the burst release was much more pronounced, and (ii) the standard deviations were much higher. This can be explained by the fact that the initial burst release is likely attributable to drug particles (and agglomerates of thereof), which are located close to the film surface and have either direct access to the latter from the beginning, or have/get rapidly access via small pores. Looking at the optical macroscopy pictures in Figure 3.2, it becomes clear that in the case of nonmilled dexamethasone phosphate powder, the access of a large particle agglomerate to the surface likely causes a relative important amount of drug to be released at early time points, compared to a much smaller drug particle having/getting such an access in the case of films prepared with pre-milled powder. Also, the likelihood that a large drug particle agglomerate has/gets direct surface access is higher than in the case of a tiny drug particle, if both are located in the same zone close to the surface (due to its larger dimensions). This overcompensates the higher number of numerous small particles compared to few larger particle agglomerates. The difference in the spatial drug distribution within films prepared with non-milled versus milled dexamethasone phosphate powder (Figure 3.2) can also explain the difference in the variability of drug release (Figure 3.4): The observed drug release rate is the sum of all the individual release events stemming from the dissolution of drug particles or agglomerates which are/get in contact with the surface (and hence, with the bulk fluid). In the case of large drug particle agglomerates, each of these individual events is relatively important. In contrast, in the case of numerous tiny drug particles, each individual "release event" is relatively less important. Since all these events are random, the variability of the sum is higher in the case of fewer events related to the large agglomerates compared to numerous small events associated with tiny drug particles. In practice, a reduced variability is highly desirable to assure more reliable therapeutic effects and a limited risk of potential toxic side effects. Thus, a milling time of 3 min was chosen for further experiments.

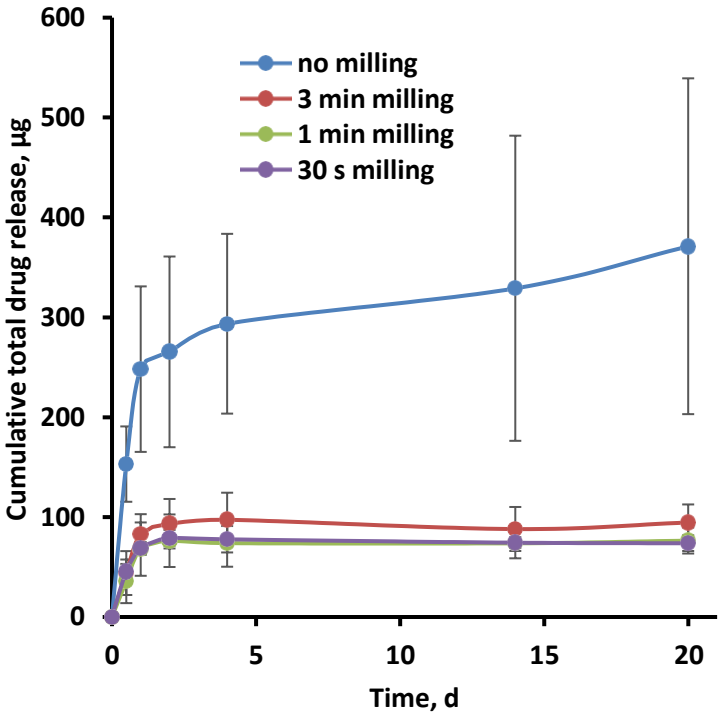

Figure 3.4. Cumulative absolute total drug release from silicone films loaded with 1 % dexamethasone phosphate upon exposure to artificial perilymph at 37 °C. The drug powder was optionally milled before incorporation into the silicone (as indicated).

3.1.3. Conversion of dexamethasone phosphate into dexamethasone

Please note that the absolute cumulative drug release curves shown in Figure 3.4 encompass both: the prodrug dexamethasone phosphate as well as the parent drug dexamethasone (generated by the hydrolysis of dexamethasone phosphate upon contact with water). Both species were detected in the release medium (by HPLC-UV analysis) and considered for the calculation of the "total drug release". To estimate the conversion rate of dexamethasone phosphate into dexamethasone under the given conditions, a solution of this drug in artificial perilymph was studied at 37 °C under horizontal shaking (80 rpm) (under the same conditions as for the in vitro drug release measurements). For reasons of comparison, the stability of dexamethasone phosphate was also monitored in pure water (MilliQ) and aqueous

solutions of the different components of the artificial perilymph: 145 mmol sodium chloride, 1.2 mmol calcium chloride, 5 mmol HEPES, 2 mmol magnesium sulfate tetrahydrate, or 2.7 mmol potassium chloride. Figure 3.5 shows the obtained results. About 5 mg drug were dissolved in 100 mL medium. The blue curve in the diagram at the top shows the degradation kinetics of dexamethasone phosphate in artificial perilymph. Clearly, the ester is relatively rapidly hydrolyzed. The brown curve in the same diagram shows the respective dexamethasone phosphate degradation in pure water: As it can be seen, in the latter case the ester hydrolysis is much slower. Thus, the presence of the co-dissolved salts in the artificial perilymph has an impact on the hydrolysis of the phosphate ester. The diagram in the middle of Figure 3.5 differentiates between the impact of the different types of salts. The following rank order was observed with respect to the acceleration of dexamethasone phosphate degradation: NaCl < CaCl2 < HEPES < MgSO4 < KCl. For reasons of comparison, also the stability of the parent drug dexamethasone dissolved in artificial perilymph at 37 °C was studied (bottom diagram in Figure 3.5): There were no signs for any noteworthy degradation during the observation period (1 month).

Please note that in the case of controlled release silicone films or cochlear implants, the conversion of dexamethasone phosphate into dexamethasone can occur within the well-agitated bulk fluid (after the release of the prodrug), or within the drug delivery system (once water has reached the drug). It was beyond the scope of this work to study this aspect in more detail. For the therapeutic effects, most important is the conversion rate, not the location of this conversion.

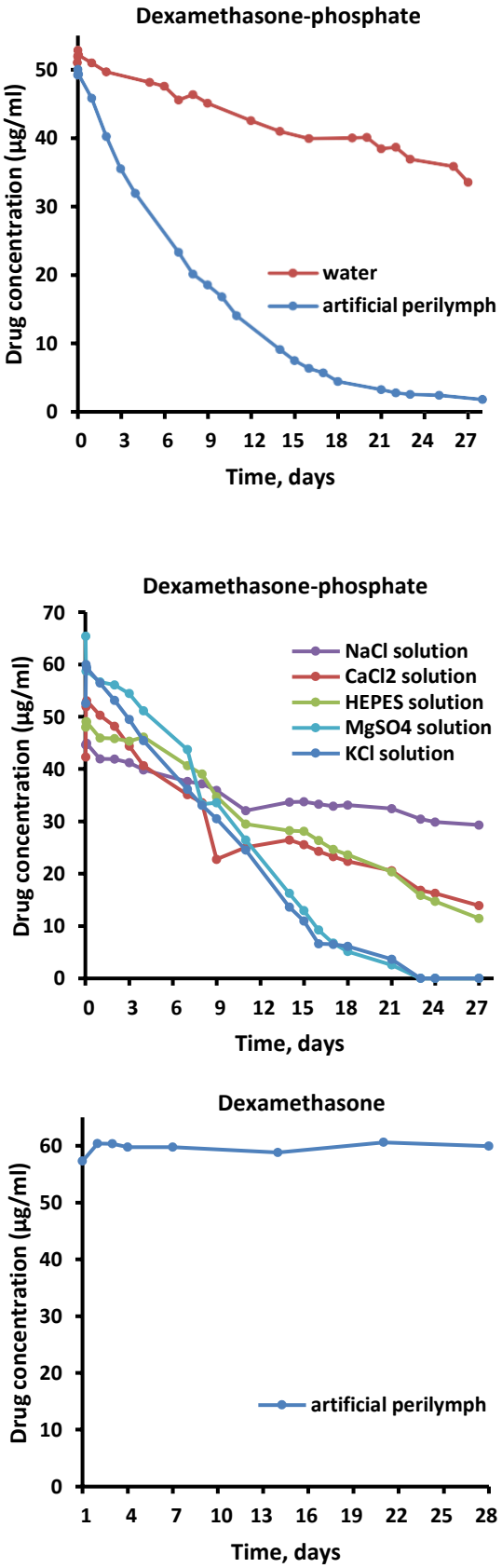

Figure 3.5. Stability of dexamethasone or dexamethasone phosphate in artificial perilymph, pure water or different types of aqueous salt solutions (as indicated) at 37 °C.

Figure 3.6 shows the HPLC chromatograms of samples of release medium withdrawn after 2 h or 11 days exposure of thin silicone films loaded with 11% dexamethasone phosphate to artificial perilymph at 37 °C (80 rpm). As it can be seen, after 2 h, only dexamethasone phosphate was detected, no dexamethasone. In contrast, after 11 days, a dexamethasone peak was clearly visible in addition to the dexamethasone phosphate peak. Please note that: (i) The dexamethasone phosphate peak was much larger than the dexamethasone peak after 11 days in the HPLC chromatogram, which was obtained during the drug release measurements from thin silicone films (Figure 3.6). (ii) In contrast, most of the dexamethasone phosphate was degraded after 11 days when dissolved from the beginning in artificial perilymph at 37 °C (blue curve in the diagram at the top of Figure 3.5). This indicates that the entrapment of the dexamethasone phosphate particles in the silicone matrix protects the drug from hydrolysis (avoiding the contact with water). However, this is not necessarily a 100% protection, since upon water penetration into the system, dexamethasone phosphate can be expected to be also hydrolyzed within the drug delivery system, prior to its release.

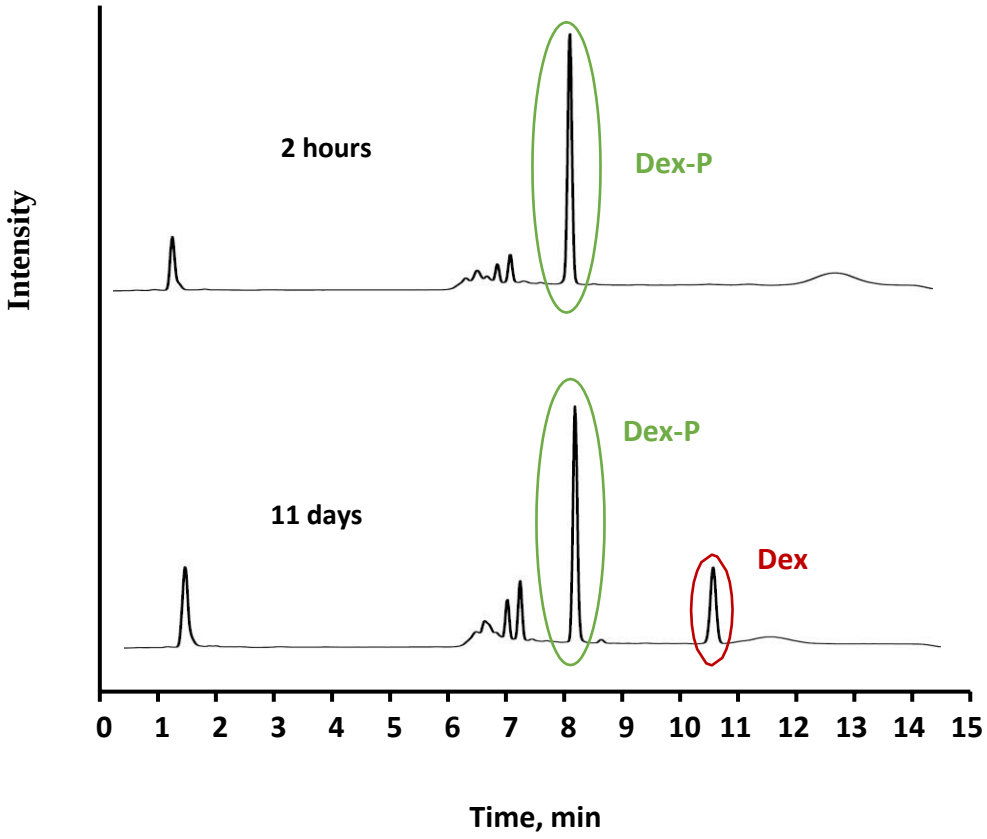

Figure 3.6. HPLC chromatograms of samples of release medium withdrawn after 2 h and 11 d. Silicone films loaded with 11 % dexamethasone phosphate were exposed to artificial perilymph at 37 °C.

The left diagram in Figure 3.7 shows the concentrations of the prodrug dexamethasone phosphate detected in samples, which were withdrawn from the release medium at different time points upon exposure of a silicone film loaded with 11% dexamethasone phosphate to artificial perilymph at 37 °C. The volume of the well agitated bulk fluid was 10 mL. At each sampling time point, 1 mL bulk fluid was withdrawn and replaced with 1 mL fresh medium. Thus, the observed decrease in the concentration of released dexamethasone phosphate can in part be attributed to a dilution effect. However, the observed decrease is much more pronounced than this dilution effect, indicating that dexamethasone phosphate conversion into dexamethasone in the release medium plays a major role, as expected from the discussion above. For reasons of comparison, the diagram on the right-hand side of Figure 3.7 shows the dexamethasone concentrations measured in samples withdrawn from the release medium in the case of thin silicone films loaded with 11% dexamethasone. As it can be seen, in this case, the drug concentration monotonically increased with time, because the accumulation of drug in the bulk fluid due to its continuous release from the film was more important than the dilution effect due to sampling & medium replacement (and the drug was stable under the given conditions, bottom diagram in Figure 3.5).

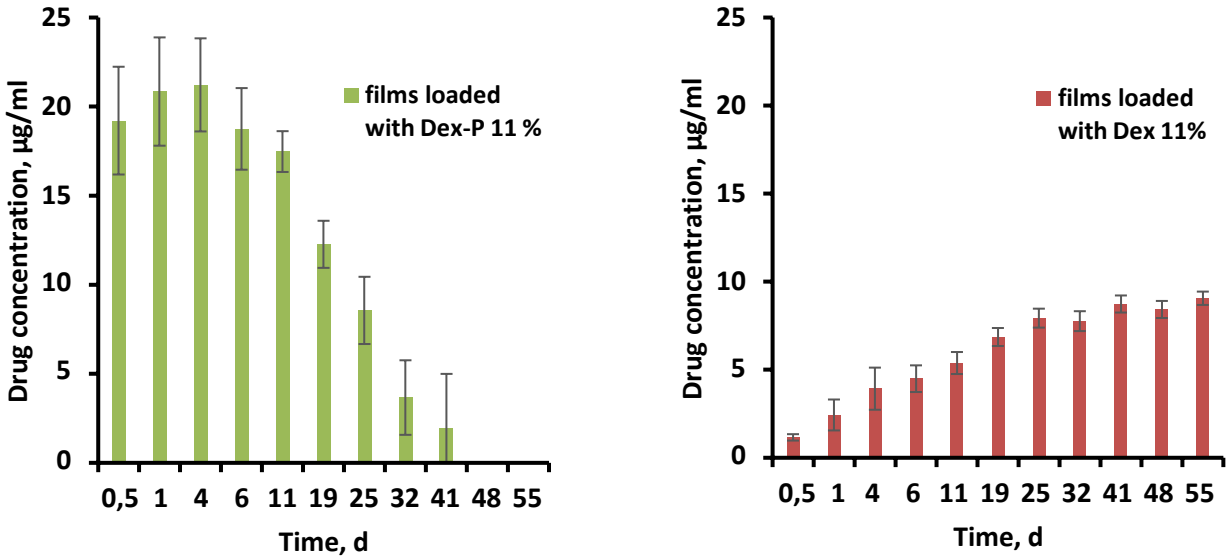

Figure 3.7. Released drug concentration from silicone films loaded with either 11 % dexamethasone or 11 % dexamethasone phosphate milled for 3 min upon exposure to artificial perilymph at 37°C.

3.1.4. Impact of the relative drug loadings

The basic idea of this study was to increase the dexamethasone release rate during the initial "burst phase" from silicone-based delivery systems by the addition of the more hydrophilic dexamethasone phosphate ester. In order to evaluate whether this strategy is successful, a series of thin silicone films was prepared, loaded with 11% total drug content, varying the concentrations of dexamethasone and dexamethasone phosphate as follows: 1 + 10, 2 + 9, 3 + 8, 4 + 7, 5 + 6, 6 + 5, 7 + 4, 8 + 3, 9 + 2 and 10 + 1%. Figure 3.8 shows optical macroscopy pictures of the different films. The dexamethasone phosphate powder was milled for 3 min prior to incorporation into the silicone matrix to minimize the formation of drug particle agglomerates. Nevertheless, an increasing number of white agglomerates was visible with increasing dexamethasone phosphate contents. This can be attributed to the higher hydrophilicity of this drug compared to dexamethasone and the hydrophobic nature of the

silicone, as discussed above. Please note that the pictures shown in Figure 3.2 had a drug loading of 1% only.

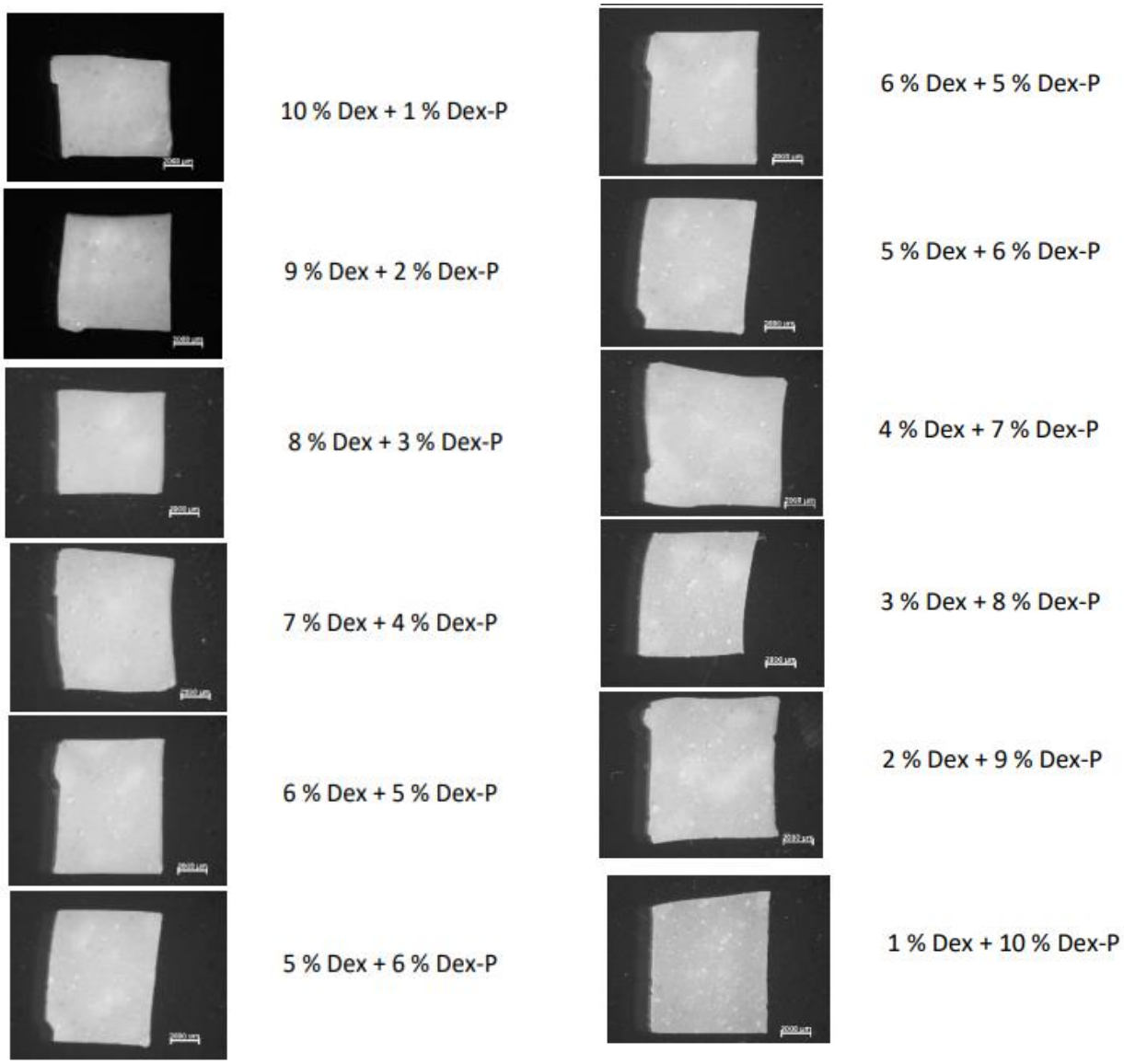

Figure 3.8. Macroscopic pictures of silicone films loaded with different amounts of dexamethasone and dexamethasone phosphate milled for 3 min. The total drug content was constant (11 %).

The resulting total absolute drug release rates from the different films in artificial perilymph at 37 °C are illustrated in Figure 3.9. The amounts of both, dexamethasone and dexamethasone phosphate, are considered. Importantly, this diagram clearly shows that the formulation

strategy is successful: Despite the constant total drug loading, the release rate increased with increasing dexamethasone phosphate content. This can be expected to be beneficial for the patient, providing higher drug concentrations during the first hours/days/weeks after implant placement, when the risk of trauma, inflammation and fibrosis is particularly elevated. Please note that the shape of the drug release curve of films containing 1% dexamethasone phosphate and 10% dexamethasone (bottom curve in Figure 3.9) is different from that of films containing only 1% dexamethasone phosphate (bottom curve in Figure 3.4). This is because the presence of the additional 10% dexamethasone has an important effect on drug release: Upon leaching of dexamethasone phosphate or dexamethasone, the porosity of the films and their water content increase, facilitating the release of remaining drug. In the case of films containing only 1% dexamethasone phosphate, the "pore creating effect" of the 10% dexamethasone is missing. Thus, some kind of "plateau" is observed after a few days (Figure 3.4): Drug particles/agglomerates with direct surface access have been released and it takes more time for drug particles/agglomerates located in deeper film regions to be released. In contrast, in films loaded with 1% dexamethasone phosphate and 10% dexamethasone (Figure 3.9), the release of drug particles/agglomerates located in deeper film regions is facilitated by the presence of an important number of pores and channels in direct contact with the surface, created by drug leaching at earlier time points.

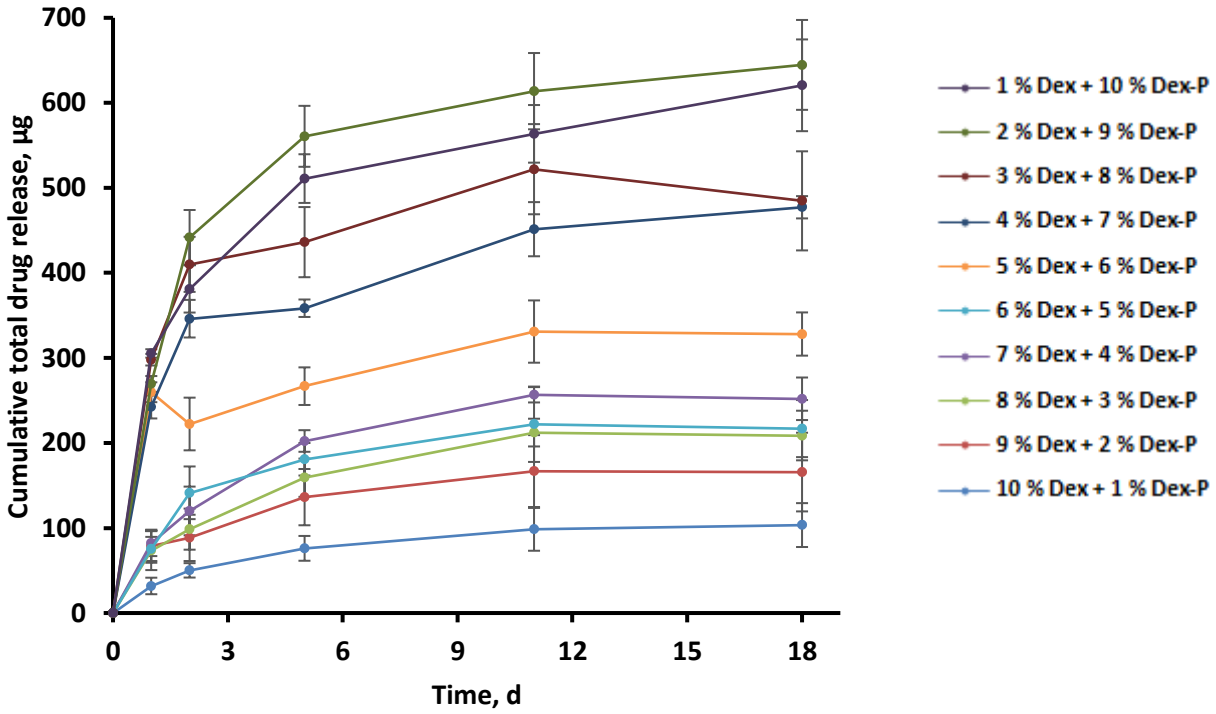

Figure 3.9. Cumulative total drug release from silicone films loaded with different concentrations of dexamethasone and dexamethasone phosphate (as indicated) in artificial perilymph at 37 °C. The total drug content was constant (11 %).

The optical macroscopy pictures in Figure 3.10 are consistent with this hypothesis: Films loaded with "10 % dexamethasone + 1 % dexamethasone phosphate" or with "1 % dexamethasone + 10 % dexamethasone phosphate" are illustrated before and after 32 days exposure to artificial perilymph: The initially clearly visible white drug particles/agglomerates of drug particles became water filled cavities. In the case of high dexamethasone phosphate

loadings this effect was more pronounced, due to the prodrug being more hydrophilic than dexamethasone, facilitating water penetration into the system and drug dissolution.

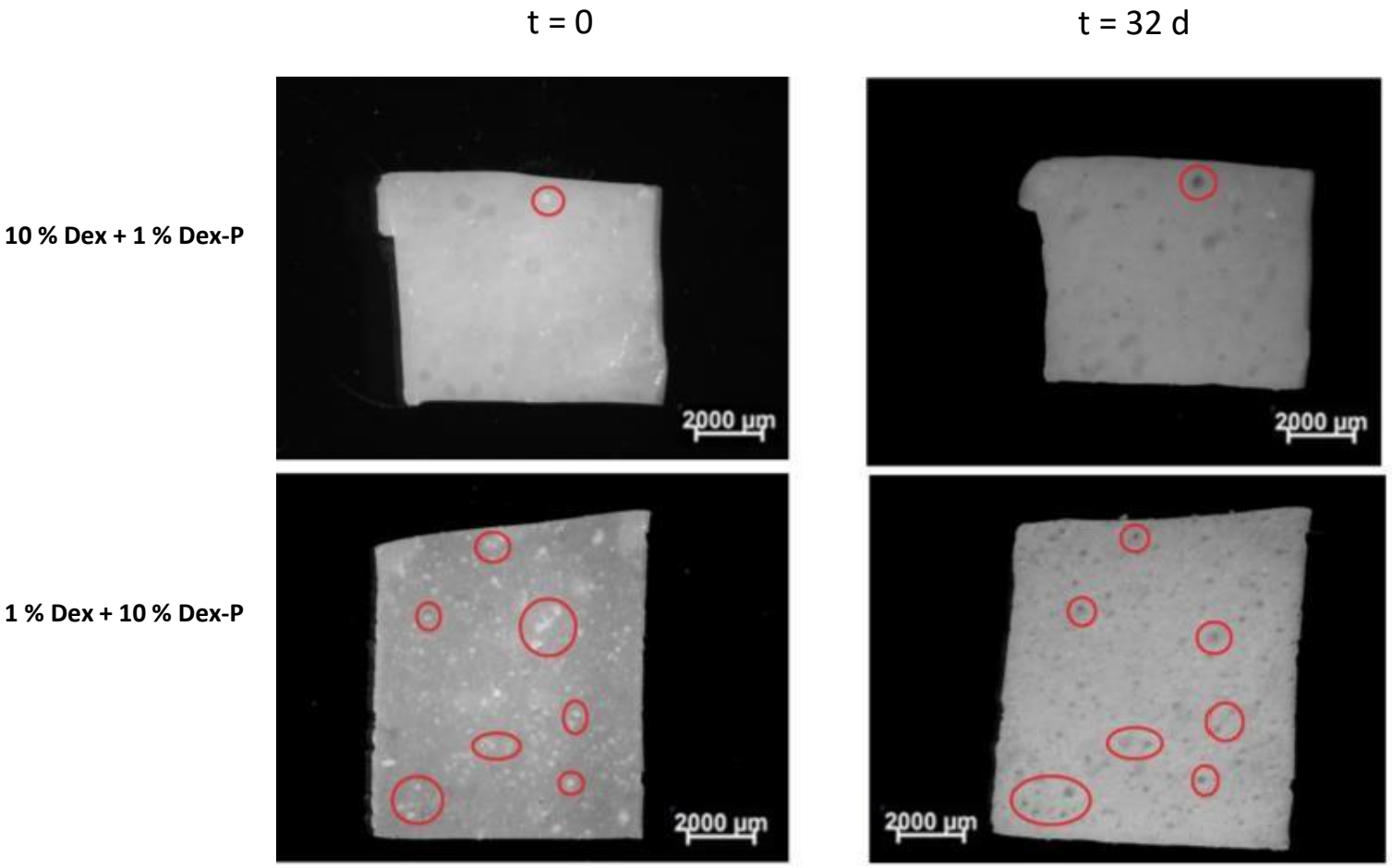

Figure 3.10. Macroscopic pictures of silicone films loaded with varying concentrations of dexamethasone and dexamethasone phosphate before and after 32 d exposure to artificial perilymph (37 °C). The red ovals indicate drug agglomerates (left-hand side) and holes (right hand-side), respectively.

However, the addition of a more hydrophilic compound to a hydrophobic silicone matrix can also lead to a much more pronounced system swelling. In the case of miniaturized implants which are placed into the cochlea of a patient this effect must be limited, because the inner ear is a tiny and sensitive organ. Substantial implant swelling can be expected to cause damage.

This is the reason why the dynamic changes in the wet mass and thickness of the silicone films loaded with different dexamethasone and dexamethasone phosphate contents was also monitored upon exposure to artificial perilymph at 37 °C. As it can be seen in Figure 3.11, film swelling became much more pronounced at higher dexamethasone phosphate contents. Thus, the strategy of adding a more hydrophilic prodrug to increase the initial burst release was successful, but must be used with caution: A compromise has to be found between the desired drug release rate and acceptable system swelling. Please note that even though sink conditions were maintained throughout the observation periods in the surrounding, well-agitated bulk fluid, limited drug solubility effects are likely playing a crucial role within the investigated drug delivery systems: The amounts of water penetrating into the silicone matrices can be expected to be insufficient to dissolve all drug immediately (even upon addition of up to 10% dexamethasone phosphate). The potential importance of limited drug solubility effects within a drug delivery system, in contrast to drug saturation effects in the surrounding release medium, has recently been highlighted and explained in more detail.

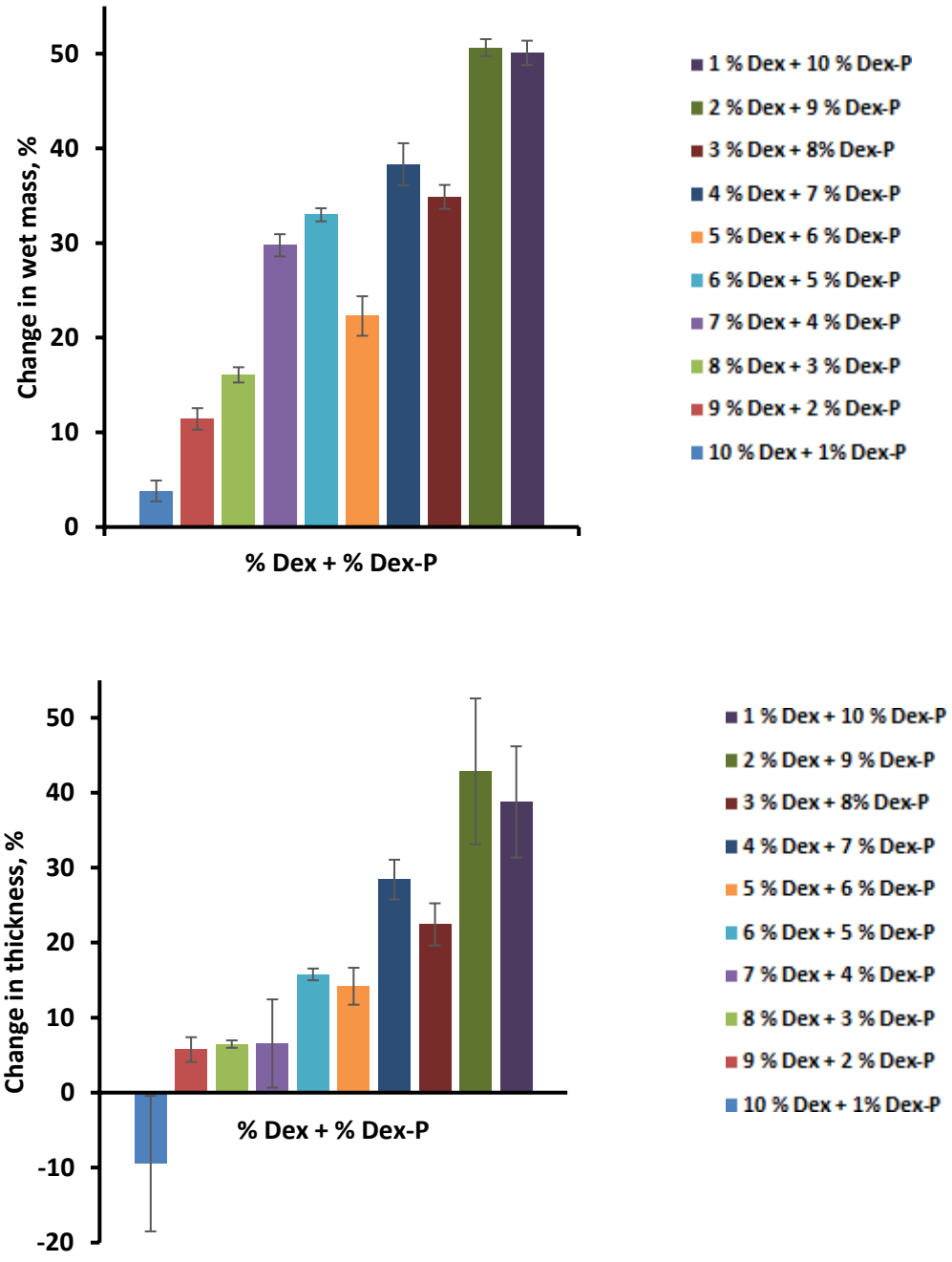

Figure 3.11. Dynamic changes in the wet mass and thickness of silicone films loaded with varying concentrations of dexamethasone and dexamethasone phosphate (as indicated) upon exposure to artificial perilymph at 37 °C. The total drug content was constant (11 %).

3.1.5. Drug release from cochlear implants

Based on the above described results obtained with thin silicone films, miniaturized inner ear implants were prepared with dimensions allowing for administration in human cochleae[122]. The systems were loaded with "10 % dexamethasone + 1 % dexamethasone phosphate" or with "10 % dexamethasone" for reasons of comparison. Please note that metal electrodes were not incorporated (but their impact on the investigated formulation effects, can be expected to be limited). Figure 3.12 shows optical macroscopy pictures of the implants, which appeared to be rather homogenous.

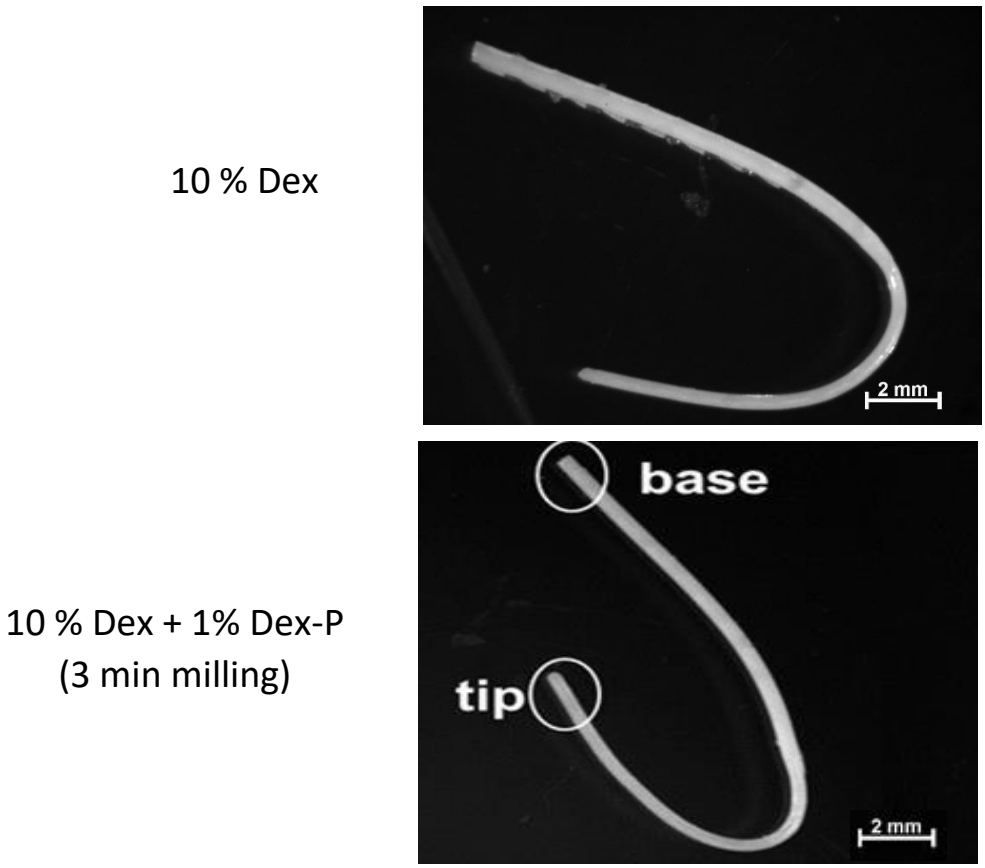

Figure 3.12. Optical macroscopy pictures of cochlear implants loaded with "10 % dexamethasone" or "10 % dexamethasone + 1 % dexamethasone phosphate (milled for 3 min)", before exposure to the release medium.

The resulting cumulative drug release kinetics in artificial perilymph are illustrated in Figure 3.13. Importantly, the strategy was successful: The addition of only 1% dexamethasone phosphate significantly increased the initial burst release during the first few days/weeks. Please note that an average volume of only 76 µL perilymph has been reported for humans.

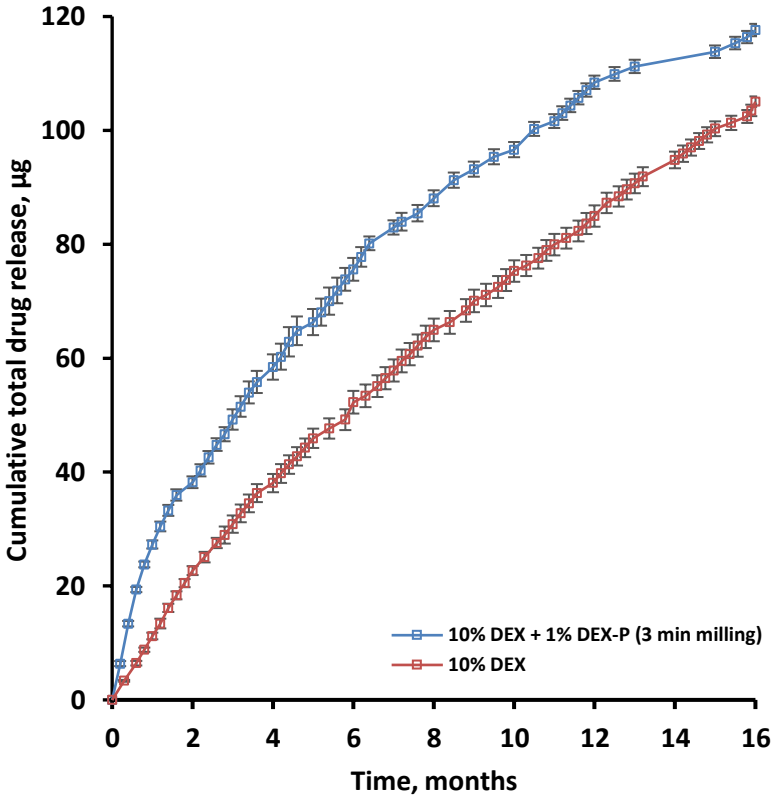

Figure 3.13. Impact of adding 1 % dexamethasone phosphate to cochlear implants loaded with 10 % dexamethasone on the resulting cumulative absolute total drug release kinetics in artificial perilymph (37 °C). The dexamethasone phosphate powder was milled for 3 min prior to incorporation into the silicone.

Thus, the observed increase in the total drug release rate is likely relevant in vivo. At the same time, the addition of only 1% dexamethasone phosphate to the 10% dexamethasone containing silicone-based implants did not lead to noteworthy system swelling during at least 1 year, as illustrated in Figure 3.14: The dynamic changes in the diameters of the "tips" and "bases" of the implants (shown in Figure 3.12) were monitored upon exposure to artificial perilymph (37 °C, 80 rpm) by optical macroscopy. From a clinical perspective, this type of behavior can be expected to be acceptable.

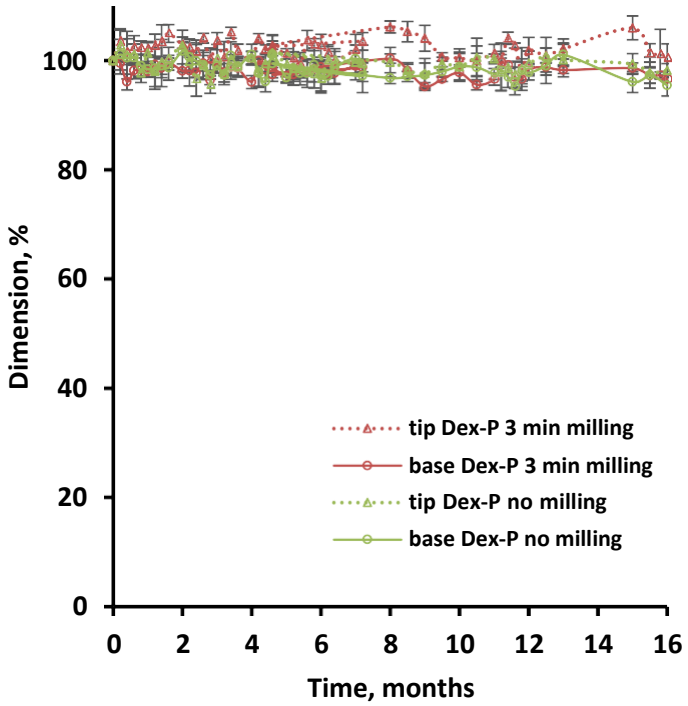

Figure 3.14. Absence of noteworthy swelling or shrinking: Dynamic changes in the dimensions of cochlear implants loaded with 10 % dexamethasone and 1 % dexamethasone phosphate upon exposure to artificial perilymph (37 °C). The dexamethasone phosphate powder was optionally milled for 3 min prior to incorporation into the silicone.

3.2 Long term behavior of dexamethasone-loaded cochlear implants

3.2.1 Physical state and distribution of the drug after manufacturing

The picture at the top of Figure 3.15 shows a cochlear implant loaded with 10 % dexamethasone for humans after manufacturing. The implant consists of silicone and drug only, no metal electrodes were included. For the dexamethasone release measurements and swelling studies, the part of the implant which is not inserted into the cochlea (on the right-hand side) was cut off (as illustrated in the 2 pictures at the top of Figure 3.15).

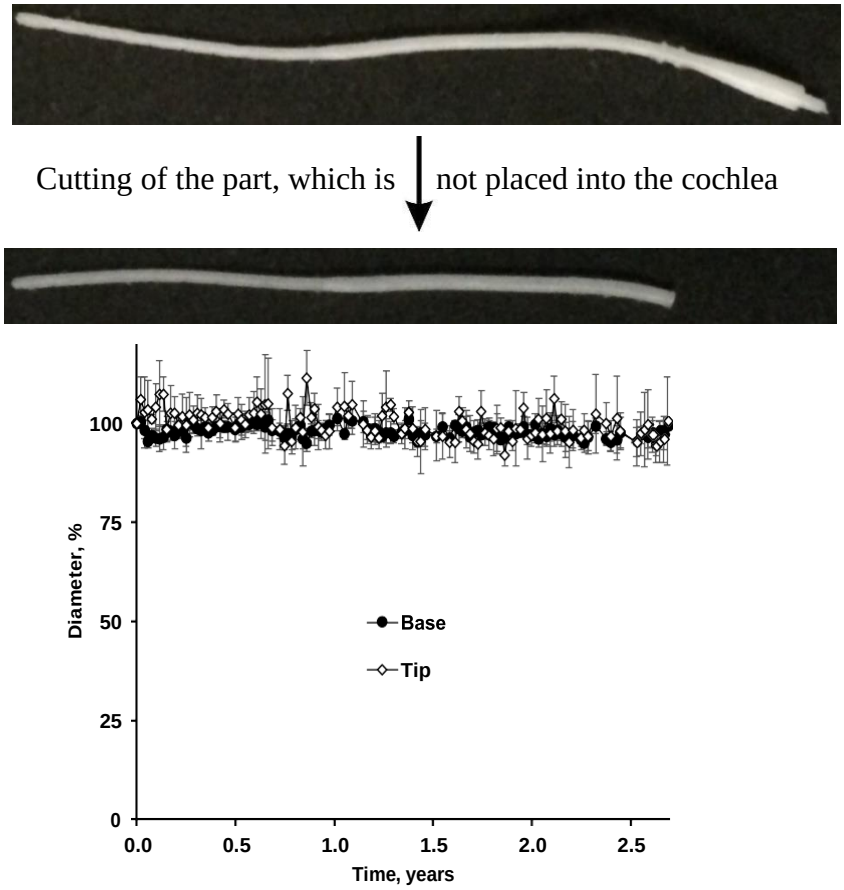

Figure 3.15. *Top:* Optical microscopy pictures of a cochlear implant for use in humans (without metal electrodes), loaded with 10 % dexamethasone (after manufacturing). For the drug release and swelling studies, the part of the implant which is not placed into the cochlea, was cut off. *Bottom:* Dynamic changes in the diameters of the "tips" and "bases" of the implants upon long term exposure to artificial perilymph at 37 °C (in vitro).

The images on the left-hand side of Figure 3.16 show optical microscopy pictures of radial cross-sections of such an implant (at different magnifications). For reasons of comparison, the picture on the right-hand side in Figure 3.16 shows a radial cross-section through a cochlear implant *free* of drug (placebo). As it can be seen, the latter (consisting of silicone only) was transparent. In contrast, darker regions were visible in the dexamethasone-loaded implant. They likely indicate the presence of drug particles, hindering the visible light to pass through the sample. This is consistent with previously reported Scanning Electron Microscopy pictures of polymeric films and cylindrical extrudates based on the same silicone and drug: Krenzlin et al evidenced the presence of tiny dexamethasone crystals distributed throughout such silicone matrices[122]. Importantly, the drug crystal distribution seems to be homogenous throughout the implant (Figure 3.16, left hand side). Similar observations were made with the cochlear implants for use in *gerbils* (which were smaller).

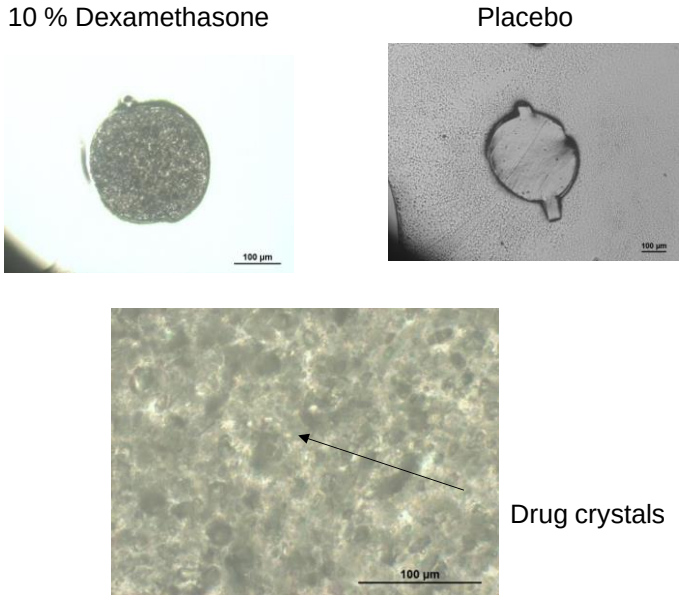

Figure 3.16. Optical microscopy pictures of radial cross-sections of cochlear implants for humans (without metal electrodes) after manufacturing: Loaded with 10 % dexamethasone (left hand side) or free of drug (placebo, right hand side).

Since two polymorphic forms of dexamethasone have recently been reported (Forms A and B), it was interesting to know which polymorph was present in the investigated cochlear implants. For this reason, X-ray diffraction patterns of the implants were recorded as well as of the 2 known polymorphic forms of dexamethasone. As it can be seen in Figure 3.17, the diffraction patterns of dexamethasone Form A (drug powder as received) and Form B (prepared by milling and heating) can be distinguished by several peaks observed at different angles. Clearly, the diffraction patterns of the drug-loaded implants corresponded to those of dexamethasone Form A. Please note that the implant had been exposed for 1 month to artificial perilymph. Thus, neither the manufacturing process of the cochlear implants used in this study nor exposure to the release medium changed the polymorphic form of the drug

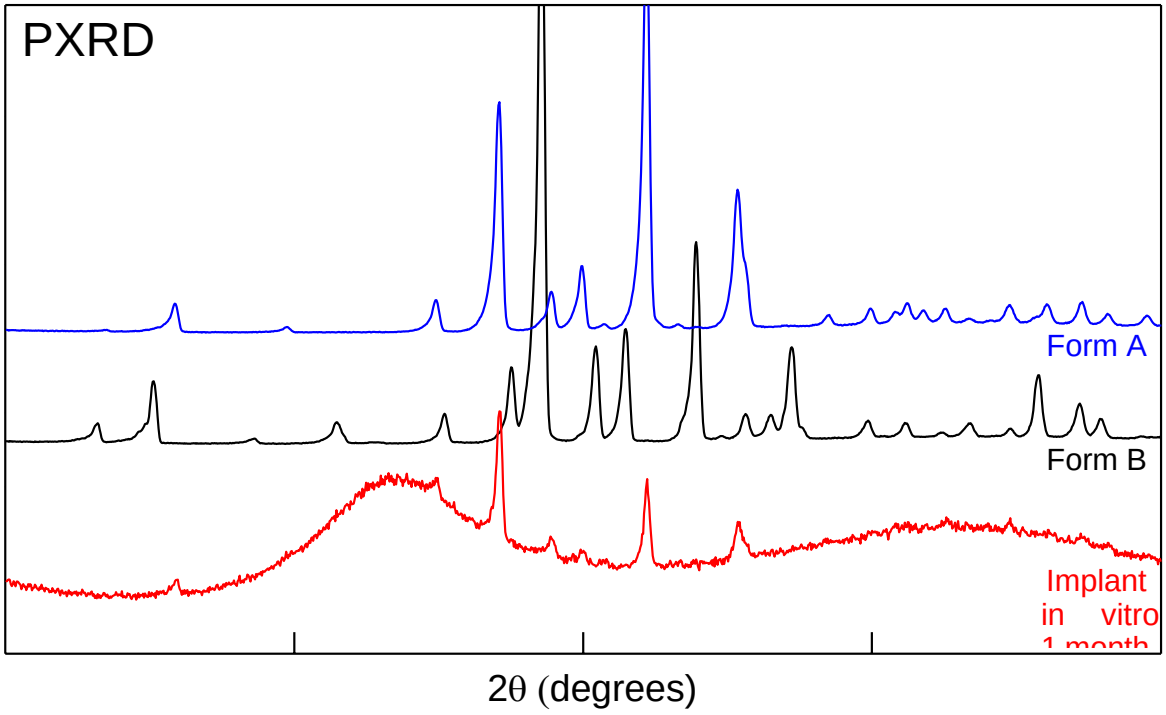

Figure 3.17. X-ray diffraction patterns of cochlear implants for humans loaded with 10 % dexamethasone after 1 month exposure to artificial perilymph at 37 °C (in vitro). For reasons of comparison, also the X-ray diffraction patterns of the 2 known polymorphic forms of dexamethasone are shown.

3.2.2 Implant swelling and drug release in vitro

From a practical point of view, it is critically important that the cochlear implants do not substantially swell upon contact with aqueous media. Otherwise, the inner ear might be damaged. To monitor potential changes in the dimensions of the investigated implants in vitro, the latter were exposed to artificial perilymph at 37 °C and horizontally shaken at 80 rpm. At pre-determined time points, samples were withdrawn and their diameters were measured using a Nikon Eclipse SMZ-U microscope, equipped with an AxioCam ICc 1 Zeiss camera. The pictures in the middle of Figure 3.15 show the locations for these measurements: at the "tips" and "bases" of the implants. The diagram at the bottom of Figure 3.15 shows the swelling behavior during long term exposure (3 years) to artificial perilymph. Importantly, no substantial variations in the systems' diameters were observed. The implants did neither swell, nor shrink to a noteworthy extent. The observed arbitrary and limited "fluctuations" can probably be explained as follows: The radial cross-section of an implant was not *perfectly* spherical (see for instance the two pictures at the top of Figure 3.16). Thus, the *exact position* of the implant during the microscopic observation impacts the measured diameter to a certain degree. This *technical* bias does not reflect real implant swelling/shrinking.

The experimentally measured dexamethasone release kinetics from cochlear implants for humans loaded with 10 % drug in artificial perilymph are illustrated in the diagram at the top of Figure 3.18. The error bars are too small to be visible. Clearly, drug release is controlled during several years (e.g., about 40 % of the initial dexamethasone loading was released after 3.2 years). This is in good agreement with results previously reported on silicone-based cochlear implants of the same composition, but containing also metal electrodes. Thus, the presence/absence of the metal wires does not substantially impact drug release. This is consistent with the hypothesis that drug diffusion through the silicone matrix plays a major role in the control of dexamethasone release from this type of advanced drug delivery systems: Upon

contact with aqueous fluids, water penetrates into the system and dissolves the drug. Once dissolved the dexamethasone slowly diffuses out into the surrounding environment. The following equation has been proposed for the quantification of drug release from such electrode-containing implants (assuming cylindrical geometry):

$$\frac{M_t}{M_\infty} = 1 - \frac{32}{\pi^2} \cdot \sum_{n=1}^{\infty} \frac{1}{q_n^2} \cdot \exp\left(-\frac{q_n^2}{R^2} \cdot D \cdot t\right) \cdot \sum_{p=0}^{\infty} \frac{1}{(2 \cdot p + 1)^2} \cdot \exp\left(-\frac{(2 \cdot p + 1)^2 \cdot \pi^2}{H^2} \cdot D \cdot t\right) \quad (1)$$

where M_t and M_∞ are the absolute cumulative amounts of drug released at time *t* and *infinity*, respectively; *n* and *p* are a dummy variables; q_n are the roots of the Bessel function of the first kind of zero order [$J_0(q_n)=0$]; *D* is the "apparent" diffusion coefficient of dexamethasone within the silicone matrix; *R* and *H* denote the radius and height of the cylindrical implants.

This equation can be derived from Fick's second law of diffusion, assuming that: (i) drug diffusion is the dominant mass transport process (e.g. is much faster than drug dissolution and water diffusion), (ii) perfect sink conditions are provided throughout the experiments, (iii) the drug is initially homogeneously distributed throughout the system, (iv) the diffusion coefficient of the drug is not dependent on time or position, (v) the implants are of cylindrical geometry, (vi) drug diffusion occurs in radial and axial direction, and (vii) the implant does not dissolve or swell upon exposure to the release medium.

Krenzlin et al. used Equation 1 to theoretically predict dexamethasone release from cochlear implants based on the same silicone, loaded with 10-30 % drug[122]. But in that study, the implants contained metal electrodes and the release medium was not agitated. The apparent diffusion coefficient of the drug in the polymeric matrix had been estimated by fitting an appropriate solution of Fick's second law of diffusion to experimentally determined dexamethasone release kinetics from thin *films* of the same composition (free of electrodes).

Importantly, in that previous study drug release was only monitored during 80 d. Relatively good agreement between theory and experiment had been observed. In the present study, the same apparent dexamethasone diffusion coefficient for this type of silicone, loaded with 10 % drug was used to predict the release patterns from the investigated electrode-free implants upon exposure to well agitated artificial perilymph at 37 °C. The black curves in the diagrams at the bottom of Figure 3.18 show these theoretical predictions. The diagram on the right hand side is a zoom on the first 7 months and shows the release kinetics from 4 individual implants. As it can be seen, the agreement between theoretical prediction and independent experiment is *rather* good, but there are clear and systematic deviations: At early time points, the theory overestimates drug release, at later time points, dexamethasone release is underestimated. This can probably be attributed to the simplifying assumption Equation 1 is based on that the diffusion coefficient of the drug is *constant* over time and independent of the position in the implant. In reality, this is likely not the case for the following reason: Upon exposure to the release medium, drug crystals located in surface near regions can be expected to dissolve *first*. Once dissolved, the drug diffuses out. Consequently, water-filled "pores" remain. To a certain extend these "pores" might be closed by (even limited) swelling/expansion of surrounding silicone. In any case, it is likely that these locations in the silicone matrix become more permeable for the drug. Thus, dexamethasone which subsequently diffuses from the center of the implants to the surface can be expected to be more mobile in such drug-exhausted regions. Equation 1 does not take such effects into account. The apparent diffusion coefficient (being a measure for the mobility of the drug in the polymeric matrix) used in this equation presents a "*time-averaged*" value. It overestimates the real diffusion coefficient at early time points and underestimates drug mobility at late time points ("ignoring" the creation of "higher mobility regions" during drug release). The diagram on the right hand side at the bottom of Figure 3.18 nicely illustrates this initial overestimation and subsequent underestimation of drug release

from the investigated cochlear implants. Please note that a more comprehensive mathematical theory, taking into account time-dependent diffusion coefficients (and ideally also position-dependent diffusivities), can be expected to be able to more reliably describe the observed drug release kinetics. However, the development of such a model was beyond the scope of this study.

The fact the diffusion coefficient used for the above predictions was determined in *non-agitated* artificial perilymph likely only plays a minor role (if at all), since the effects of bulk fluid agitation on drug release were shown to be of negligible importance on dexamethasone release from thin films based on the same type of silicone[122]. Furthermore, the fact that *perfect sink conditions* were not always maintained in the surrounding bulk fluid might contribute to the observed deviations between theory and experiment (Figure 3.18). However, the degree of drug saturation in the release medium relatively rarely exceeded 30 % (and very rarely 50 %). Furthermore, high drug concentrations in the release medium were observed *throughout* the observation period (due to occasional prolonged non-sampling periods during holidays or COVID lockdowns), whereas the under- and overestimation of drug release was systematic: overestimation at early time points, underestimation at later time points (Figure 3.18).

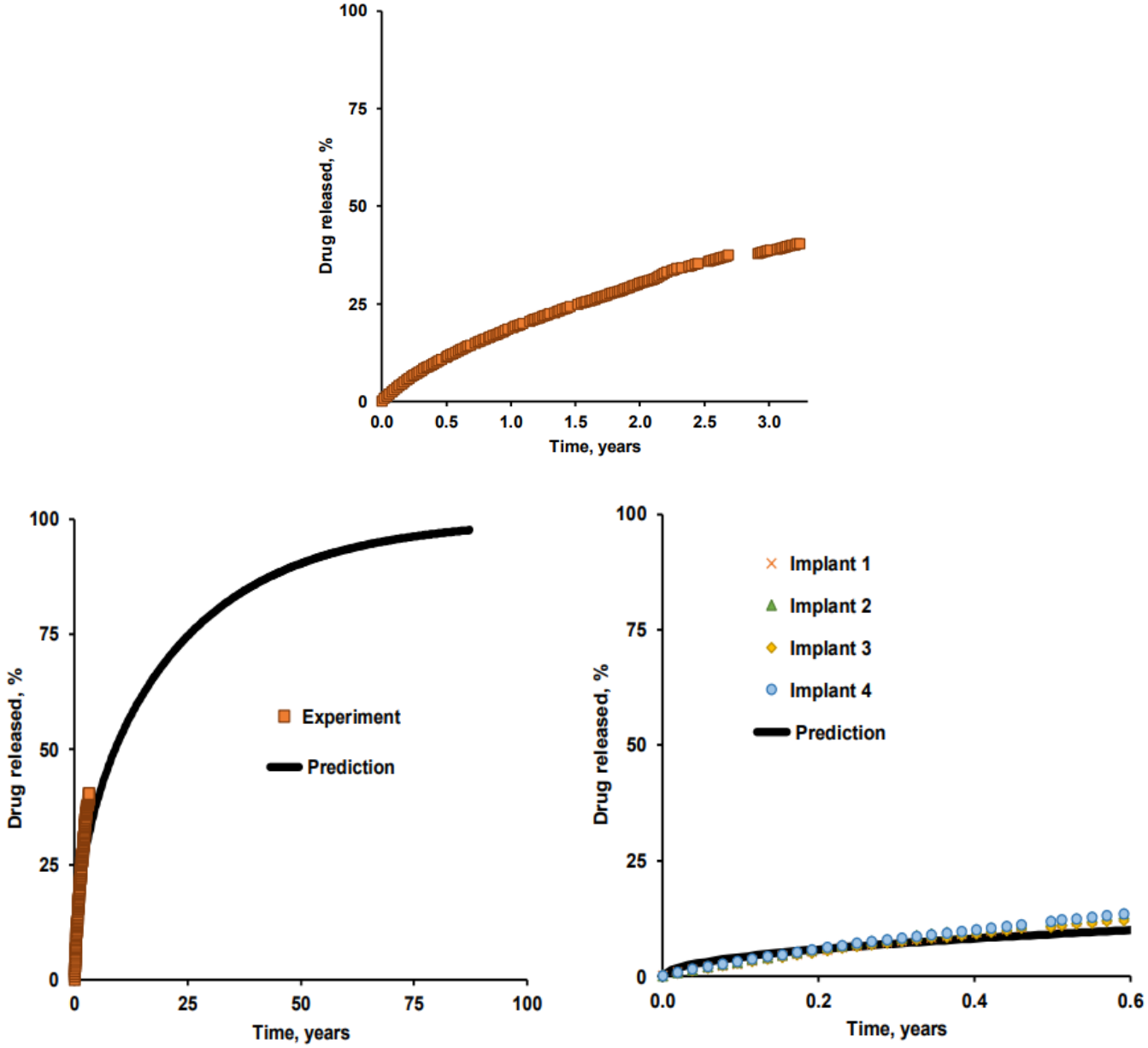

Figure 3.18. In vitro drug release from cochlear implants for humans (without metal electrodes) loaded with 10 % dexamethasone in artificial perilymph at 37 °C. The upper diagram shows the experimentally measured values (n = 4, error bars are too small to be visible). The diagrams at the bottom illustrate in addition the theoretically predicted release profile (calculated using Equation 1, details are given in the text). The diagram on the right hand side shows a zoom on the first 7 months, illustrating the release profiles from 4 individual implants.

3.2.3. Raman imaging in vitro and ex vivo

Figure 3.19 shows the Raman spectra of the investigated pure silicone (cochlear implants free of drug) and dexamethasone (powder as received). Importantly, the two spectra show multiple Raman shifts at different wavelengths. These differences can be used to distinguish between the two compounds and, thus, allow for Raman imaging of cross-sections of implants before and after exposure to artificial perilymph or implantation into gerbils.

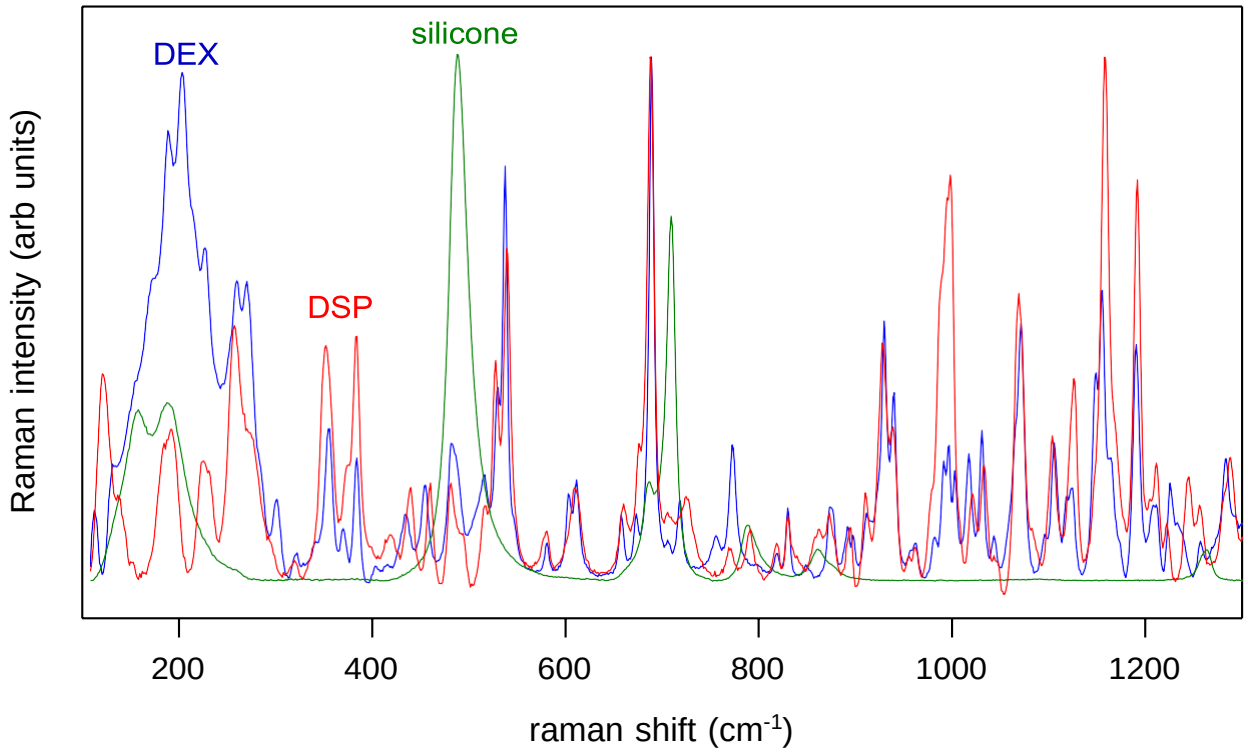

Figure 3.19. Raman spectra of the investigated silicone and dexamethasone. Drug-free silicone implants and drug powder as received were studied.

A radial cross-section of a cochlear implant loaded with 10 % dexamethasone (for use in humans, but free of metal electrodes) is shown in Figure 3.20 (before exposure to release media or implantation in vivo). From the left to the right the following images can be seen: an optical microscopy picture, an image highlighting the silicone-rich regions in red, an image highlighting the dexamethasone-rich regions in green, and an overlap picture of the two (green

and red being “false colors”). The cross-section was divided into small “pixels” and the Raman spectrum of each pixel was recorded. The relative importance of the contribution of dexamethasone and silicone was calculated, based on the reference spectra. Pixels which rich in silicone are marked in red, pixels rich in dexamethasone are marked in green. So, please note that a red color does not strictly exclude the presence of any dexamethasone, nor does the green color strictly exclude the presence of any silicone. The penetration depth for these measurements is about 20-25 µm. As it can be seen in Figure 3.20, the dexamethasone is indeed homogeneously distributed throughout the implant, confirming the hypothesis based on the optical microscopy picture above.

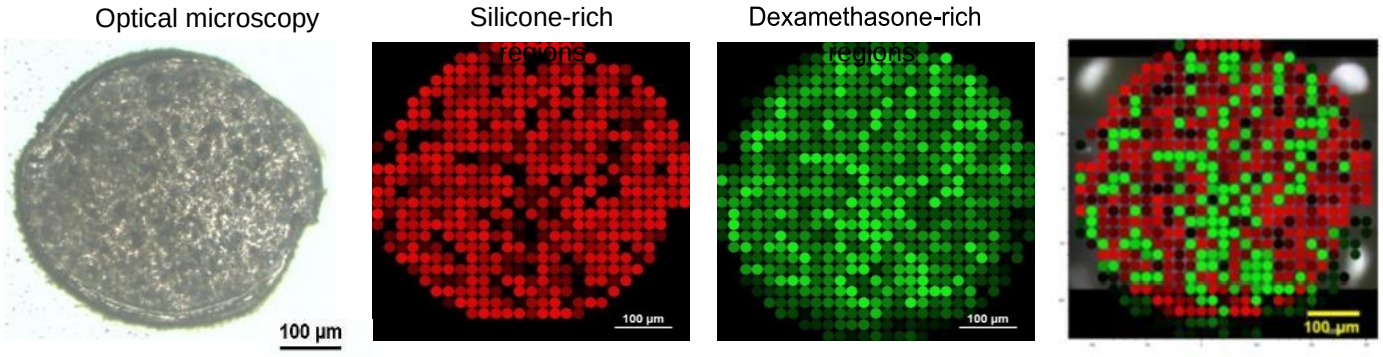

Figure 3.20. Optical microscopy picture and Raman images of a radial cross-section of a cochlear implant for humans (without metal electrodes), loaded with 10 % dexamethasone *after manufacturing*.

Figure 3.21 shows an optical microscopy picture and Raman images of a radial cross-section of a cochlear implant *after 1 month exposure* to artificial perilymph at 37 °C *in vitro*. As it can be seen, dexamethasone-rich regions are still distributed *throughout* the implant, with a very few exceptions appearing in black close to the system’s surface, which might indicate

regions from which drug crystals have been released (highlighted by the white flashes). These pictures are in good agreement with the experimentally measured drug release kinetics (Figure 3.18): After 1 month, only very minor amounts of drug are released. Furthermore, the Raman images are consistent with the hypothesized drug release mechanism: Water penetrating into the implants first reaches surface-near dexamethasone crystals, which dissolve and disappear.

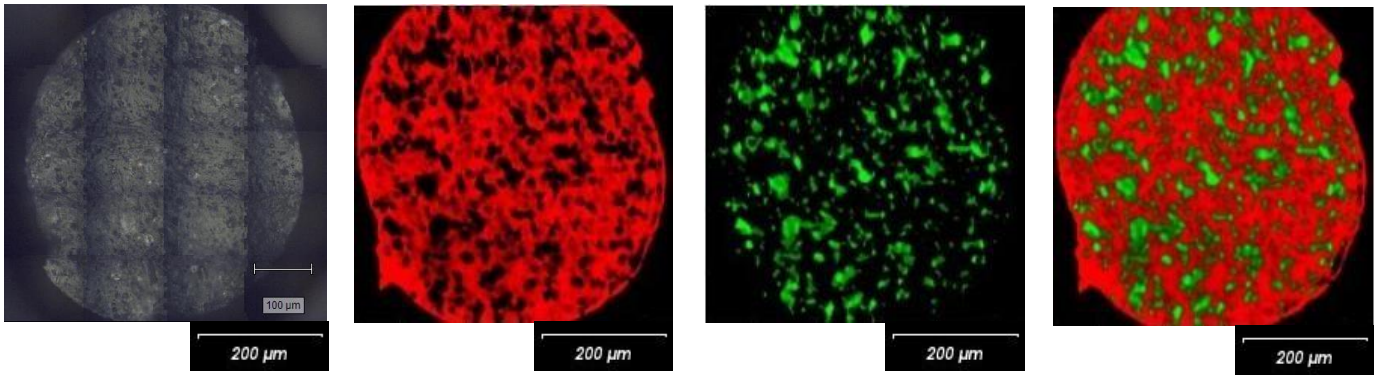

Figure 3.21. Optical microscopy picture and Raman images of a radial cross-section of a cochlear implant for humans (without metal electrodes), loaded with 10 % dexamethasone *after 1 month exposure to artificial perilymph at 37 °C (in vitro)*. The white flashes highlight regions which might correspond to dexamethasone-depleted regions.

To better understand the *in vivo* fate of this type of advanced drug delivery systems, the dexamethasone-loaded cochlear implants were placed into gerbils and explanted after 2 years. Figure 3.22 shows Raman images of *axial* cross-sections of such implant samples. The pictureat the top on the left-hand side shows the distribution of silicone-rich regions. Dexamethasone- rich regions are illustrated in the middle, the picture on the right-hand side is an overlap of thetwo images. Clearly, especially surface-near regions were depleted of dexamethasone, while regions closer to the center of the implants still contained numerous drug crystals. This further confirms the hypothesis that drug

diffusion is the dominant mass transport mechanism in this type of miniaturized implants. The bottom row in Figure 3.22 shows examples for Raman spectra recorded in silicone-rich and dexamethasone-rich pixels (the reference spectra of the two pure components are shown for reasons of comparison on the left-hand side).

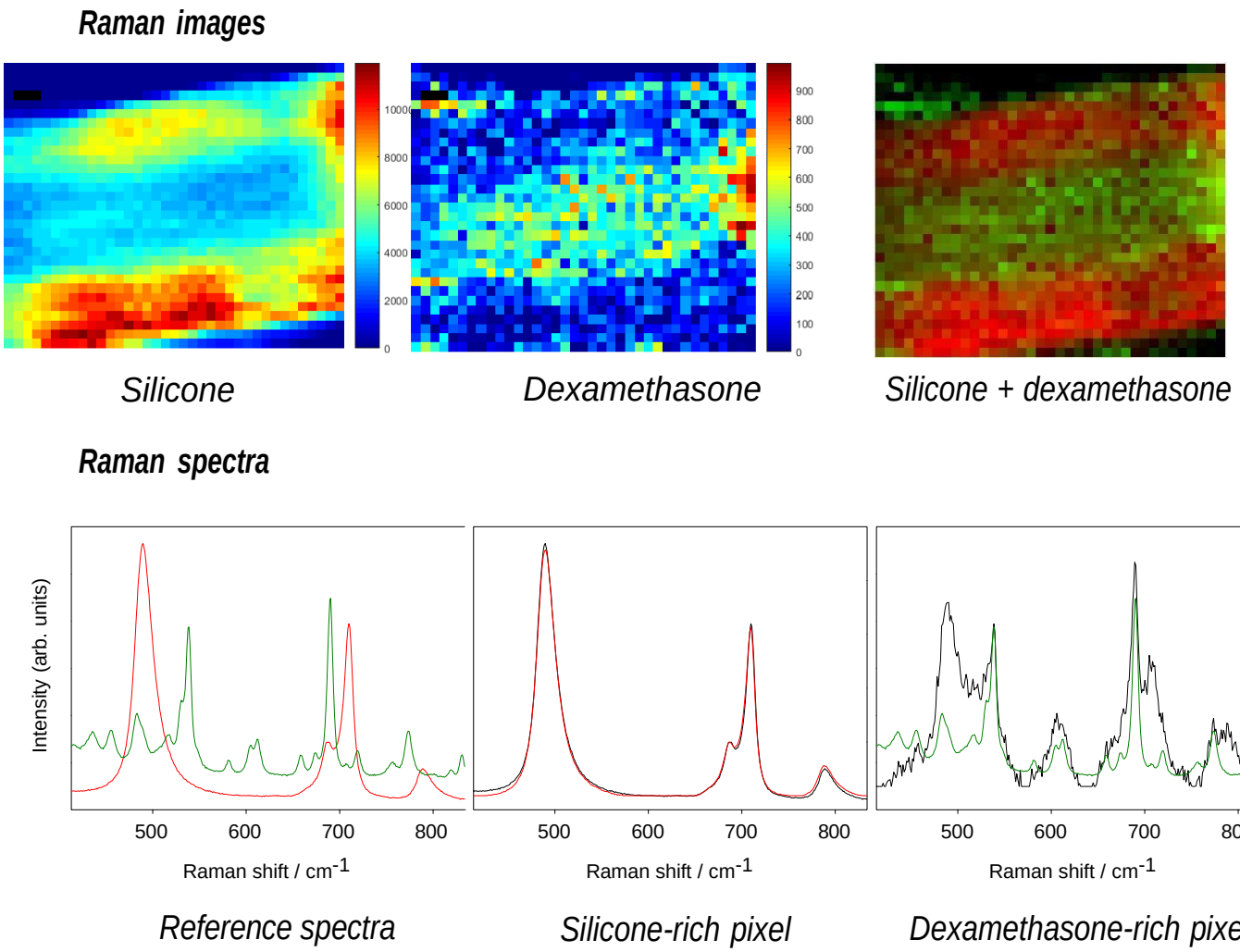

Figure 3.22. Raman images (pixel size: 20 x 20 µm) and Raman spectra of a longitudinal cross-section of a cochlear implant, which was explanted from a gerbil after 2 years.

Figure 3.23 shows Raman images of two *radial* cross-sections of a cochlear implant, which was explanted from a gerbil after 2 years. The pictures at the top correspond to one cross-section, the pictures at the bottom to the other (obtained at a different position). The implant

was initially loaded with 10 % dexamethasone. Again, silicone-rich regions are marked in red, dexamethasone-rich regions in green. The picture on the right hand side at the top is an overlap image. Clearly, in the cross-section shown in the top row, a relatively large drug crystal (or an agglomeration of smaller dexamethasone crystals) can be seen. In contrast, in the cross-section shown in the bottom row, no drug-rich regions are visible. This further confirms the hypothesis that the drug is initially homogeneously distributed throughout the cylindrical implants in the form of tiny dexamethasone crystals and that drug diffusion through the silicone matrix plays a major role. By chance, the images in the top row of Figure 3.23 show a cross-section containing a dexamethasone crystal (or agglomerate of smaller crystals), which has (have) not yet been released after 2 years in vivo implantation, whereas the pictures in the bottom row show a cross-section, from which all drug has been released at this time point, or which never contained any drug (the initial drug loading was 10 %).

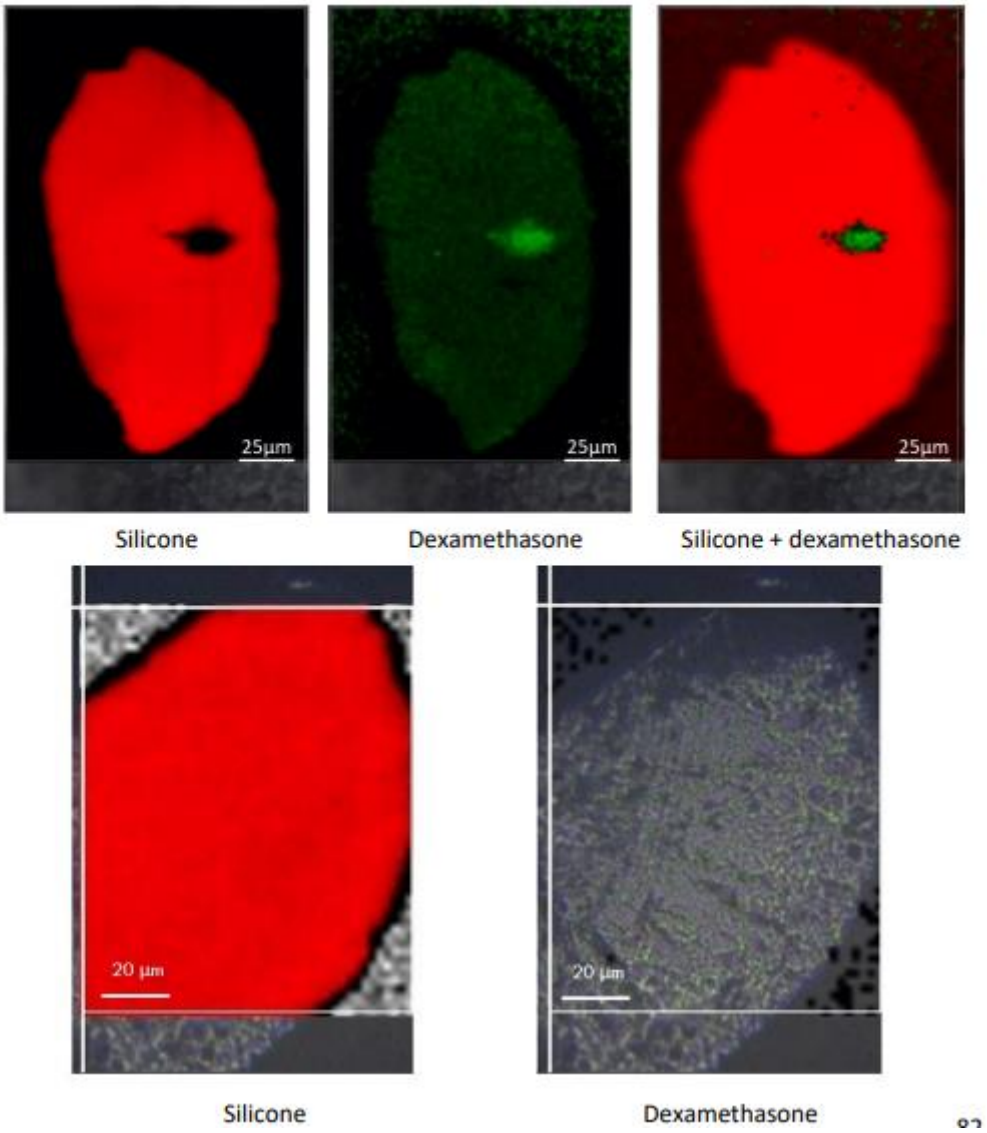

Figure 3.23. Raman images of two radial cross-sections of a cochlear implant, which was explanted from a gerbil after 2 years. The pictures at the top correspond to one cross- section, the pictures at the bottom to the other cross-section. The implant was initially loaded with 10 % dexamethasone.

3.2.4. Optical microscopy before and after 2 years implantation in gerbils

Figure 3.24 shows optical microscopy pictures of cochlear implants for gerbils loaded with 0, 1 or 10 % dexamethasone (as indicated). The images at the top were obtained before implantation, those at the bottom after 2 years implantation into the animals. As it can be seen, drug-free implants were transparent after manufacturing. The addition of increasing amounts of dexamethasone rendered the systems more and more opaque. This can be explained by the presence of dexamethasone in the form of tiny crystals in the silicone matrices, which are distributed throughout the devices. Importantly, the drug distribution is homogenous throughout the entire cochlear implants. In contrast, after 2 years implantation in gerbils, the systems have become transparent in surface-near regions, while the center of the devices remained opaque (bottom row of images in Figure 3.24). This is a further confirmation of the above described, hypothesized drug release mechanism: Upon water penetration into the implants, first drug crystals located close to the systems' surface dissolve and disappear.

After manufacturing

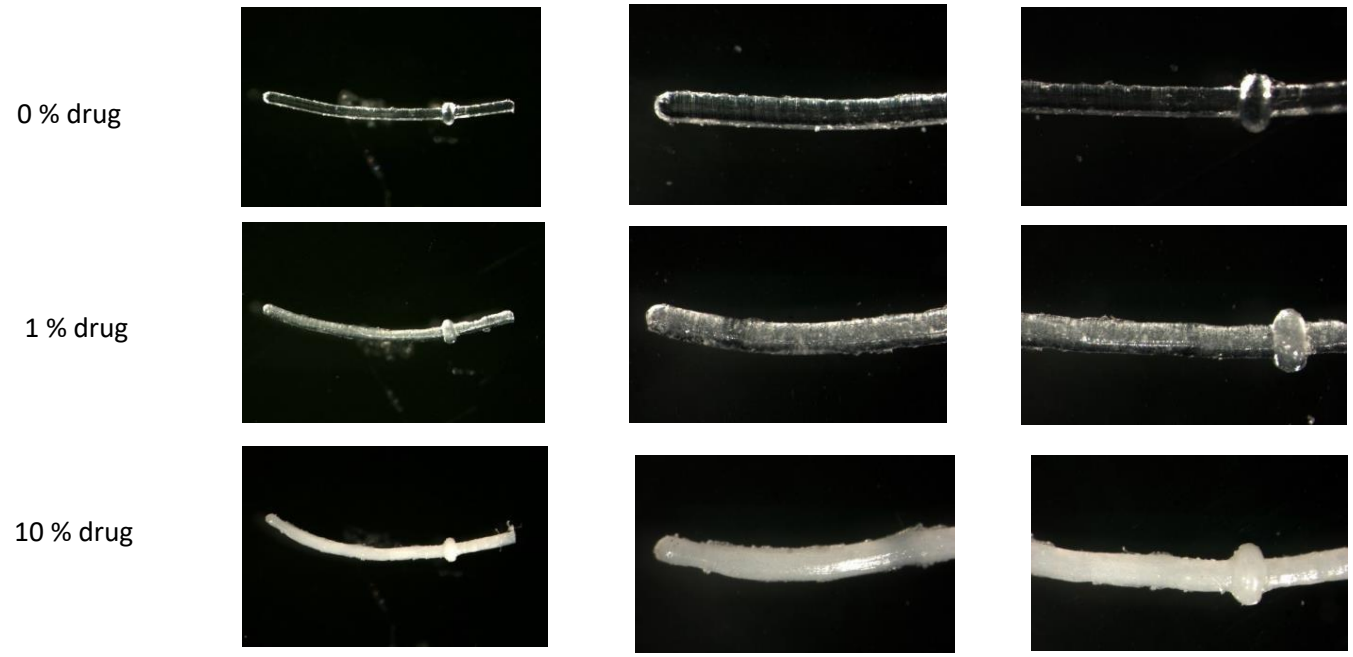

After 2 years implantation in gerbils

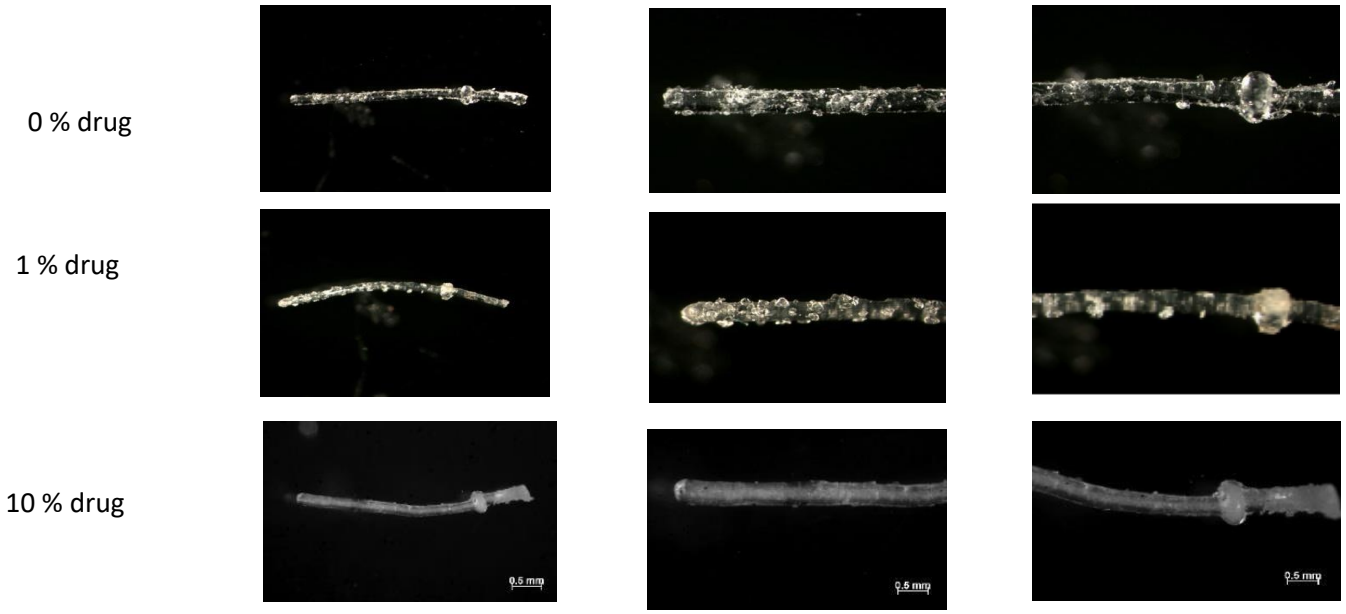

Figure 3.24. Optical microscopy pictures of cochlear implants for gerbils before (top) implantation and after 2 years implantation in vivo (bottom). The initial dexamethasone loading was 0, 1 or 10 % (as indicated on the left hand side). Please note that in the case of implants explanted after 2 years from gerbils, which were initially loaded with 10 % drug, particle deposits on the systems' surface had been removed before taking the picture (in contrast to the other samples).

Interestingly, particle deposits were visible on the surface of all implants after 2 years implantation into gerbils, irrespective of the initial drug loading (please note that the deposits were removed prior to taking the pictures in the case of 10 % drug loading, for reasons of visibility). These deposits might potentially be salts contained in the perilymph, dexamethasone or stemming from the silicone matrix. To know whether this was the case, Raman spectra of such particle deposits were recorded: Optical microscopy pictures of them are shown on the left-hand side of Figure 3.25. The Raman spectra are shown at the top on the right-hand side of Figure 3.25. Clearly, multiple peaks are visible in all 3 samples, at the same wavelengths. Importantly, these peaks did not correspond to those observed in the spectra of the reference substances. Thus, the deposits formed in vivo have a different (biological) origin. It was beyond the scope of this study to analyze their composition in more detail.

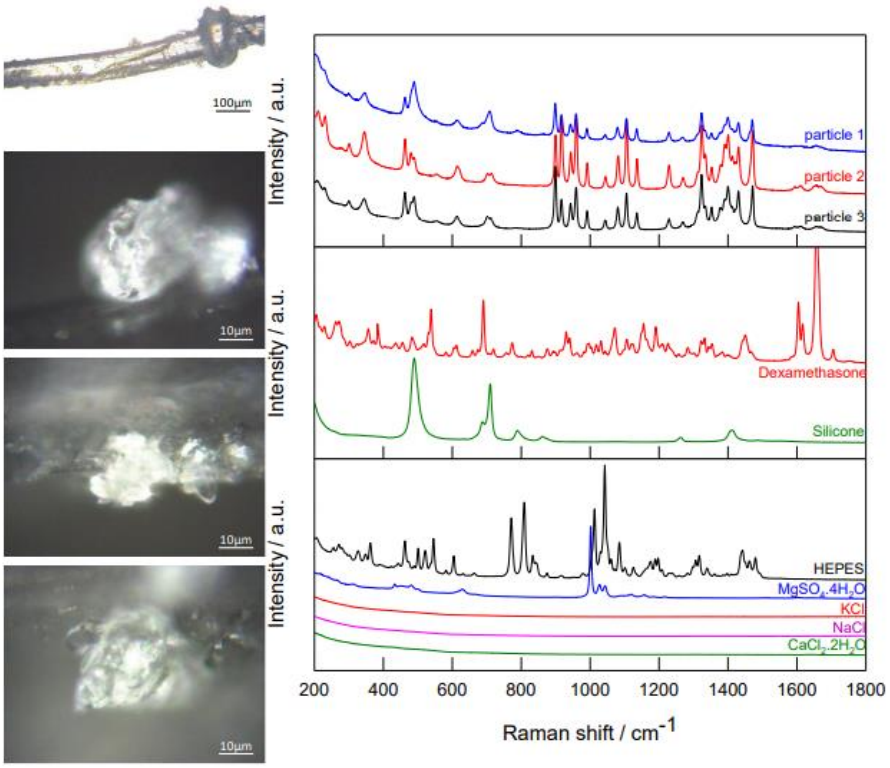

Figure 3.25. *Left hand side:* Optical microscopy picture of a cochlear implant explanted from a gerbil after 2 years (top), and zooms on deposits observed at the implant's surface. *Right hand side:* Raman spectra of 3 particle deposits and different reference substances (as indicated).

3.3 Understanding the mechanisms behind controlled dexamethasone release

3.3.1. Films prepared with crystalline vs. amorphous drug

The physical state of a drug might significantly affect its solubility in water and, thus, the rate at which it is released from a pharmaceutical dosage form. For instance, if the drug is distributed throughout a polymeric matrix in the form of drug *particles*, it first has to dissolve to become mobile and subsequently diffuse out of the system (due to concentration gradients). If the solubility of the drug and/or the amounts of water available for drug dissolution *within* the system are limited, this might very much slow down drug release. Silicone matrices are generally hydrophobic. Thus, only minor amounts of water can penetrate into the device and limited drug saturation effects might be crucial. A drug in an *amorphous* form might exhibit a much higher aqueous solubility than in a crystalline state. Dexamethasone is known to form at least 2 different polymeric forms: Form A and Form B. The dexamethasone in the investigated 3 batches (as received) was crystalline in all cases. To transform it into an amorphous form, samples of Batch 1 (Form A) were milled in a stainless-steel jar with a stainless-steel ball for 3 min at 30 Hz. The optical microscopy pictures on the left hand-side of Figure 3.26 show images of the powder before and after milling.

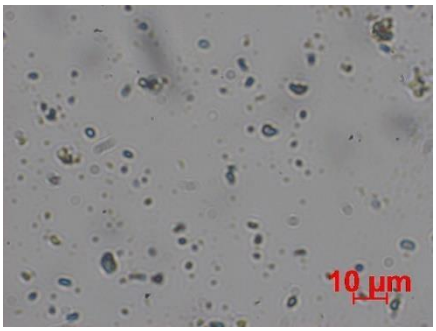

Crystalline dexamethasone (raw material, Form A)

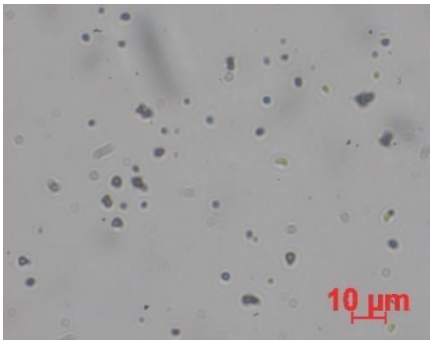

Amorphous dexamethasone

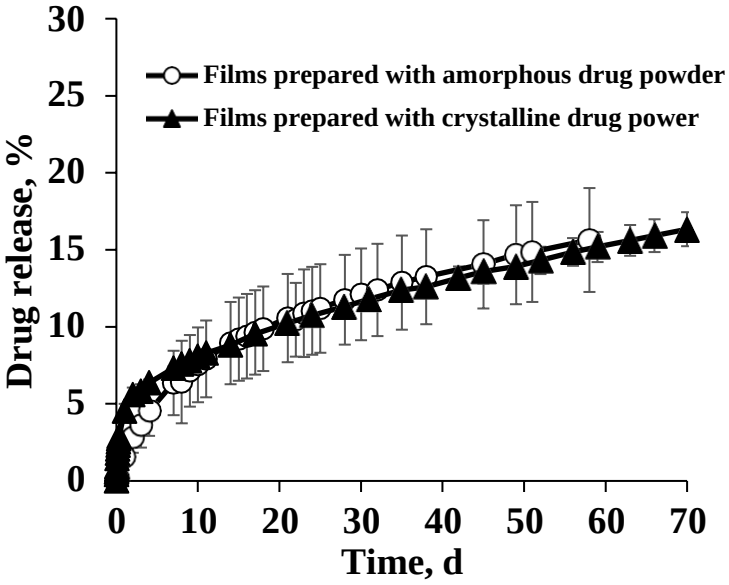

Figure 3.26. Dexamethasone release from silicone films prepared with crystalline (Form A) or amorphous drug powders upon exposure to artificial perilymph at 37 °C. The optical microscopy pictures on the left-hand side show the respective drug powders.

Figure 3.27 shows the corresponding X-ray diffraction patterns (pink and black curves). As it can be seen, the milling process successfully transformed the crystalline Form A into an X-ray amorphous state. Using the 2 types of powders, dexamethasone-loaded silicone films were prepared (10 % w/w drug content). Figure 3.27 also shows the X-ray diffraction patterns of these films (green and red curves). Clearly, the polymorphic form of the crystalline dexamethasone (Form A) did not change during film manufacturing: Sharp diffraction peaks are located at the same angles for the green and pink curves. However, the silicone films prepared with amorphous dexamethasone exhibited also sharp diffraction peaks (red curve). The latter cannot be attributed to the silicone (which was amorphous). Furthermore, the peak

positions did not correspond to those of crystalline dexamethasone *Form A* (which was used for film preparation, pink curve in Figure 3.27). But they corresponded to the diffraction peaks of crystalline dexamethasone *Form B* (blue curve in Figure 3.27). This indicates that the amorphous dexamethasone used for film preparation was at least partially transformed into the crystalline Form B during manufacturing and/or storage prior to the X-ray measurements.

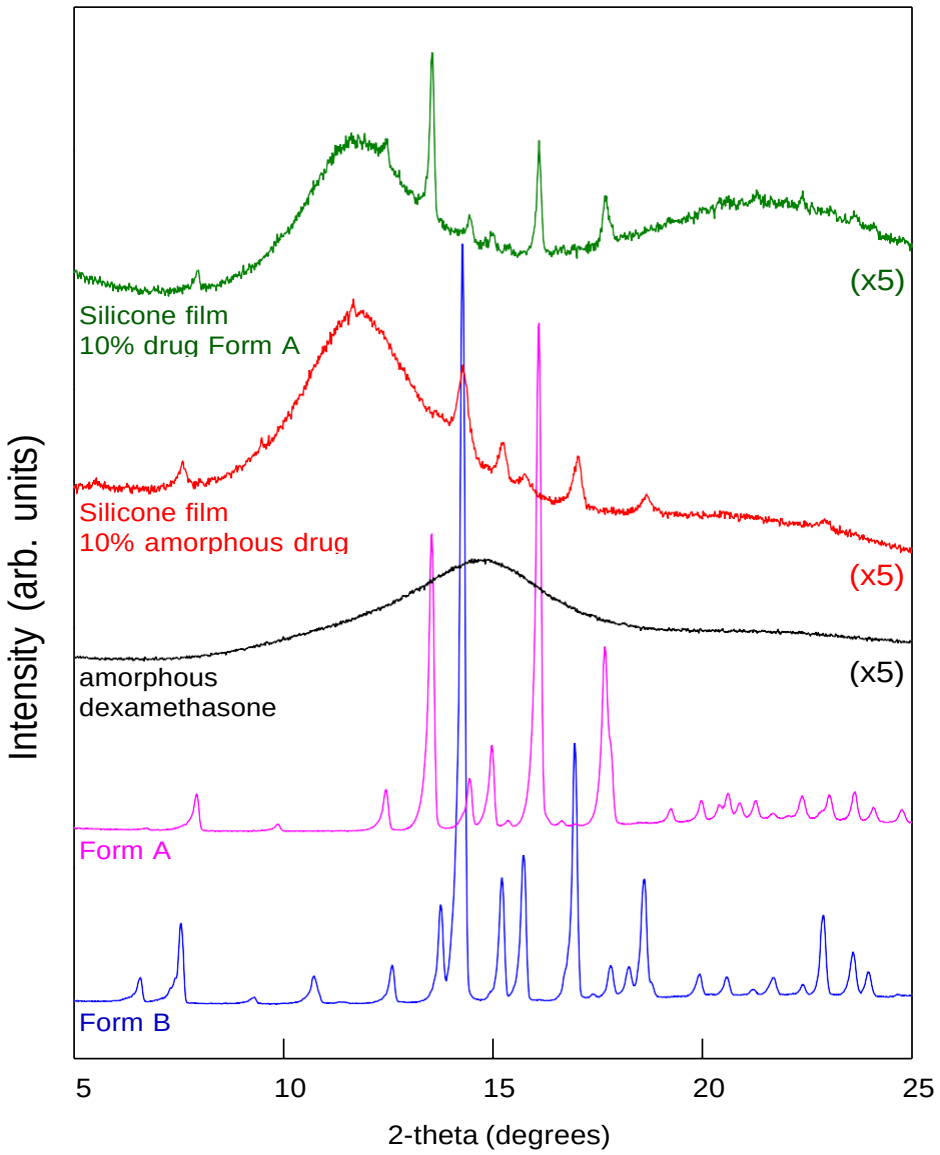

Figure 3.27. X-ray diffraction patterns of silicone films prepared with amorphous or crystalline (Form A) dexamethasone powder. For reasons of comparison, also the X-ray diffraction patterns of the dexamethasone powders used for film preparation are shown (crystalline Form A and amorphous), as well as crystalline Form B.

The DSC thermograms shown in Figure 3.28 indicate that this solid state transformation was not complete: The behavior of a silicone film prepared with 10 % amorphous dexamethasone upon heating to about 190 °C is illustrated. For reasons of comparison, also the thermogram of amorphous drug is shown. In both cases, multiple endothermic events were visible, likely indicating recrystallisation. The fact that not only one single recrystallisation event was observed might be attributable to the fact that differences in the size of the drug particles can potentially affect the energies required to initiate this process. The green curve in Figure 3.28 shows the thermal behavior of a silicone film prepared with dexamethasone Form A crystals: No signs for physical state transformations are visible until the substance melts at about 250 °C (corresponding to the endothermic event observed with crystalline dexamethasone Form A reference substance, pink curve).

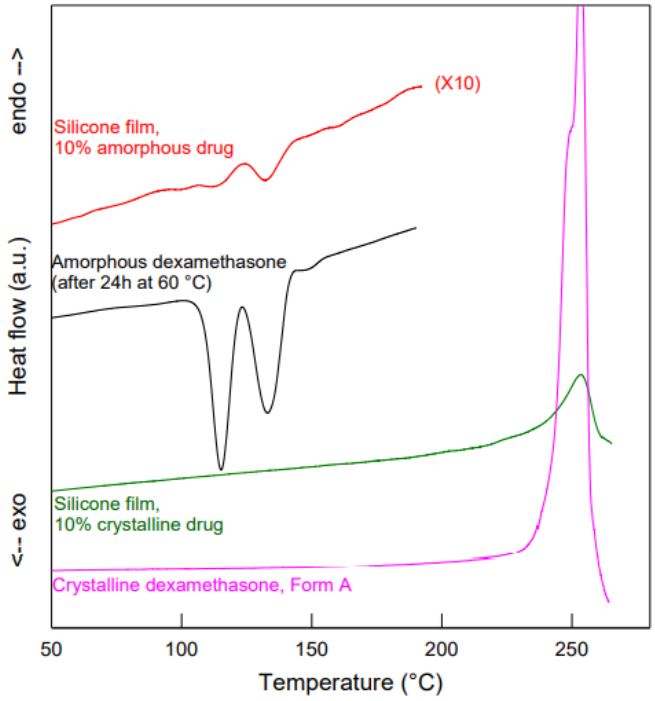

Figure 3.28. DSC thermograms of silicone films prepared with amorphous or crystalline (Form A) dexamethasone powder. For reasons of comparison, also the DSC thermograms of crystalline dexamethasone (Form A) and amorphous drug powder (upon heating to 60 °C for 24 h = treatment to assure complete silicone cross-linking in films) are shown.

Importantly, the above discussed transformations of the physical state of the drug did not affect the resulting dexamethasone release kinetics from silicone films, as shown in Figure 3.26: The drug release patterns were similar from films prepared with crystalline dexamethasone Form A (filled triangles) and from films prepared with amorphous drug (open circles), which at least partially re-crystallized into the polymorphic Form B. The absence of any noteworthy effect on drug release might be explained by the fact that other phenomena than limited drug solubility effects are release rate controlling, or that the differences in drug solubility of the respective forms are not sufficiently important to be visible, and/or that the less soluble form rather rapidly reprecipitates during drug release. It was beyond the scope of this study to investigate this aspect in more detail. From a practical point of view, it is most important that this type of formulation can be expected to be rather robust ("forgiving") with respect to the physical state of the drug in the formulation.

3.3.2. Films prepared with different drug batches and different thickness

To evaluate the potential sensitivity of the key properties of dexamethasone-loaded silicone matrices (drug release and swelling behavior) to batch-to-batch variability of the drug raw material and variations in the film thickness, different types of films were prepared with 2 drug batches (Batch 2 and Batch 3, used as received from the supplier) and about 0.35 vs. 2 mm thickness. The optical microscopy pictures in Figure 3.29 show that there were no noteworthy differences in the particle sizes of the two drug batches (being in the lower micrometer size range).

Batch 2

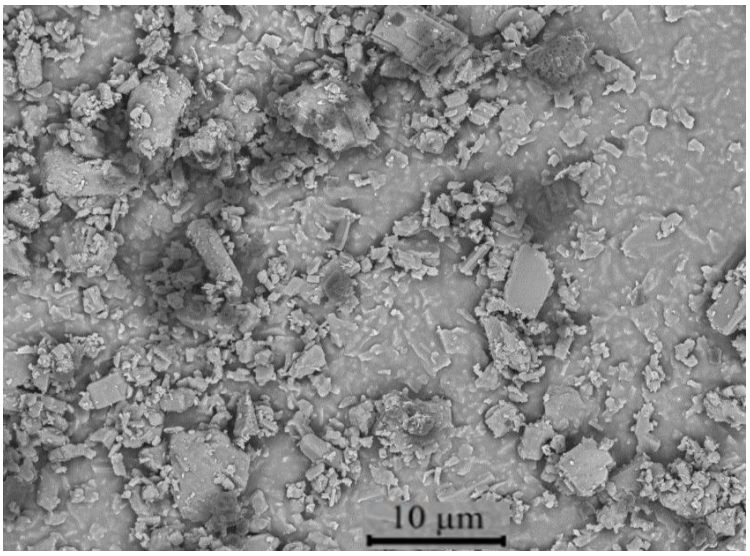

Batch 3

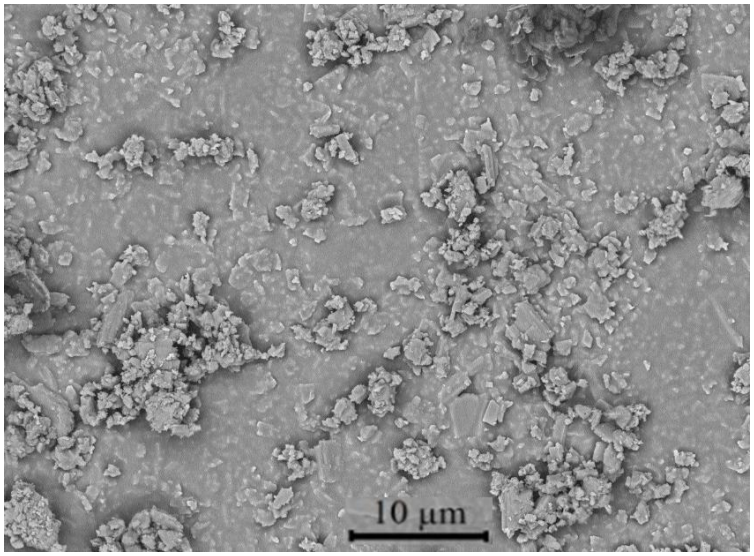

Figure 3.29. SEM pictures of dexamethasone powder samples (as received) of Batch 2 and Batch 3.

Interestingly, the two drug batches consisted of a blend of dexamethasone Form A and dexamethasone Form B (Form A being dominant), in contrast to Batch 1: Figure 3.30 shows the X-ray diffraction patterns of the 3 drug batches, together with the reference patterns of dexamethasone Form A and Form B. As it can be seen, the peaks of Batch 1 correspond well to the peaks of dexamethasone Form A, whereas the peaks visible in drug Batches 2 and 3 correspond to the peaks of *both* polymorphic forms: A and B (the dashed pink and blue lines are intended to help comparing key peaks of the two crystal forms).

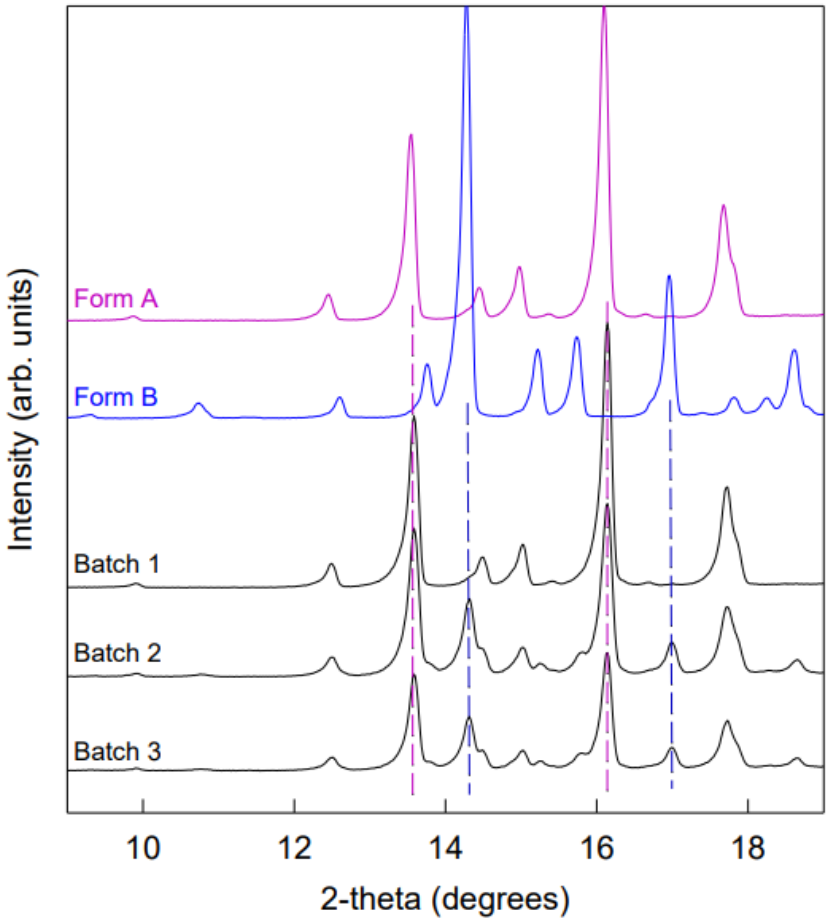

Figure 3.30. X-ray diffraction patterns of the investigated 3 batches of dexamethasone (as received), exhibiting similar particle sizes in the lower micrometer range, but different crystalline forms. For reasons of comparison, also the X-ray diffraction patterns of crystalline dexamethasone (Forms A and B) reference powders are shown.

The resulting drug release kinetics from “thinner” (about 350 µm, dotted curves) and “thicker” (about 2 mm, solid curves) silicone films loaded with 10 % drug, prepared with the drug Batches 2 and 3 are shown in Figure 3.31: At the top, the observed *absolute* drug release rates are illustrated, at the bottom the respective *relative* drug release rates. Clearly, the drug batch had no noteworthy impact on the resulting drug release kinetics in this case, irrespective of the film thickness. Comparing the solid and dashed curves in the upper diagram in Figure 3.31, it is visible that the *absolute* drug release rates are higher for “thicker” than for “thinner” films. This can be explained by the higher surface area available for diffusion (2.8 cm^2 versus 2.14 cm^2). In contrast, the *relative* drug release rates are lower from the “thicker” films than from the “thinner” films (solid versus dashed curves in the bottom diagram in Figure 3.31). This is because of the different 100 % reference values (total drug loadings) of the film samples (and, in the long run, due to the prolonged diffusion pathway lengths for drug located in the center of the films).

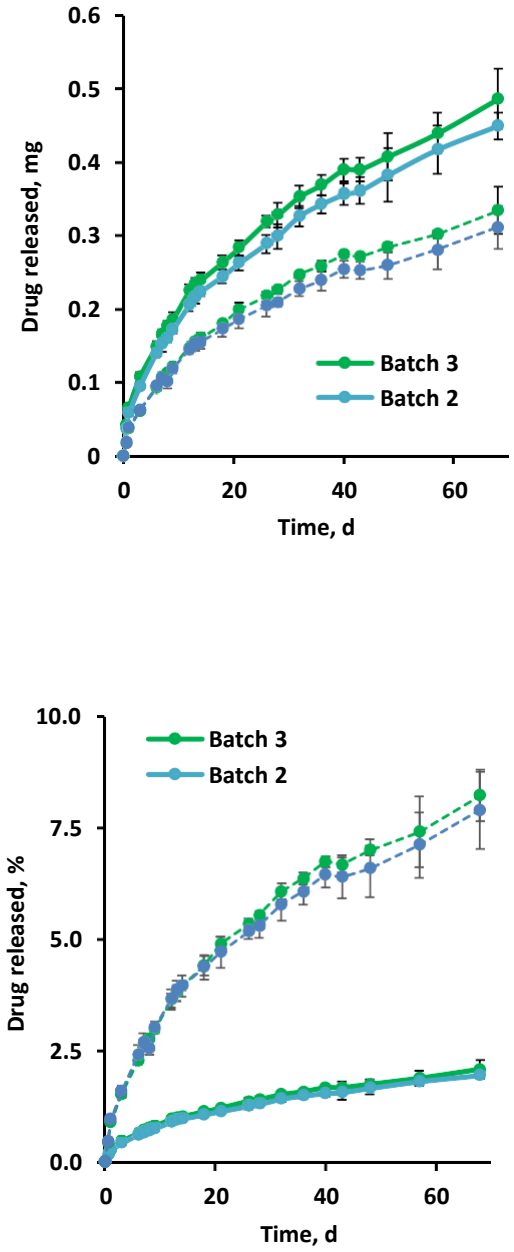

Figure 3.31. Dexamethasone release from silicone films in artificial perilymph. "Thinner" (about 350 µm, dashed curves) and "thicker" (about 2 mm, solid curves) films were studied. In each case, 2 different batches of dexamethasone (Batches 2 and 3) were used for film preparation. At the top, the cumulative *absolute* amounts of drug release are shown, at the bottom the respective *relative* amounts of drug.

Figure 3.32 shows the swelling behavior of the “thinner” and “thicker” silicone films loaded with 10 % dexamethasone, prepared with drug Batches 2 and 3. The films were exposedto artificial perilymph for 68 d at 37 °C. The top row illustrates the wet mass (%), the bottom row the film thickness (%). The 100 % reference values are the film mass and thickness before exposure to the release medium. Clearly, there were no signs for noteworthy film swelling or shrinkage, irrespective of the film thickness and drug batch. From a practical point of view, thiscan be a crucial aspect: For instance, if the drug delivery system is placed into the inner ear, significant device swelling can damage the highly sensitive organ.

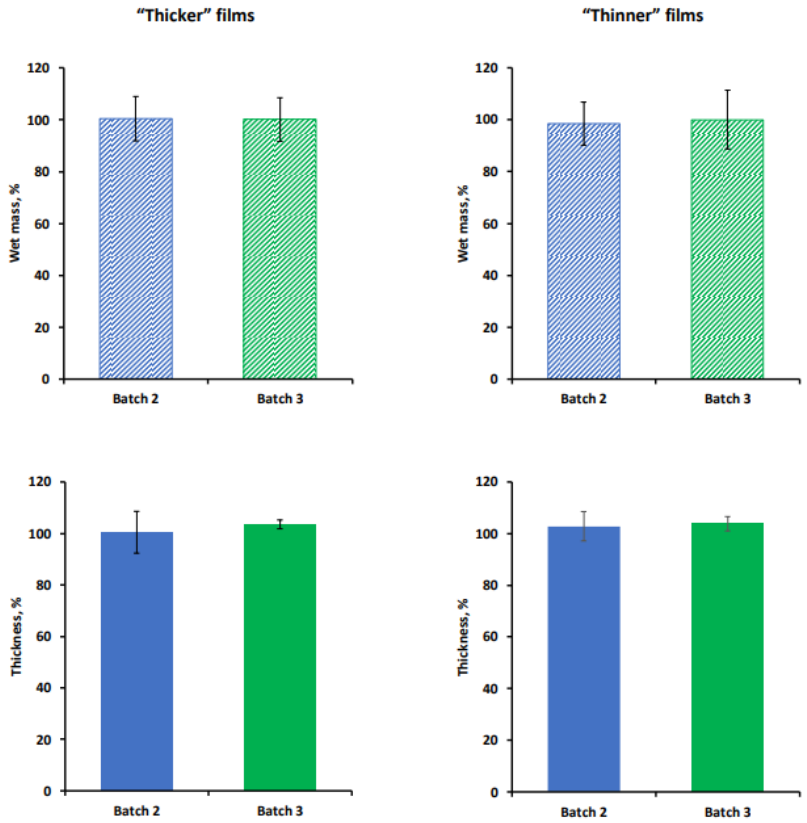

Figure 3.32. Absence of noteworthy film swelling or shrinking upon exposure artificial perilymph: Wet mass (%) and film thickness (%) of the films after 68 d exposure at 37 °C. The 100 % reference values are the initial sample mass and thickness. On the x-axes, the drug batches used for film preparation are indicated. Mean values +/- SD are reported.

3.3.3. Raman imaging before and during drug release

To better understand how drug release is controlled from the investigated silicone matrices, Raman imaging was applied. The diagram on the left hand-side of Figure 3.33 shows the Raman spectra of dexamethasone and silicone. As it can be seen, multiple Raman bands are located at different frequencies, allowing to distinguish between the two substances. On the right hand-side of Figure 3.33, an optical microscopy picture (top) and the corresponding Raman image of the surface of a silicone film before exposure to the release medium are shown. The film was loaded with 10 % dexamethasone (prepared with crystalline drug, Batch 1: Form A). The film was divided into small pixels and the Raman spectrum of each pixel was recorded. A linear combination of the spectra of dexamethasone and silicone was fitted to the spectra of each pixel using the DCLS (Direct Classical Least Square) method. This allowed identifying pixels rich in silicone, marked in green, and pixels rich in dexamethasone, marked in red in Figure 3.33 (false colours). As it can be seen, certain surface regions are particularly rich in drug. When comparing the optical microscopy picture and Raman image in Figure 3.33, it seems that these drug-rich regions correspond to zones with dexamethasone crystals.

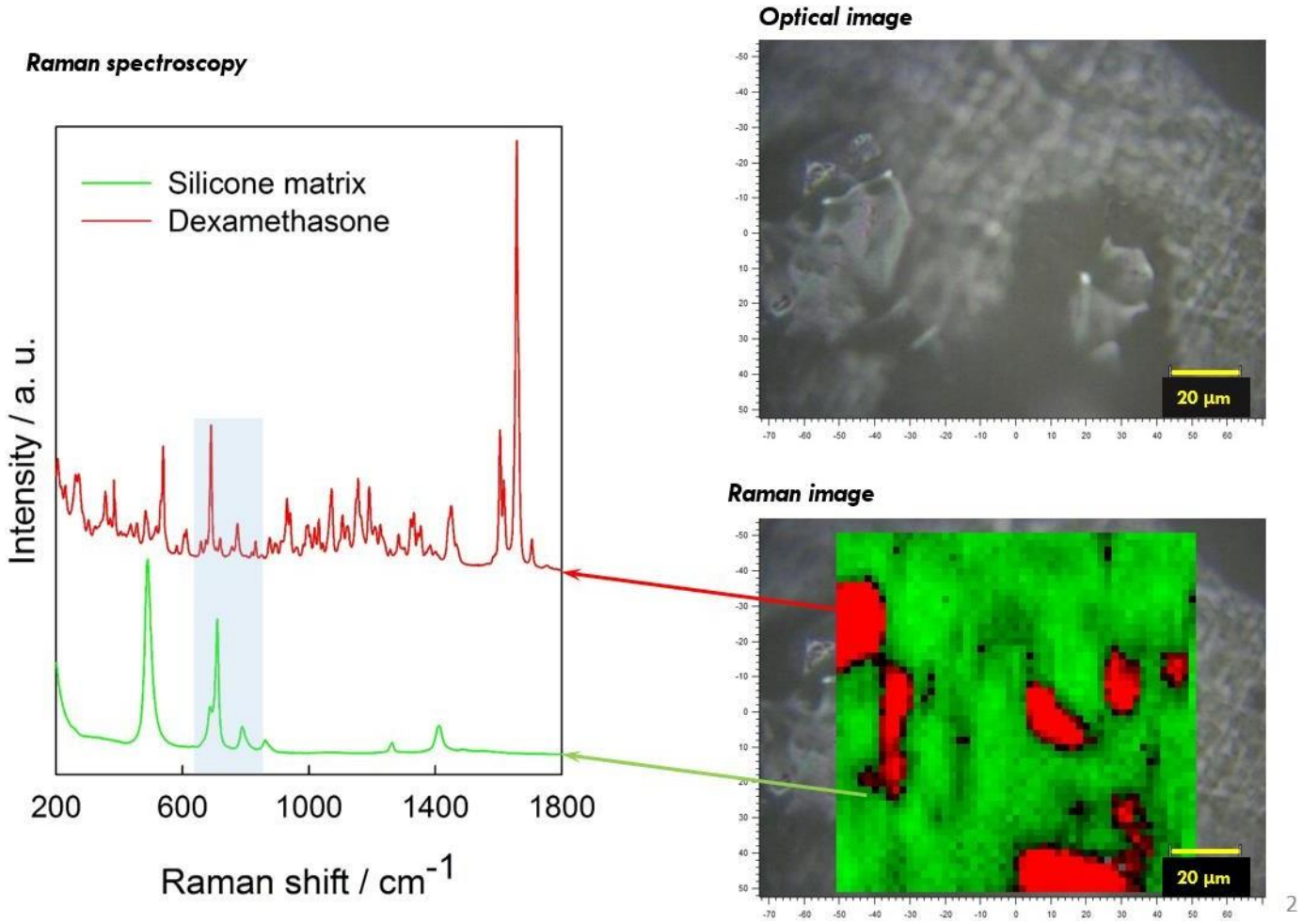

Figure 3.33. Left-hand side: Raman spectra of silicone and dexamethasone. Right-hand side: Optical microscopy picture and Raman image of the surface of a silicone film loaded with 10 % dexamethasone (prepared with crystalline drug, Batch 1: Form A) *before* exposure to the release medium. Silicone-rich regions are marked in green, dexamethasone-rich regions in red (false colors).

Figure 3.34 shows series of optical microscopy pictures and Raman images of a specific surface region of a silicone film initially loaded with 10 % crystalline drug (Batch 1: Form A) before and after exposure to artificial perilymph at 37 °C. The exposure times are indicated in the left hand-side. The aim was to analyze the same film region at each time point. This at least partially succeeded: The black circles in the Raman images at the top highlight the same drug particles. The numbers correspond to specific drug particles, which

could be recognized at different time points. It must be pointed out that the Raman measurements detect dexamethasone up to a depth of about 20-25 µm. Thus, drug crystals visible in the top row of Figure 3.33 (before exposure to the release medium) might be directly located at the films surface, or might be separated from the surface by a thin silicone layer. This explains why not all dexamethasone particles disappear upon exposure to the artificial perilymph: Only those with direct surface access (an, thus direct contact with water) can rapidly dissolve. Looking at Figure 3.34, it seems that the majority of the drug crystals does not have immediate surface access and remains within the film during the observation period. This is in good agreement with the very slow drug release observed from these films (please see above). Please also notethat the film samples were dried prior to Raman imaging. Thus, dissolved drug might have precipitated in the 20-25 µm outer film surface layer ("being on its way to diffuse out of the film").

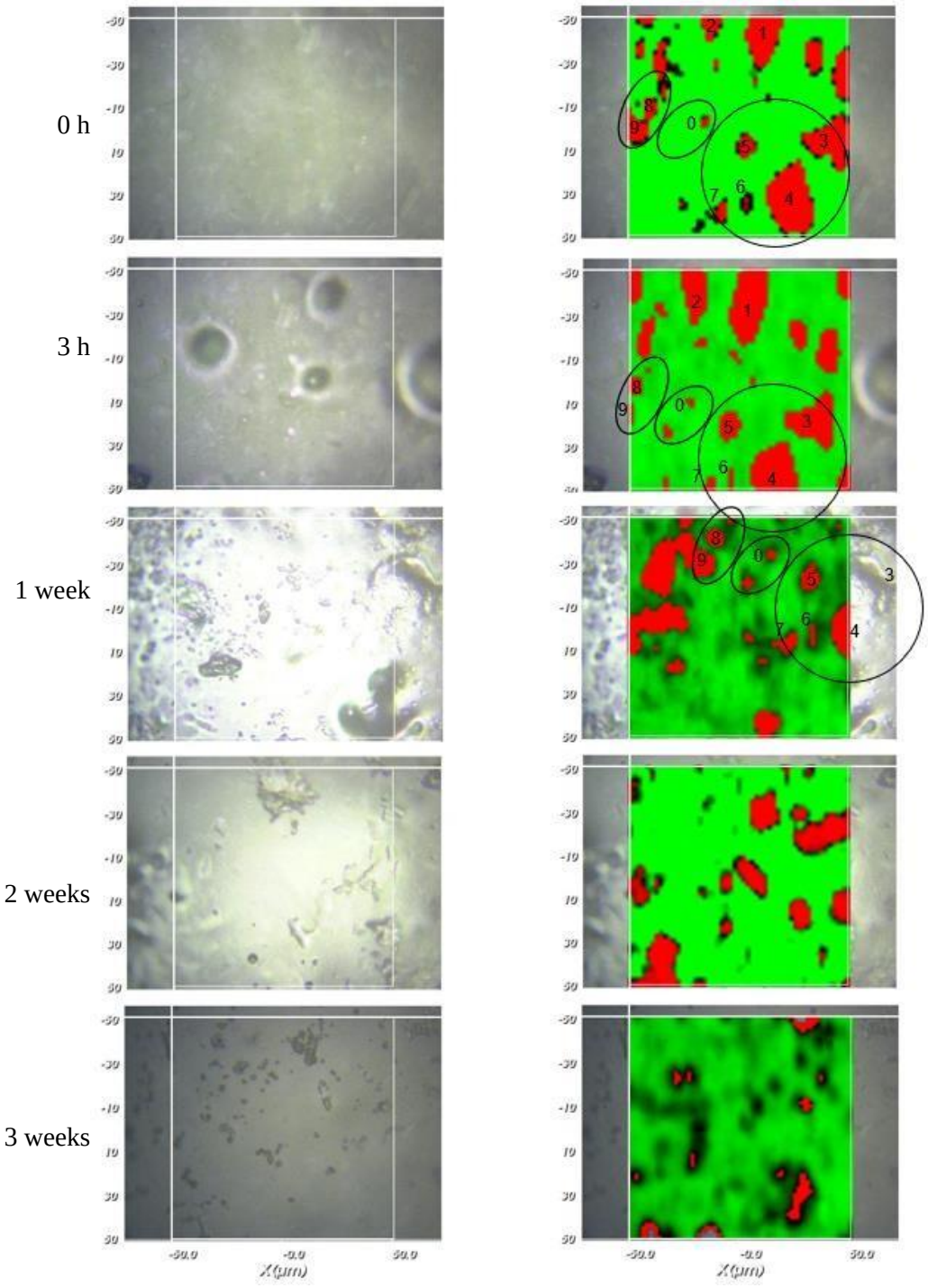

Figure 3.34. Optical microscopy pictures (left column) and Raman images (right column) of silicone films initially loaded with 10 % dexamethasone (prepared with crystalline drug, Batch 1: Form A) *after different exposure times* to artificial perilymph at 37 °C (as indicated on the left hand-side). The numbers and circles highlight examples of specific locations, which are the same at different time points. Silicone-rich regions are marked in green, dexamethasone-rich regions in red (false colors).

It has recently been shown that also the Raman spectrum of dexamethasone *phosphate* shows distinct differences in its Raman bands compared to dexamethasone and silicone. Thus, Raman imaging allows distinguishing between the 3 compounds and identifying pixel particularly rich in silicone, dexamethasone or dexamethasone phosphate. Figure 3.35 shows an optical microscopy picture and a Raman image of a silicone film loaded with 10 % dexamethasone and 1 % dexamethasone phosphate before exposure to the release medium. Both drugs were crystalline (dexamethasone Batch 1: Form A was used for the preparation). Silicone-rich regions are marked in green, dexamethasone-rich regions in blue and dexamethasone *phosphate*-rich regions in red (false colors). Interestingly, the dexamethasone and dexamethasone phosphate particles seem to be located in the same regions. This can probably be explained by the fact that both types of drug particles do not have a high affinity towards the investigated silicone (neither to the compounds used for film preparation: Parts A and B of the MED-4735 kits). To reduce the contact surface area "drug – silicone", the drug particles partially agglomerated. This is important information for the underlying drug release mechanism: Once an interconnected drug particle network gets access to the films surface (e.g., via a water-filled pore), it can be expected that all "connected" particles can rather rapidly diffuse out into the surrounding bulk fluid.

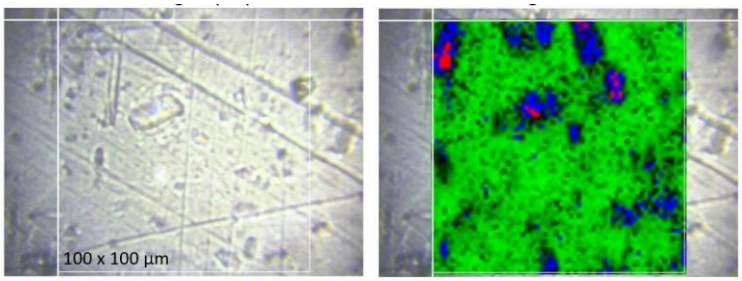

Figure 3.35. Optical microscopy picture (left) and Raman image (right) of the surface of a silicone film loaded with 10 % dexamethasone and 1 % dexamethasone phosphate (both crystalline, dexamethasone Batch 1: Form A) *before* exposure to the release medium. Silicone-rich regions are marked in green, dexamethasone-rich regions in blue and dexamethasone phosphate-rich regions in red (false colors).

Figure 3.36 shows an optical microscopy picture and Raman image of a silicone film loaded with 1 % dexamethasone (Batch 1: Form A) and 10 % dexamethasone phosphate before exposure to the release medium. So, the dexamethasone: dexamethasone *phosphate* ratio was inversed compared to the film illustrated in Figure 3.35 (1:10 instead of 10:1). The dominance of dexamethasone phosphate compared to dexamethasone is clearly visible in this outer film layer. This can be expected to have important consequences for the resulting drug release kinetics: Dexamethasone phosphate is much more soluble in water than dexamethasone. Thus, it likely attracts more water into the system upon exposure to the artificial perilymph. It has recently been shown that, in fact, the addition of small amounts of dexamethasone phosphate to dexamethasone loaded silicone films increases the "initial burst release".

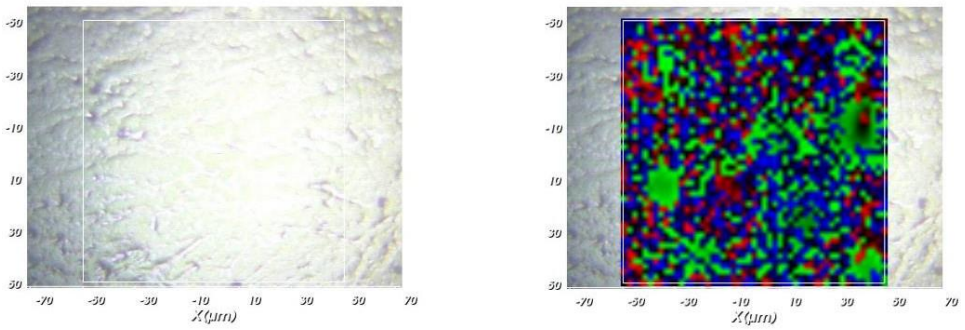

Figure 3.36. Optical microscopy picture (left) and Raman image (right) of the surface of a silicone film loaded with 1 % dexamethasone (Batch 1: Form A) and 10 % dexamethasone phosphate *before* exposure to the release medium. Silicone is marked in green, dexamethasone in blue and dexamethasone phosphate in orange (false colors).

This is consistent with the Raman images shown in Figure 3.37 of a silicone film initially loaded with 10 % dexamethasone *phosphate before and after* different exposure times to artificial perilymph at 37 °C. Before exposure to the release medium, large drug clusters canbe seen, even larger than those observed with dexamethasone (e.g., Figures 3.33 and Figure 3.34). This might be explained by the higher hydrophilicity of dexamethasone *phosphate* compared to dexamethasone, silicone being hydrophobic. Interestingly, after 1 week exposure to the artificial perilymph, no drug is detectable

anymore. This contrasts with the observed behavior of dexamethasone (which could still be detected in considerable amounts at this timepoint, Figure 3.34). The reason is likely the higher hydrophilicity of this drug, attracting more water into the system.

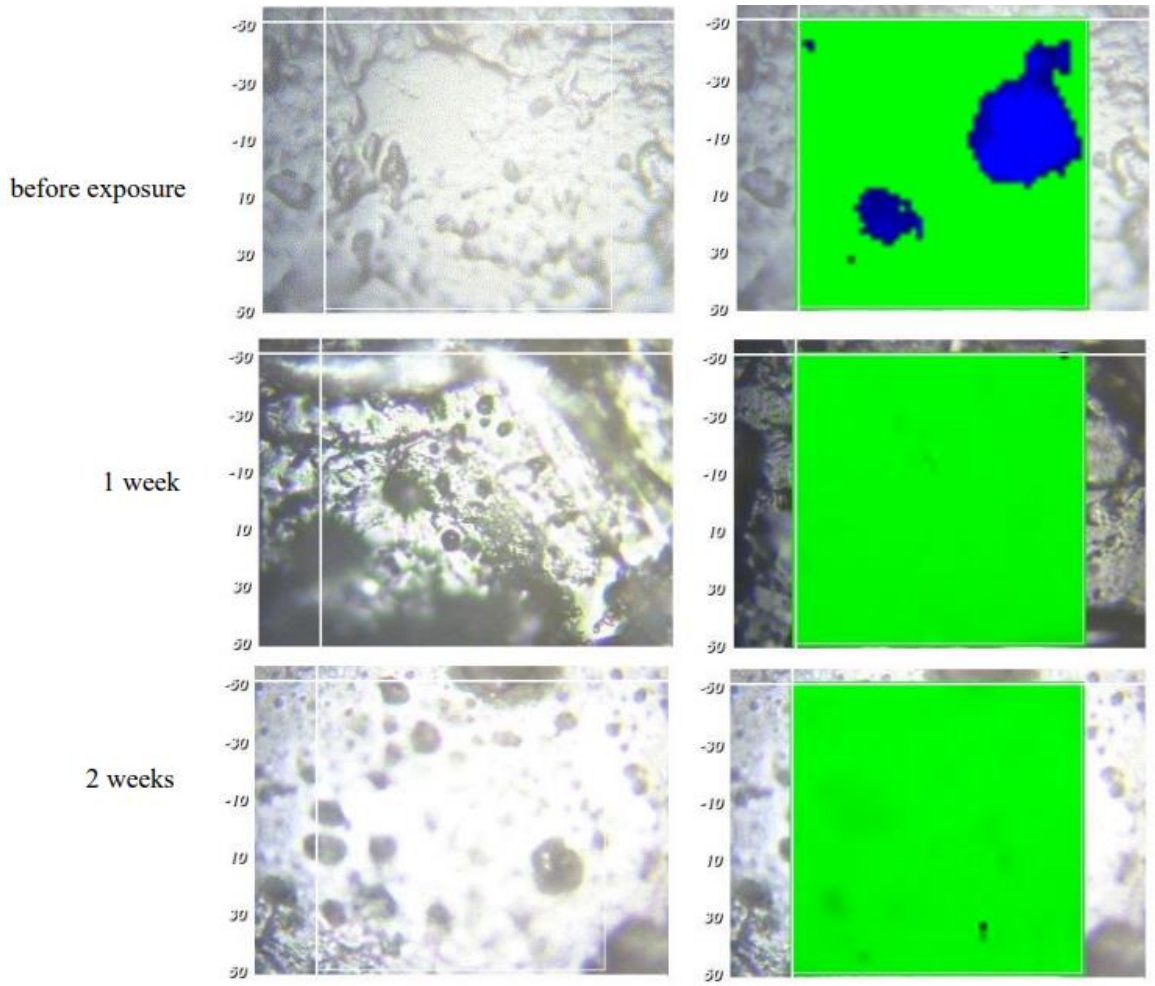

Figure 3.37. Optical microscopy pictures (left column) and Raman images (right column) of silicone films initially loaded with 10 % dexamethasone phosphate *before and after different exposure times* to artificial perilymph at 37 °C (as indicated on the left hand-side, scales are in µm). Silicone is marked in green, dexamethasone phosphate in orange (false colors).

4. Conclusion

The addition of small amounts of dexamethasone phosphate to silicone-based miniaturized cochlear implants for controlled dexamethasone release can effectively increase the initial burst release. This is expected to be beneficial for the patient, since it can help: (i) to limit local trauma and inflammation caused by the invasive insertion of the electrode array, and (ii) to limit the formation of fibrotic tissue around the foreign body (fibrosis decreasing the performance of the implants, as the transmission of electrical signals is hindered). The effect on drug release can be explained by the more hydrophilic nature of the prodrug dexamethasone phosphate compared to its parent drug dexamethasone, facilitating water penetration into the system and hence, drug dissolution and diffusion. Importantly, at limited dexamethasone phosphate contents, implant swelling remains clinically acceptable.

Moreover, silicone-based cochlear implants can reliably control dexamethasone release over several years. Diffusional mass transport combined with drug saturation effects *within* the implants seem to play a major role. The polymeric matrix being hydrophobic, only limited amounts of water are available for dexamethasone dissolution inside the implants. The drug is initially homogeneously distributed throughout the devices in the form of tiny dexamethasone crystals. With time, first surface-near regions become depleted of drug (in vitro as well as in vivo), as evidenced by optical microscopy and Raman imaging. Importantly, the implants do not swell or shrink to a noteworthy extent upon exposure to living tissue or artificial perilymph for several years.

References

(1) Chan, Y.; Goddard, J. C. *K.J. Lee's Essential Otolaryngology: Head and Neck Surgery*; 2019.

(2) Chittka, L.; Brockmann, A. Perception Space—The Final Frontier. *PLoS Biol.* **2005**, *3* (4), e137. https://doi.org/10.1371/journal.pbio.0030137.

(3) Gelfand, S. A. *Essentials of Audiology*, 3rd ed.; Thieme: New York, 2009.

(4) Robles, L.; Ruggero, M. A. Mechanics of the Mammalian Cochlea. *Physiol. Rev.* **2001**, *81* (3), 1305–1352. https://doi.org/10.1152/physrev.2001.81.3.1305.

(5) Thorne, M.; Salt, A. N.; DeMott, J. E.; Henson, M. M.; Henson, O. W.; Gewalt, S. L. Cochlear Fluid Space Dimensions for Six Species Derived From Reconstructions of Three-Dimensional Magnetic Resonance Images. *The Laryngoscope* **1999**, *109* (10), 1661–1668. https://doi.org/10.1097/00005537-199910000-00021.

(6) El Kechai, N.; Agnely, F.; Mamelle, E.; Nguyen, Y.; Ferrary, E.; Bochot, A. Recent Advances in Local Drug Delivery to the Inner Ear. *Int. J. Pharm.* **2015**, *494* (1), 83–101. https://doi.org/10.1016/j.ijpharm.2015.08.015.

(7) Lawton, B. W.; Great Britain; Health and Safety Executive. *Damage to Human Hearing by Airborne Sound of Very High Frequency or Ultrasonic Frequency.*; Great Britain, Health and Safety Executive, 2001.

(8) Neurones.co.uk http://neurones.co.uk/Neurosciences/Tutorials/M4/M.4.2c%20Auditory%20Pathway.html (accessed Sep 27, 2020).

(9) Hickok, G.; Poeppel, D. The Cortical Organization of Speech Processing. *Nat. Rev. Neurosci.* **2007**, *8* (5), 393–402. https://doi.org/10.1038/nrn2113.

(10) Hughes, G. B.; Freedman, M. A.; Haberkamp, T. J.; Guay, M. E. Sudden Sensorineural Hearing Loss. *Otolaryngol. Clin. North Am.* **1996**, *29* (3), 393–405. https://doi.org/10.1016/S0030-6665(20)30362-5.

(11) Rabinowitz, P. Noise-Induced Hearing Loss. *Am. Fam. Physician* **2000**, *61* (9), 2749–2756.

(12) Lopez-Escamez, J. A.; Carey, J.; Chung, W.-H.; Goebel, J. A.; Magnusson, M.; Mandalà, M.; Newman-Toker, D. E.; Strupp, M.; Suzuki, M.; Trabalzini, F.; Bisdorff, A. Diagnostic Criteria for Menière's Disease. *J. Vestib. Res.* **2015**, *25* (1), 1–7. https://doi.org/10.3233/VES-150549.

(13) Waters, F.; Blom, J. D.; Jardri, R.; Hugdahl, K.; Sommer, I. E. C. Auditory Hallucinations, Not Necessarily a Hallmark of Psychotic Disorder. *Psychol. Med.* **2018**, *48* (4), 529–536. https://doi.org/10.1017/S0033291717002203.

(14) Brophy-Williams, S.; Jarosz, K.; Sommer, J.; Leach, A. J.; Morris, P. S. Preventative and Medical Treatment of Ear Disease in Remote or Resource-Constrained Environments. *J. Laryngol. Otol.* **2019**, *133* (1), 59–72. https://doi.org/10.1017/S0022215119000057.

(15) Volandri, G.; Di Puccio, F.; Forte, P.; Carmignani, C. Biomechanics of the Tympanic Membrane. *J. Biomech.* **2011**, *44* (7), 1219–1236. https://doi.org/10.1016/j.jbiomech.2010.12.023.

(16) Hao, J.; Li, S. K. Inner Ear Drug Delivery: Recent Advances, Challenges, and Perspective. *Eur. J. Pharm. Sci. Off. J. Eur. Fed. Pharm. Sci.* **2019**, *126*, 82–92. https://doi.org/10.1016/j.ejps.2018.05.020.

(17) Ren, Y.; Landegger, L. D.; Stankovic, K. M. Gene Therapy for Human Sensorineural Hearing Loss. *Front. Cell. Neurosci.* **2019**, *13*, 323. https://doi.org/10.3389/fncel.2019.00323.

(18) Thomson, S.; Madani, G. The Windows of the Inner Ear. *Clin. Radiol.* **2014**, *69* (3), e146–e152. https://doi.org/10.1016/j.crad.2013.10.020.

(19) Rask-Andersen, H.; Liu, W.; Erixon, E.; Kinnefors, A.; Pfaller, K.; Schrott-Fischer, A.; Glueckert, R. Human Cochlea: Anatomical Characteristics and Their Relevance for Cochlear Implantation. *Anat. Rec. Adv. Integr. Anat. Evol. Biol.* **2012**, *295* (11), 1791–1811. https://doi.org/10.1002/ar.22599.

(20) Gan, R. Z.; Feng, B.; Sun, Q. Three-Dimensional Finite Element Modeling of Human Ear for Sound Transmission. *Ann. Biomed. Eng.* **2004**, *32* (6), 847–859. https://doi.org/10.1023/B:ABME.0000030260.22737.53.

(21) King, E. B.; Salt, A. N.; Eastwood, H. T.; O'Leary, S. J. Direct Entry of Gadolinium into the Vestibule Following Intratympanic Applications in Guinea Pigs and the Influence of Cochlear Implantation. *J. Assoc. Res. Otolaryngol.* **2011**, *12* (6), 741–751. https://doi.org/10.1007/s10162-011-0280-5.

(22) King, E. B.; Salt, A. N.; Kel, G. E.; Eastwood, H. T.; O'Leary, S. J. Gentamicin Administration on the Stapes Footplate Causes Greater Hearing Loss and Vestibulotoxicity than Round Window Administration in Guinea Pigs. *Hear. Res.* **2013**, *304*, 159–166. https://doi.org/10.1016/j.heares.2013.07.013.

(23) Glueckert, R.; Johnson Chacko, L.; Rask-Andersen, H.; Liu, W.; Handschuh, S.; Schrott-Fischer, A. Anatomical Basis of Drug Delivery to the Inner Ear. *Hear. Res.* **2018**, *368*, 10–27. https://doi.org/10.1016/j.heares.2018.06.017.

(24) Juhn, S. K.; Rybak, L. P.; Fowlks, W. L. Transport Characteristics of the Blood—Perilymph Barrier. *Am. J. Otolaryngol.* **1982**, *3* (6), 392–396. https://doi.org/10.1016/S0196-0709(82)80016-1.

(25) Swan, E. E. L.; Mescher, M. J.; Sewell, W. F.; Tao, S. L.; Borenstein, J. T. Inner Ear Drug Delivery for Auditory Applications. *Adv. Drug Deliv. Rev.* **2008**, *60* (15), 1583–1599. https://doi.org/10.1016/j.addr.2008.08.001.

(26) Deafness https://www.britannica.com/science/deafness (accessed Sep 23, 2020).

(27) WHO | Hearing loss grades and the International classification of functioning, disability and health https://www.who.int/bulletin/volumes/97/10/BLT-19-230367-table-T1.html (accessed Sep 23, 2020).

(28) Different types of hearing loss | Oticon Medical https://www.oticonmedical.com/hearing-and-hearing-loss (accessed Sep 23, 2020).

(29) Deafness and hearing loss https://www.who.int/westernpacific/health-topics/hearing-loss (accessed Sep 23, 2020).

(30) Zahnert, T. The Differential Diagnosis of Hearing Loss. *Dtsch. Ärztebl. Int.* **2011**, *108* (25), 433–444. https://doi.org/10.3238/arztebl.2011.0433.

(31) Oroei, M.; Peyvandi, A. A.; Mokhtarinejad, F. Opioid Drugs and Sensorineural Hearing Loss. *Addict. Health* **2018**, *10* (1), 64–66. https://doi.org/10.22122/ahj.v10i1.560.

(32) Schacht, J.; Talaska, A. E.; Rybak, L. P. Cisplatin and Aminoglycoside Antibiotics: Hearing Loss and Its Prevention. *Anat. Rec. Hoboken NJ 2007* **2012**, *295* (11), 1837–1850. https://doi.org/10.1002/ar.22578.

(33) Cannizzaro, E.; Cannizzaro, C.; Plescia, F.; Martines, F.; Soleo, L.; Pira, E.; Coco, D. L. Exposure to Ototoxic Agents and Hearing Loss: A Review of Current Knowledge. *Hear. Balance Commun.* **2014**, *12* (4), 166–175. https://doi.org/10.3109/21695717.2014.964939.

(34) Kuhn, M.; Heman-Ackah, S. E.; Shaikh, J. A.; Roehm, P. C. Sudden Sensorineural Hearing Loss. *Trends Amplif.* **2011**, *15* (3), 91–105. https://doi.org/10.1177/1084713811408349.

(35) Lin, C.; Lin, S.-W.; Weng, S.-F.; Lin, Y.-S. Risk of Sudden Sensorineural Hearing Loss in Patients with Systemic Lupus Erythematosus: A Population-Based Cohort Study. *Audiol. Neurootol.* **2013**, *18* (2), 95–100. https://doi.org/10.1159/000345512.

(36) Hellmann, M. A.; Steiner, I.; Mosberg-Galili, R. Sudden Sensorineural Hearing Loss in Multiple Sclerosis: Clinical Course and Possible Pathogenesis. *Acta Neurol. Scand.* **2011**, *124* (4), 245–249. https://doi.org/10.1111/j.1600-0404.2010.01463.x.

(37) Mosnier, I.; Stepanian, A.; Baron, G.; Bodenez, C.; Robier, A.; Meyer, B.; Fraysse, B.; Bertholon, P.; Defay, F.; Ameziane, N.; Ferrary, E.; Sterkers, O.; de Prost, D. Cardiovascular and Thromboembolic Risk Factors in Idiopathic Sudden Sensorineural Hearing Loss: A Case-Control Study. *Audiol. Neurootol.* **2011**, *16* (1), 55–66. https://doi.org/10.1159/000312640.

(38) Hopkins, K. Chapter 27 - Deafness in Cochlear and Auditory Nerve Disorders. In *Handbook of Clinical Neurology*; Aminoff, M. J., Boller, F., Swaab, D. F., Eds.; The Human Auditory System; Elsevier, 2015; Vol. 129, pp 479–494. https://doi.org/10.1016/B978-0-444-62630-1.00027-5.

(39) Byl, F. M. Sudden Hearing Loss: Eight Years' Experience and Suggested Prognostic Table. *The Laryngoscope* **1984**, *94* (5 Pt 1), 647–661.

(40) Conlin, A. E.; Parnes, L. S. Treatment of Sudden Sensorineural Hearing Loss: I. A Systematic Review. *Arch. Otolaryngol. Neck Surg.* **2007**, *133* (6), 573–581. https://doi.org/10.1001/archotol.133.6.573.

(41) Wilson, W. R.; Byl, F. M.; Laird, N. The Efficacy of Steroids in the Treatment of Idiopathic Sudden Hearing Loss. A Double-Blind Clinical Study. *Arch. Otolaryngol. Chic. Ill 1960* **1980**, *106* (12), 772–776. https://doi.org/10.1001/archotol.1980.00790360050013.

(42) Cinamon, U.; Bendet, E.; Kronenberg, J. Steroids, Carbogen or Placebo for Sudden Hearing Loss: A Prospective Double-Blind Study. *Eur. Arch. Otorhinolaryngol.* **2001**, *258* (9), 477–480. https://doi.org/10.1007/s004050100366.

(43) Kubo, T.; Matsunaga, T.; Asai, H.; Kawamoto, K.; Kusakari, J.; Nomura, Y.; Oda, M.; Yanagita, N.; Niwa, H.; Uemura, T.; Komune, S. Efficacy of Defibrinogenation and Steroid Therapies on Sudden Deafness. *Arch. Otolaryngol. - Head Neck Surg.* **1988**, *114* (6), 649–652. https://doi.org/10.1001/archotol.1988.01860180063031.

(44) Nageris, B. I.; Ulanovski, D.; Attias, J. Magnesium Treatment for Sudden Hearing Loss. *Ann. Otol. Rhinol. Laryngol.* **2004**, *113* (8), 672–675. https://doi.org/10.1177/000348940411300814.

(45) Joachims, H. Z.; Segal, J.; Golz, A.; Netzer, A.; Goldenberg, D. Antioxidants in Treatment of Idiopathic Sudden Hearing Loss: *Otol. Neurotol.* **2003**, *24* (4), 572–575. https://doi.org/10.1097/00129492-200307000-00007.

(46) Topuz, E.; Yigit, O.; Cinar, U.; Seven, H. Should Hyperbaric Oxygen Be Added to Treatment in Idiopathic Sudden Sensorineural Hearing Loss? *Eur. Arch. Otorhinolaryngol.* **2004**, *261* (7). https://doi.org/10.1007/s00405-003-0688-6.

(47) Shemirani, N. L.; Schmidt, M.; Friedland, D. R. Sudden Sensorineural Hearing Loss: An Evaluation of Treatment and Management Approaches by Referring Physicians. *Otolaryngol.--Head Neck Surg. Off. J. Am. Acad. Otolaryngol.-Head Neck Surg.* **2009**, *140* (1), 86–91. https://doi.org/10.1016/j.otohns.2008.09.022.

(48) Merchant, S. N.; Durand, M. L.; Adams, J. C. Sudden Deafness: Is It Viral? *ORL* **2008**, *70* (1), 52–62. https://doi.org/10.1159/000111048.

(49) Wei, B. P. C.; Mubiru, S.; O'Leary, S. Steroids for Idiopathic Sudden Sensorineural Hearing Loss. *Cochrane Database Syst. Rev.* **2006**, No. 1, CD003998. https://doi.org/10.1002/14651858.CD003998.pub2.

(50) R. J. Stokroos, E. M. T., F. W. J. Albers. Antiviral Treatment of Idiopathic Sudden Sensorineural Hearing Loss: A Prospective, Randomized, Double-Blind Clinical Trial. *Acta Otolaryngol. (Stockh.)* **1998**, *118* (4), 488–495. https://doi.org/10.1080/00016489850154603.

(51) Treatment of Idiopathic Sudden Sensorineural Hearing Loss with Antiviral Therapy: A Prospective, Randomized, Double-Blind Clinical Trial - Boris Olivier Westerlaken, Robert Jan Stokroos, Hero Piet Wit, Inge Johanna Maria Dhooge, Frans Willem Jan Albers, 2003 https://journals.sagepub.com/doi/10.1177/000348940311201113 (accessed Sep 24, 2020).

(52) Tucci, D. L.; Farmer, J. C. J.; Kitch, R. D.; Witsell, D. L. Treatment of Sudden Sensorineural Hearing Loss with Systemic Steroids and Valacyclovir. *Otol. Neurotol.* **2002**, *23* (3), 301–308.

(53) Uri, N.; Doweck, I.; Cohen-Kerem, R.; Greenberg, E. Acyclovir in the Treatment of Idiopathic Sudden Sensorineural Hearing Loss. *Otolaryngol.--Head Neck Surg. Off. J. Am. Acad. Otolaryngol.-Head Neck Surg.* **2003**, *128* (4), 544–549. https://doi.org/10.1016/s0194-5998(03)00004-4.

(54) Blanchemain, N.; Siepmann, F.; Siepmann, J. Implants pour la délivrance de principes actifs. *médecine/sciences* **2017**, *33* (1), 32–38. https://doi.org/10.1051/medsci/20173301006.

(55) Salt, A. N.; Plontke, S. K. Pharmacokinetic Principles in the Inner Ear: Influence of Drug Properties on Intratympanic Applications. *Hear. Res.* **2018**, *368*, 28–40. https://doi.org/10.1016/j.heares.2018.03.002.

(56) Hahn, H.; Kammerer, B.; DiMauro, A.; Salt, A. N.; Plontke, S. K. Cochlear Microdialysis for Quantification of Dexamethasone and Fluorescein Entry into Scala Tympani during Round Window Administration. *Hear. Res.* **2006**, *212* (1–2), 236–244. https://doi.org/10.1016/j.heares.2005.12.001.

(57) Herraiz, C.; Miguel Aparicio, J.; Plaza, G. [Intratympanic drug delivery for the treatment of inner ear diseases]. *Acta Otorrinolaringol. Esp.* **2010**, *61* (3), 225–232. https://doi.org/10.1016/j.otorri.2009.03.008.

(58) Ng, J. H.; Ho, R. C. M.; Cheong, C. S. J.; Ng, A.; Yuen, H. W.; Ngo, R. Y. S. Intratympanic Steroids as a Salvage Treatment for Sudden Sensorineural Hearing Loss? A Meta-Analysis. *Eur. Arch. Oto-Rhino-Laryngol. Off. J. Eur. Fed. Oto-Rhino-Laryngol. Soc. EUFOS Affil. Ger. Soc. Oto-Rhino-Laryngol. - Head Neck Surg.* **2015**, *272* (10), 2777–2782. https://doi.org/10.1007/s00405-014-3288-8.

(59) Garavello, W.; Galluzzi, F.; Gaini, R. M.; Zanetti, D. Intratympanic Steroid Treatment for Sudden Deafness: A Meta-Analysis of Randomized Controlled Trials. *Otol. Neurotol.* **2012**, *33* (5), 724–729. https://doi.org/10.1097/MAO.0b013e318254ee04.

(60) In-office-Intra-tympanic-steroid-therapy.jpg (836×646) https://melbentgroup.com.au/wp-content/uploads/2019/12/In-office-Intra-tympanic-steroid-therapy.jpg (accessed Sep 27, 2020).

(61) Alles, M. J. R. C.; der Gaag, M. A.; Stokroos, R. J. Intratympanic Steroid Therapy for Inner Ear Diseases, a Review of the Literature. *Eur. Arch. Oto-Rhino-Laryngol. Head Neck* **2006**, *263* (9), 791–797. https://doi.org/10.1007/s00405-006-0065-3.

(62) Silverstein, H. Use of a New Device, the MicroWick, to Deliver Medication to the Inner Ear. *Ear. Nose. Throat J.* **1999**, *78* (8), 595–598, 600.

(63) Barriat, S.; van Wijck, F.; Staecker, H.; Lefebvre, P. P. Intratympanic Steroid Therapy Using the Silverstein Microwick™ for Refractory Sudden Sensorineural Hearing Loss Increases Speech Intelligibility. *Audiol. Neurootol.* **2012**, *17* (2), 105–111. https://doi.org/10.1159/000329367.

(64) Plontke, S. K.; Zimmermann, R.; Zenner, H.-P.; Löwenheim, H. Technical Note on Microcatheter Implantation for Local Inner Ear Drug Delivery: Surgical Technique and Safety Aspects. *Otol. Neurotol. Off. Publ. Am. Otol. Soc. Am. Neurotol. Soc. Eur. Acad. Otol. Neurotol.* **2006**, *27* (7), 912–917. https://doi.org/10.1097/01.mao.0000235310.72442.4e.

(65) Plontke, S. K.; Löwenheim, H.; Mertens, J.; Engel, C.; Meisner, C.; Weidner, A.; Zimmermann, R.; Preyer, S.; Koitschev, A.; Zenner, H.-P. Randomized, Double Blind, Placebo Controlled Trial on the Safety and Efficacy of Continuous Intratympanic Dexamethasone Delivered via a Round Window Catheter for Severe to Profound Sudden Idiopathic Sensorineural Hearing Loss after Failure of Systemic Therapy. *The Laryngoscope* **2009**, *119* (2), 359–369. https://doi.org/10.1002/lary.20074.

(66) Li, L.; Ren, J.; Yin, T.; Liu, W. Intratympanic Dexamethasone Perfusion versus Injection for Treatment of Refractory Sudden Sensorineural Hearing Loss. *Eur. Arch. Oto-Rhino-Laryngol. Off. J. Eur. Fed. Oto-Rhino-Laryngol. Soc. EUFOS Affil. Ger. Soc. Oto-Rhino-Laryngol. - Head Neck Surg.* **2013**, *270* (3), 861–867. https://doi.org/10.1007/s00405-012-2061-0.

(67) Wang, X.; Dellamary, L.; Fernandez, R.; Harrop, A.; Keithley, E. M.; Harris, J. P.; Ye, Q.; Lichter, J.; LeBel, C.; Piu, F. Dose-Dependent Sustained Release of Dexamethasone in Inner Ear Cochlear Fluids Using a Novel Local Delivery Approach. *Audiol. Neurootol.* **2009**, *14* (6), 393–401. https://doi.org/10.1159/000241896.

(68) Borden, R. C.; Saunders, J. E.; Berryhill, W. E.; Krempl, G. A.; Thompson, D. M.; Queimado, L. Hyaluronic Acid Hydrogel Sustains the Delivery of Dexamethasone across the Round Window Membrane. *Audiol. Neurotol.* **2011**, *16* (1), 1–11. https://doi.org/10.1159/000313506.

(69) Paulson, D. P.; Abuzeid, W.; Jiang, H.; Oe, T.; O'Malley, B. W.; Li, D. A Novel Controlled Local Drug Delivery System for Inner Ear Disease. *The Laryngoscope* **2008**, *118* (4), 706–711. https://doi.org/10.1097/MLG.0b013e31815f8e41.

(70) McCall, A. A.; Swan, E. E. L.; Borenstein, J. T.; Sewell, W. F.; Kujawa, S. G.; McKenna, M. J. Drug Delivery for Treatment of Inner Ear Disease: Current State of Knowledge: *Ear Hear.* **2010**, *31* (2), 156–165. https://doi.org/10.1097/AUD.0b013e3181c351f2.

(71) Du, X.; Chen, K.; Kuriyavar, S.; Kopke, R. D.; Grady, B. P.; Bourne, D. H.; Li, W.; Dormer, K. J. Magnetic Targeted Delivery of Dexamethasone Acetate Across the Round Window Membrane in Guinea Pigs: *Otol. Neurotol.* **2013**, *34* (1), 41–47. https://doi.org/10.1097/MAO.0b013e318277a40e.

(72) Kim, D.-K.; Park, S.-N.; Park, K.-H.; Park, C. W.; Yang, K.-J.; Kim, J.-D.; Kim, M.-S. Development of a Drug Delivery System for the Inner Ear Using Poly(Amino Acid)-Based Nanoparticles. *Drug Deliv.* **2015**, *22* (3), 367–374. https://doi.org/10.3109/10717544.2013.879354.

(73) Salt, A. N.; Hale, S. A.; Plonkte, S. K. R. Perilymph Sampling from the Cochlear Apex: A Reliable Method to Obtain Higher Purity Perilymph Samples from Scala Tympani. *J. Neurosci. Methods* **2006**, *153* (1), 121–129. https://doi.org/10.1016/j.jneumeth.2005.10.008.

(74) Kawamoto, K.; Kanzaki, S.; Yagi, M.; Stöver, T.; Prieskorn, D. M.; Dolan, D. F.; Miller, J. M.; Raphael, Y. Gene-Based Therapy for Inner Ear Disease. *Noise Health* **2001**, *3* (11), 37–47.

(75) 4589_313_177-facial-nerve-recess-cochlear-implant.jpg (276×437) https://www.alpfmedical.info/tympanic-membrane/images/4589_313_177-facial-nerve-recess-cochlear-implant.jpg (accessed Sep 27, 2020).

(76) Salt, A. N.; Sirjani, D. B.; Hartsock, J. J.; Gill, R. M.; Plontke, S. K. Marker Retention in the Cochlea Following Injections through the Round Window Membrane. *Hear. Res.* **2007**, *232* (1–2), 78–86. https://doi.org/10.1016/j.heares.2007.06.010.

(77) Brown, J. N.; Miller, J. M.; Altschuler, R. A.; Nuttall, A. L. Osmotic Pump Implant for Chronic Infusion of Drugs into the Inner Ear. *Hear. Res.* **1993**, *70* (2), 167–172. https://doi.org/10.1016/0378-5955(93)90155-T.

(78) Horiike, O.; Shimogori, H.; Yamashita, H. Effect of Edaravone on Streptomycin-Induced Vestibulotoxicity in the Guinea Pig: *The Laryngoscope* **2004**, *114* (9), 1630–1632. https://doi.org/10.1097/00005537-200409000-00023.

(79) Shimogori, H.; Yamashita, H. Efficacy of Intracochlear Administration of Betamethasone on Peripheral Vestibular Disorder in the Guinea Pig. *Neurosci. Lett.* **2000**, *294* (1), 21–24. https://doi.org/10.1016/S0304-3940(00)01534-2.

(80) Ayoob, A. M.; Borenstein, J. T. The Role of Intracochlear Drug Delivery Devices in the Management of Inner Ear Disease. *Expert Opin. Drug Deliv.* **2015**, *12* (3), 465–479. https://doi.org/10.1517/17425247.2015.974548.

(81) Sewell, W. F.; Borenstein, J. T.; Chen, Z.; Fiering, J.; Handzel, O.; Holmboe, M.; Kim, E. S.; Kujawa, S. G.; McKenna, M. J.; Mescher, M. M.; Murphy, B.; Leary Swan, E. E.; Peppi, M.; Tao, S. Development of a Microfluidics-Based Intracochlear Drug Delivery Device. *Audiol. Neurotol.* **2009**, *14* (6), 411–422. https://doi.org/10.1159/000241898.

(82) Emerich, D. F.; Orive, G.; Thanos, C.; Tornoe, J.; Wahlberg, L. U. Encapsulated Cell Therapy for Neurodegenerative Diseases: From Promise to Product. *Adv. Drug Deliv. Rev.* **2014**, *67–68*, 131–141. https://doi.org/10.1016/j.addr.2013.07.008.

(83) Fransson, A.; Tornøe, J.; Wahlberg, L. U.; Ulfendahl, M. The Feasibility of an Encapsulated Cell Approach in an Animal Deafness Model. *J. Controlled Release* **2018**, *270*, 275–281. https://doi.org/10.1016/j.jconrel.2017.12.014.

(84) Wang, Y.; Wise, A. K.; Tan, J.; Maina, J. W.; Shepherd, R. K.; Caruso, F. Mesoporous Silica Supraparticles for Sustained Inner-Ear Drug Delivery. *Small* **2014**, n/a-n/a. https://doi.org/10.1002/smll.201401767.

(85) Wise, A. K.; Tan, J.; Wang, Y.; Caruso, F.; Shepherd, R. K. Improved Auditory Nerve Survival with Nanoengineered Supraparticles for Neurotrophin Delivery into the Deafened Cochlea. *PLOS ONE* **2016**, *11* (10), e0164867. https://doi.org/10.1371/journal.pone.0164867.

(86) Souza, P.; Hoover, E. The Physiologic and Psychophysical Consequences of Severe-to-Profound Hearing Loss. *Semin. Hear.* **2018**, *39* (04), 349–363. https://doi.org/10.1055/s-0038-1670698.

(87) Hearing Aids https://www.nidcd.nih.gov/health/hearing-aids (accessed Sep 27, 2020).

(88) Zeng, F.-G.; Rebscher, S.; Harrison, W.; Sun, X.; Feng, H. Cochlear Implants: System Design, Integration, and Evaluation. *IEEE Rev. Biomed. Eng.* **2008**, *1*, 115–142. https://doi.org/10.1109/RBME.2008.2008250.

(89) Cochlear Implants & Other Implantable Devices. *Hearing Loss Association of America*.

(90) James, D. P.; Eastwood, H.; Richardson, R. T.; O'Leary, S. J. Effects of Round Window Dexamethasone on Residual Hearing in a Guinea Pig Model of Cochlear Implantation. *Audiol. Neurotol.* **2008**, *13* (2), 86–96. https://doi.org/10.1159/000111780.

(91) Ghavi, F. F.; Mirzadeh, H.; Imani, M.; Jolly, C.; Farhadi, M. Corticosteroid-Releasing Cochlear Implant: A Novel Hybrid of Biomaterial and Drug Delivery System. *J. Biomed. Mater. Res. B Appl. Biomater.* **2010**, *94B* (2), 388–398. https://doi.org/10.1002/jbm.b.31666.

(92) Nadol, J. B.; Burgess, B. J.; Gantz, B. J.; Coker, N. J.; Ketten, D. R.; Kos, I.; Roland, J. T.; Shiao, J. Y.; Eddington, D. K.; Montandon, P.; Shallop, J. K. Histopathology of Cochlear Implants in Humans. *Ann. Otol. Rhinol. Laryngol.* **2001**, *110* (9), 883–891. https://doi.org/10.1177/000348940111000914.

(93) Fayad, J.; Linthicum, F. H.; Galey, F. R.; Otto, S. R.; House, W. F. Cochlear Implants: Histopathologic Findings Related to Performance in 16 Human Temporal Bones. *Ann. Otol. Rhinol. Laryngol.* **1991**, *100* (10), 807–811. https://doi.org/10.1177/000348949110001004.

(94) Seyyedi, M.; Nadol, J. B. J. Intracochlear Inflammatory Response to Cochlear Implant Electrodes in Humans. *Otol. Neurotol.* **2014**, *35* (9), 1545–1551. https://doi.org/10.1097/MAO.0000000000000540.

(95) Clark, G. M.; Shepherd, R. K.; Franz, B. K. H.; Dowell, R. C.; Tong, Y. C.; Blamey, P. J.; Webb, R. L.; Pyman, B. C.; McNaughtan, J.; Bloom, D. M.; Kakulas, B. A.; Siejka, S. The Histopathology of the Human Temporal Bone and Auditory Central Nervous System Following Cochlear Implantation in a Patient: *Correlation with Psychophysics and Speech Perception Results*. *Acta Otolaryngol. (Stockh.)* **1988**, *105* (sup448), 1–65. https://doi.org/10.3109/00016488809098972.

(96) Boggess, W. J.; Baker, J. E.; Balkany, T. J. Loss of Residual Hearing after Cochlear Implantation. *The Laryngoscope* **1989**, *99* (10), 1002–1005. https://doi.org/10.1288/00005537-198210000-00005.

(97) O'Leary, S. J.; Monksfield, P.; Kel, G.; Connolly, T.; Souter, M. A.; Chang, A.; Marovic, P.; O'Leary, J. S.; Richardson, R.; Eastwood, H. Relations between Cochlear Histopathology and Hearing Loss in Experimental Cochlear Implantation. *Hear. Res.* **2013**, *298*, 27–35. https://doi.org/10.1016/j.heares.2013.01.012.

(98) Eshraghi, A. A.; Van De Water, T. R. Cochlear Implantation Trauma and Noise-Induced Hearing Loss: Apoptosis and Therapeutic Strategies. *Anat. Rec. A. Discov. Mol. Cell. Evol. Biol.* **2006**, *288A* (4), 473–481. https://doi.org/10.1002/ar.a.20305.

(99) Wilk, M.; Hessler, R.; Mugridge, K.; Jolly, C.; Fehr, M.; Lenarz, T.; Scheper, V. Impedance Changes and Fibrous Tissue Growth after Cochlear Implantation Are Correlated and Can Be Reduced Using a Dexamethasone Eluting Electrode. *PLOS ONE* **2016**, *11* (2), e0147552. https://doi.org/10.1371/journal.pone.0147552.

(100) Reich, U.; Warnecke, A.; Szczepek, A. J.; Mazurek, B.; Olze, H. Establishment of an Experimental System to Study the Influence of Electrical Field on Cochlear Structures. *Neurosci. Lett.* **2015**, *599*, 38–42. https://doi.org/10.1016/j.neulet.2015.05.027.

(101) McCreery, D. B.; Yuen, T. G. H.; Agnew, W. F.; Bullara, L. A. Stimulus Parameters Affecting Tissue Injury during Microstimulation in the Cochlear Nucleus of the Cat. *Hear. Res.* **1994**, *77* (1–2), 105–115. https://doi.org/10.1016/0378-5955(94)90258-5.

(102) Huang, C. Q.; Tykocinski, M.; Stathopoulos, D.; Cowan, R. Effects of Steroids and Lubricants on Electrical Impedance and Tissue Response Following Cochlear Implantation. *Cochlear Implants Int.* **2007**, *8* (3), 123–147. https://doi.org/10.1179/cim.2007.8.3.123.

(103) Lo, J.; Campbell, L.; Sale, P.; Chambers, S.; Hampson, A.; Eastwood, H.; O'Leary, S. The Role of Preoperative Steroids in Atraumatic Cochlear Implantation Surgery: *Otol. Neurotol.* **2017**, *38* (8), 1118–1124. https://doi.org/10.1097/MAO.0000000000001505.

(104) Rajan, G. P.; Kuthubutheen, J.; Hedne, N.; Krishnaswamy, J. The Role of Preoperative, Intratympanic Glucocorticoids for Hearing Preservation in Cochlear Implantation: A Prospective Clinical Study. *The Laryngoscope* **2012**, *122* (1), 190–195. https://doi.org/10.1002/lary.22142.

(105) Torres, R.; Drouillard, M.; De Seta, D.; Bensimon, J.-L.; Ferrary, E.; Sterkers, O.; Bernardeschi, D.; Nguyen, Y. Cochlear Implant Insertion Axis Into the Basal Turn: A Critical Factor in Electrode Array Translocation. *Otol. Neurotol.* **2018**, *39* (2), 168–176. https://doi.org/10.1097/MAO.0000000000001648.

(106) Kikkawa, Y. S.; Nakagawa, T.; Ying, L.; Tabata, Y.; Tsubouchi, H.; Ido, A.; Ito, J. Growth Factor-Eluting Cochlear Implant Electrode: Impact on Residual Auditory Function, Insertional Trauma, and Fibrosis. *J. Transl. Med.* **2014**, *12* (1), 280. https://doi.org/10.1186/s12967-014-0280-4.

(107) Chikar, J. A.; Hendricks, J. L.; Richardson-Burns, S. M.; Raphael, Y.; Pfingst, B. E.; Martin, D. C. The Use of a Dual PEDOT and RGD-Functionalized Alginate Hydrogel Coating to Provide Sustained Drug Delivery and Improved Cochlear Implant Function. *Biomaterials* **2012**, *33* (7), 1982–1990. https://doi.org/10.1016/j.biomaterials.2011.11.052.

(108) Golomb, G.; Fisher, P.; Rahamim, E. The Relationship between Drug Release Rate, Particle Size and Swelling of Silicone Matrices. *J. Controlled Release* **1990**, *12* (2), 121–132. https://doi.org/10.1016/0168-3659(90)90088-B.

(109) Geers, A.; Tobey, E.; Moog, J.; Brenner, C. Long-Term Outcomes of Cochlear Implantation in the Preschool Years: From Elementary Grades to High School. *Int. J. Audiol.* **2008**, *47* (sup2), S21–S30. https://doi.org/10.1080/14992020802339167.

(110) Helbig, S.; Adel, Y.; Rader, T.; Stöver, T.; Baumann, U. Long-Term Hearing Preservation Outcomes After Cochlear Implantation for Electric-Acoustic Stimulation. *Otol. Neurotol.* **2016**, *37* (9), e353–e359. https://doi.org/10.1097/MAO.0000000000001066.

(111) Kim, J.; Peng, C.-C.; Chauhan, A. Extended Release of Dexamethasone from Silicone-Hydrogel Contact Lenses Containing Vitamin E. *J. Controlled Release* **2010**, *148* (1), 110–116. https://doi.org/10.1016/j.jconrel.2010.07.119.

(112) Mond, H. G.; Stokes, K. B. The Steroid-Eluting Electrode: A 10-Year Experience. *Pacing Clin. Electrophysiol.* **1996**, *19* (7), 1016–1020. https://doi.org/10.1111/j.1540-8159.1996.tb03407.x.

(113) Malcolm, K.; Woolfson, D.; Russell, J.; Tallon, P.; McAuley, L.; Craig, D. Influence of Silicone Elastomer Solubility and Diffusivity on the in Vitro Release of Drugs from Intravaginal Rings. *J. Controlled Release* **2003**, *90* (2), 217–225. https://doi.org/10.1016/S0168-3659(03)00178-0.

(114) Kamath, K. R.; Barry, J. J.; Miller, K. M. The Taxus™ Drug-Eluting Stent: A New Paradigm in Controlled Drug Delivery. *Adv. Drug Deliv. Rev.* **2006**, *58* (3), 412–436. https://doi.org/10.1016/j.addr.2006.01.023.

(115) Perin, E. C. Choosing a Drug-Eluting Stent: A Comparison between CYPHER and TAXUS. *Rev. Cardiovasc. Med.* **2005**, *6 Suppl 1*, S13-21.

(116) Farhadi, M.; Jalessi, M.; Salehian, P.; Ghavi, F. F.; Emamjomeh, H.; Mirzadeh, H.; Imani, M.; Jolly, C. Dexamethasone Eluting Cochlear Implant: Histological Study in Animal Model. *Cochlear Implants Int.* **2013**, *14* (1), 45–50. https://doi.org/10.1179/1754762811Y.0000000024.

(117) Douchement, D.; Terranti, A.; Lamblin, J.; Salleron, J.; Siepmann, F.; Siepmann, J.; Vincent, C. Dexamethasone Eluting Electrodes for Cochlear Implantation: Effect on Residual Hearing. *Cochlear Implants Int.* **2015**, *16* (4), 195–200. https://doi.org/10.1179/1754762813Y.0000000053.

(118) Gehrke, M.; Sircoglou, J.; Vincent, C.; Siepmann, J.; Siepmann, F. How to Adjust Dexamethasone Mobility in Silicone Matrices: A Quantitative Treatment. *Eur. J. Pharm. Biopharm.* **2016**, *100*, 27–37. https://doi.org/10.1016/j.ejpb.2015.11.018.

(119) Siepmann, J.; Siepmann, F. Mathematical Modeling of Drug Delivery. *Int. J. Pharm.* **2008**, *364* (2), 328–343. https://doi.org/10.1016/j.ijpharm.2008.09.004.

(120) Dash, S.; Murthy, P. N.; Nath, L.; Chowdhury, P. Kinetic Modeling on Drug Release from Controlled Drug Delivery Systems. *Acta Pol. Pharm.* **2010**, *67* (3), 217–223.

(121) Siepmann, J.; Siepmann, F. Modeling of Diffusion Controlled Drug Delivery. *J. Controlled Release* **2012**, *161* (2), 351–362. https://doi.org/10.1016/j.jconrel.2011.10.006.

(122) Krenzlin, S.; Vincent, C.; Munzke, L.; Gnansia, D.; Siepmann, J.; Siepmann, F. Predictability of Drug Release from Cochlear Implants. *J. Controlled Release* **2012**, *159* (1), 60–68. https://doi.org/10.1016/j.jconrel.2011.12.032.

(123) PubChem. Dexamethasone https://pubchem.ncbi.nlm.nih.gov/compound/5743 (accessed Sep 27, 2020).

(124) Dexamethasone sodium phosphate - DrugBank https://go.drugbank.com/salts/DBSALT000843 (accessed Sep 27, 2020).

Résumé

L'oreille interne est l'organe responsable de la perception auditive et le maintien de l'équilibre. L'OMS estime que 360 millions personnes dans le monde (plus que 5 % de la population) souffrent d'une perte auditive handicapante, soit 40 dB dans l'oreille qui entend le mieux. L'impact sur la vie personnelle ainsi que professionnelle est considérable : Dans certaines sociétés les patients sont stigmatisés ou partiellement exclus du système éducatif. Ils ont beaucoup plus de mal à accéder au monde du travail et, par conséquence, cela impacte leur niveau de pauvreté.

L'oreille peut être divisée en trois parties : (i) l'oreille externe avec l'auricule et le conduit auditif externe. Le tympan sépare cette partie de (ii) l'oreille moyenne qui contient la chaîne ossiculaire (le marteau, l'enclume et l'étrier) et le trompe d'eustache qui lie l'oreille moyenne au rhinopharynx et sert à équilibrer les différences de pression. La fenêtre ovale et la fenêtre ronde sont des membranes semi-perméables qui lient l'oreille moyenne avec l'oreille interne. (iii) L'oreille interne consiste de deux parties : la cochlée et le système vestibulaire.

Dans la cochlée saine, une onde sonore est transformée en signaux mécaniques. La perception auditive se fait en plusieurs étapes μ Le son arrive à l'auricule de l'oreille externe et est canalisé et transmis pour faire vibrer le tympan. Cette vibration est amplifiée par la chaîne ossiculaire qui fait vibrer la fenêtre ovale. Par conséquence, les différents espaces liquidiens de l'oreille interne sont déplacés. Ces signaux font balancer des cellules ciliées en fonction de la fréquence et de l'amplitude du signal original. Le mouvement des cellules ciliées induit un signal électrique qui est transformé en perception sensorielle dans le cerveau.

La perception de la position de la tête et de son accélération est la fonction principale du système vestibulaire de l'oreille interne. Le mouvement de la tête induit un déplacement de liquide dans les canaux semi-circulaires dans la direction opposée. Par conséquent, les cellules ciliées du système vestibulaire balancent. Ce signal est ensuite traduit en signal électrique et

transmis au cerveau pour assurer l'équilibre du corps.

Quand ces systèmes de perception sont perturbés ou endommagés, différentes maladies de l'oreille interne peuvent se manifester, ex : la surdité, les acouphènes, les réactions auto-immunes de l'oreille interne et la maladie de Menière. Souvent, en clinique un mélange des différentes maladies est observé.

L'administration d'un principe actif dans l'oreille interne constitue un véritable challenge de par la barrière hémato-cochléaire qui est comparable à la barrière hémato-encéphalique et protège l'oreille de substances toxiques. L'administration d'un principe actif par les voies classiques (orale, intraveineuse, intramusculaire) ne permet pas d'atteindre des concentrations suffisantes au niveau de l'oreille interne pour traiter une maladie. Les jonctions serrées de la barrière hémato-cochléaire peuvent être contournées par un dosage systémique très élevé du principe actif. Une dose élevée de dexaméthasone peut par exemple être une bonne prévention contre la perte de perception auditive lors de l'insertion d'un implant cochléaire. Cependant, un dosage systémique élevé peut mener à des effets secondaires très graves. De la même façon, l'injection locale dans l'oreille interne d'un principe actif ne semble pas favorable car la solution peut s'écouler par le canal d'injection. De plus, pour le traitement d'une maladie chronique plusieurs injections sont nécessaires, augmentant le risque d'infection. La cochlée, est relativement étanche et extrêmement sensible aux changements mineurs de pression et représente donc un espace assez délicat avec un volume très faible.

C'est pourquoi, une administration locale et unique peut fournir de grands avantages. Plusieurs possibilités pour une administration prolongée ont été décrites. L'application d'un hydrogel semi-solide sur la fenêtre ronde peut créer une matrice qui libère le principe actif d'une manière prolongée. Par contre, le gel ne pouvant pas être fixé in vivo, il risque d'être éliminé très rapidement. En outre, le temps d'exposition et l'anatomie de la fenêtre ronde peut varier d'un patient à l'autre. De plus, la périlymphe (fluide principal dans la cochlée) peut être

considérée comme un fluide non-agité avec un transport de masse négligeable. Par conséquence, un principe actif administré dans l'oreille moyenne risque de ne pas être distribué de manière homogène dans la périlymphe de l'oreille interne. D'un point de vue clinique, un autre obstacle doit être surmonté: la taille minuscule de la cochlée et sa difficulté anatomique d'accès.

Le traitement est aussi relié à la cause de la maladie. Si celle-ci est connue, le patient est traité en conséquence. Sinon, le patient reçoit souvent des stéroïdes par voie orale ou intra-tympaniques. Ces stéroïdes sont utilisés pour prévenir les inflammations ou œdèmes pouvant endommager les très sensibles cellules ciliées de l'oreille interne. D'autres stratégies incluent l'administration orale de principes actifs antiviraux, de diurétiques, de vasodilatateurs, d'antioxydants, un traitement avec de l'oxygène hyperbare ou des traitements chirurgicaux de l'oreille. L'application d'un appareil auditif tel que l'implantation d'un implant cochléaire peut être nécessaire si la surdité persiste. Un implant cochléaire transforme de la même façon que les cellules ciliées un son en signal électrique qui peut être retraduit en perception auditive dans le cerveau. L'électrode est reliée à un amplificateur implanté derrière l'oreille du patient. L'implantation d'une électrode dans la scala tympani de l'oreille interne peut alors aider à reconstituer la perception sensorielle.

Ces implants cochléaires étant en silicone, il est possible de les charger en principes actifs. La libération de principe actif à partir de silicone peut être maintenue pendant des années : Du silicone chargé en dexaméthasone a été implanté avec succès dans des pacemakers. Après 10 ans d'implantation, une amélioration du fonctionnement de l'électrode est observée comparativement aux pacemakers non chargés en principe actif. Pour ajuster la libération du principe actif, plusieurs paramètres peuvent être variés tels que le type de chaînes latérales, l'ajout d'additifs, ou encore le taux de principe actif. De plus, la géométrie et les dimensions du système peuvent avoir une grande influence sur la libération car ils impactent la longueur

du « trajet » à parcourir par le principe actif pour être libéré. Ceci est d'autant plus important vu la nature plutôt hydrophobe du polymère ralentissant la pénétration de l'eau dans la matrice et par conséquent la libération du principe actif.

Les principaux objectifs de cette thèse étaient d'approfondir les travaux de Krenzlin et al. et Gehrke et al. pour une meilleure compréhension des implants cochléaires à élution de dexaméthasone par de nouveaux moyens de caractérisation, et par l'optimisation des paramètres de formulation en ajoutant divers médicaments pour compléter l'effet thérapeutique de la dexaméthasone.

1) Libération à long terme in vitro des implants cochléaires chargés en dexaméthasone :

Au début de cette thèse, la libération de la dexaméthasone pouvait être prédite en utilisant la deuxième loi de diffusion de Fick, mais jusqu'à présent, les expériences indépendantes utilisées pour confirmer notre théorie ne duraient que quelques mois. Maintenant que les taux de charge de silicone et de médicament les plus prometteurs ont été sélectionnés, la décision a été prise d'étudier la libération in vitro des implants cochléaires chargés de dexaméthasone aussi longtemps que possible (c'est-à-dire plusieurs années).

2) Développement et caractérisation de matrices de silicone combinant dexaméthasone et dexaméthasone phosphate :

Il a été démontré que les matrices de silicone chargées en dexaméthasone étaient capables d'assurer une libération continue sur plusieurs mois/années, mais il faut souligner que l'action anti-inflammatoire du médicament est particulièrement vitale pendant les premiers jours après la pose de l'implant. Afin de minimiser les conséquences du traumatisme induit à ce stade précoce, il peut être judicieux de renforcer la libération du médicament pendant cette période cruciale.

La faible solubilité de la dexaméthasone dans l'eau (89 mg/L)[123] est l'une des principales raisons pour lesquelles elle se libère si lentement. Le fait de disposer d'un médicament anti-

inflammatoire présentant une solubilité plus élevée pourrait nous donner la possibilité d'une libération plus rapide aux premiers stades. Le phosphate de dexaméthasone s'est avéré être le candidat le plus probable, puisqu'il s'agit d'une forme hautement hydrophile de dexaméthasone avec des valeurs de solubilité énormes (1,52 g/L)[124].

Nous avons supposé qu'avec l'ajout de dexaméthasone phosphate, l'absorption d'eau serait plus élevée à l'intérieur des matrices de silicone, solubilisant les cristaux de médicament plus rapidement, et fournissant une libération en rafale qui peut nous aider à atteindre des concentrations anti-inflammatoires élevées pendant les premiers jours après la chirurgie, complétant ainsi la libération lente et continue de la dexaméthasone.

Fournir une libération rapide dans les premiers jours

L'ajout de petites quantités de dexaméthasone phosphate aux implants cochléaires miniaturisés à base de silicone pour une libération contrôlée de la dexaméthasone peut augmenter efficacement la libération initiale. On s'attend à ce que cela soit bénéfique pour le patient, car cela peut aider à : (i) limiter le traumatisme local et l'inflammation provoqués par l'insertion invasive du réseau d'électrodes, et (ii) limiter la formation de tissu fibrotique autour du corps étranger (la fibrose diminuant les performances des implants, car la transmission des signaux électriques est entravée). L'effet sur la libération du principe actif peut s'expliquer par la nature plus hydrophile de la dexaméthasone phosphate, facilitant la pénétration de l'eau dans le système et donc la dissolution et la diffusion du principe actif. Il est important de noter qu'à des teneurs limitées de dexaméthasone phosphate, le gonflement de l'implant reste cliniquement acceptable.

Comportement à long terme des implants cochléaires chargés en principes actifs

Comme les périodes de libération visées sont très longues (plusieurs années), l'optimisation del'implant cochléaire chargé en principes actifs est un véritable défi. Jusqu'à présent, on ne connaît que peu de choses sur le comportement à long terme de ces systèmes, y compris leurs modes de libération ainsi que leur gonflement ou leur rétrécissement potentiel lors de l'exposition à des milieux aqueux ou à des tissus vivants. Différents types d'implants cochléaires cylindriques ont été préparés par moulage par injection, en faisant varier leurs dimensions (utilisables chez l'homme ou la gerbille) et leur charge initiale en médicament (0, 1 ou 10 %). La libération de dexaméthasone a été suivie in vitro lors de l'exposition à la périlymphe artificielle à 37 °C pendant plus de 3 ans. La microscopie optique, la diffraction des rayons X et l'imagerie Raman ont été utilisées pour caractériser les implants avant et après l'exposition au milieu de libération in vitro, ainsi qu'après 2 ans d'implantation chez la gerbille. Fait important, dans tous les cas, la libération de la dexaméthasone a été fiable pendant les périodes d'observation. Le transport de masse par diffusion et les effets de solubilité limitée du médicament au sein des matrices en silicone semblent jouer un rôle majeur. Initialement, la dexaméthasone est distribuée de manière homogène dans les matrices polymères sous forme de cristaux minuscules. Lors de l'exposition à un milieu aqueux ou à un tissu vivant, des quantités limitées d'eau pénètrent dans le dispositif, dissolvent le principe actif, qui diffuse ensuite. Les régions proches de la surface sont épuisées en premier, ce qui entraîne une augmentation de la diffusivité apparente du médicament avec le temps. Aucun signe de gonflement ou de rétractionnotable de l'implant n'a été observé in vitro, ni in vivo.

Conclusion

L'ajout de dexaméthasone phosphate à hauteur de 10 % aux matrices de silicone a considérablement augmenté le taux de libération aux premiers stades. On peut s'attendre à ce que cela améliore l'action du médicament et la fonctionnalité de l'implant. Cependant, il reste à noter qu'à des charges élevées le gonflement du dispositif est devenu important. La cochlée étant un organe minuscule et sensible, une augmentation potentielle des dimensions de l'implant au fil du temps doit donc être limitée.

Les implants cochléaires à base de silicone peuvent contrôler de manière fiable la libération de dexaméthasone sur plusieurs années. Le transport de masse par diffusion combiné aux effets de saturation à l'intérieur des implants semble jouer un rôle majeur. La matrice polymérique étant hydrophobe, seules des quantités limitées d'eau sont disponibles pour la dissolution de la dexaméthasone à l'intérieur des implants. Le principe actif est initialement distribué de manière homogène dans les dispositifs sous la forme de minuscules cristaux de dexaméthasone. Avec le temps, les premières régions proches de la surface deviennent appauvries en principe actif (in vitro comme in vivo), comme le montrent la microscopie optique et l'imagerie Raman. Il est important de noter que les implants ne gonflent pas et ne rétrécissent pas de manière notable lorsqu'ils sont exposés à des tissus vivants ou à une périlymphe artificielle pendant plusieurs années.

Research articles

A. Qnouch, V. Solarczyk, J. Verin, G. Tourrel, P. Stahl, F. Danede, J.F Willart, J. Siepmann & F. Siepmann (2021). Dexamethasone-loaded cochlear implants: How to provide a desired "burst release". International Journal of Pharmaceutics: X, 3, 100088.

T. Rongthong, A. Qnouch, M. Gehrke, L. Paccou, P. Oliveira, F. Danede, J. Verin, P.E. Lemesre, C. Vincent, J.F. Willart, F. Siepmann, J. Siepmann. Silicone matrices for controlled dexamethasone release: Towards a better understanding of the underlying mechanisms. *Submitted.*

T. Rongthong, A. Qnouch, M. Gehrke, F. Danede, J.F. Willart, P. Oliveira, L. Paccou, G. Tourrel, P. Stahl, P.E. Lemesre, C. Vincent, F. Siepmann, J. Siepmann. Long term behavior of dexamethasone-loaded cochlear implants in vitro & in vivo (gerbils). *Submitted.*

Oral communications

A. Qnouch, J. Verin, F. Siepmann, J. Siepmann (2019). Silicone matrices for controlled drug delivery to the inner ear: Effects of combining dexamethasone and dexamethasone sodium phosphate. 2nd International Symposium on Inner Ear Therapeutics, Hanover, Germany.

A. Qnouch, J. Verin, F. Siepmann, J. Siepmann (2019). Silicone matrices for controlled drug delivery to the inner ear: Effects of combining dexamethasone and dexamethasone sodium phosphate. 13th Pharmaceutical Solid State Cluster Annual Meeting, Düsseldorf, Germany.

Poster presentations

A. Qnouch, V. Solarczyk, J. Verin, C. Vincent, F. Siepmann, J. Siepmann (2021). Silicone films for controlled drug delivery to the inner ear: Effects of combining dexamethasone and dexamethasone sodium phosphate. 12th World Meeting on Pharmaceutics, Biopharmaceutics and Pharmaceutical Technology, virtual event.

A. Qnouch, T. Rongthong, G. Tourrel, P. Stahl, P. Oliveira, J.F Willart, L. Paccou, C. Vincent, F. Siepmann, J. Siepmann (2021). Monitoring the distribution and release of dexamethasone and dexamethasone sodium phosphate inside silicone matrices using Raman imaging. 12th World Meeting on Pharmaceutics, Biopharmaceutics and Pharmaceutical Technology, virtual event.

A. Qnouch, V. Solarczyk, J. Verin, G. Tourrel, P. Stahl, C. Vincent, F. Siepmann, J. Siepmann (2021). Influence of milling on the drug release and swelling of cochlear implants combining dexamethasone and dexamethasone sodium phosphate. 12th World Meeting on Pharmaceutics, Biopharmaceutics and Pharmaceutical Technology, virtual event.

A. Qnouch, T. Rongthong, J. Verin, G. Tourrel, P. Stahl, C. Vincent, F. Siepmann, J. Siepmann (2019). Predictability of drug release from dexamethasone loaded cochlear implants: Long term results. 3rd European Conference on Drug Delivery and Pharmaceutical Technology, Bologna, Italy.

A. Qnouch, J. Verin, F. Siepmann, J. Siepmann (2019). Silicone matrices for controlled drug delivery to the inner ear: Effects of combining dexamethasone and dexamethasone sodium

phosphate. 3rd European Conference on Drug Delivery and Pharmaceutical Technology, Bologna, Italy.